PONTIFICIA UNIVERSIDAD CATOLICA DE CHILE

SCHOOL OF ENGINEERING

ORGANOLEPTICAL PROPERTIES OF NATURAL, NON-CALORIC SWEETENERS: MOLECULAR SIMULATION, MIXTURE OPTIMIZATION AND EXPERIMENTAL VALIDATION IN CARBONATED SOFT DRINKS

WALDO ANDRÉS ACEVEDO CASTILLO

Thesis submitted to the Office of Graduate Studies in partial fulfillment of the requirements for the Degree of Doctor in Engineering Sciences

Advisor:

EDUARDO AGOSIN

Santiago de Chile, November, 2017

PONTIFICIA UNIVERSIDAD CATOLICA DE CHILE
SCHOOL OF ENGINEERING

ORGANOLEPTICAL PROPERTIES OF NATURAL, NON-CALORIC SWEETENERS: MOLECULAR SIMULATION, MIXTURE OPTIMIZATION AND EXPERIMENTAL VALIDATION IN CARBONATED SOFT DRINKS

WALDO ANDRÉS ACEVEDO CASTILLO

Members of the Committee:

EDUARDO AGOSIN T.

RICARDO PÉREZ C.

DANILO GONZÁLEZ N.

JAVIER SÁINZ L.

PIERO A. TEMUSSI

JORGE VÁSQUEZ P.

Thesis submitted to the Office of Graduate Studies in partial fulfillment of the requirements for the Degree of Doctor in Engineering Sciences

Santiago de Chile, November, 2017

To my family, Ximena, Valentina and Sebastián.
To my parent, Marlene and Sergio
To my grandmother, Teresa
To my brother, Aroldo

ACKNOWLEDGMENTS

I would like to thank all people who have contributed to this work either in the research area or with everyday support. Many thanks also to everyone in the Biotechnology laboratory of the Chemical Engineering and Bioprocess Department and "Centro de Aromas y Sabores – DICTUC" for their friendship and for making the laboratory an agreeable place to work.

I would like to express my sincere gratitude to my advisor, Professor Eduardo Agosin, for his continuous support, motivation, and patience, his valuable supervision, his sharp observations and good advice throughout this thesis. His guidance helped me in all the time of research and writing of this thesis. I could not have imagined having a better advisor and mentor for my Ph.D. study.

Also thanks to professors Piero A. Temussi, Danilo González, Javier Sáinz and Ricardo Pérez for their support in different stages of this thesis and for their comments and discussions to improve the final version of this manuscript and the oral presentation. In particular, I am grateful to Dr. Temussi for enlightening me the glance of research.

Thanks to the Comisión Nacional de Investigación Científica y Tecnológica (CONICYT), the Vicerrectoría de Investigación (VRI) and Pontificia Universidad Católica de Chile for providing the necessary funding to make this research possible.

Last but not the least, I would like to thank my wife, Ximena, and my children, Valentina and Sebastián, for supporting me spiritually throughout writing this thesis and my life in general.

LIST OF PUBLICATIONS

This thesis is based on the following publications.

Acevedo, W.A, González-Nilo, F., Agosin, E. 2016. Docking and Molecular Dynamics Simulations of Steviol Glycosides – Human Bitter Receptors Interactions. *Journal of Agricultural and Food Chemistry.* 64, 7585 – 7596.

Acevedo, W.A, Ramírez-Sarmiento, C., Agosin, E. 2017. Identifying the Interactions between Natural, Non-Caloric Sweeteners and the Human Sweet Receptor by Molecular Docking. (Submitted to *Journal of Food Chemistry,* Manuscript ID: FOODCHEM-S-17-0923)

Acevedo, W.A, Capitaine, C., Rodríguez, R., Araya, I., González-Nilo, F., Pérez-Correa, R, Agosin, E. 2017. Selecting Optimal Mixtures of Natural Sweeteners for Carbonated Soft Drinks through Multi-objective Decision Modeling and Sensory Validation. (Submitted to *Food Quality and Preference Journal.* Manuscript ID: FQAP_2017_5)

INDEX OF CONTENTS

FIGURE INDEX

TABLE INDEX

ABBREVIATION INDEX

ANOVA	Analysis of Variance
CHARMM	Chemistry at HARvard Macromolecular Mechanics
CMD	Conventional Molecular Dynamics
CRD	Cysteine-Rich Domain
DM	Decision Maker
DOEs	Design of Experiments
EC_{50}	Half maximal effective concentration
GPCR	G Protein-Coupled Receptor
G protein	Guanosine-5'-triphosphate (GTP)-binding protein
GRG	Generalized Reduced Gradient
GTs	Glycosylated Terpenoids
HEK	Human Embryonic Cells
K_d	Dissociation constant
LPDB	Ligand-Protein Database
mGLUR1	Metabotropic Glutamate Receptor 1
MOP	Objective Optimization Problem
MOPAC	Molecular Orbital PACKage
MPA	MultiPoint Attachment
MW	Molecular Weight
NAMD	NAnoscale Molecular Dynamics
PDB	Protein Data Bank

POPC	1-Palmitoyl-2-Oleyl-PhosphatidylCholine
QSAR	Quantitative Structure-Analysis Relationship
RB	Relative Bitterness
RMSD	Root Mean Square Deviation
RMSF	Root Mean Square Fluctuations at Cα carbon of the amino acid residues
TMD	Transmembrane Domain
hT1R2	Human Taste type 1 Receptor 2
hT1R3	Human Taste type 1 Receptor 3
hT2R1	Human Taste type 2 Receptor 1
hT2R4	Human Taste type 2 Receptor 4
hT2R14	Human Taste type 2 Receptor 14
SCFAs	Short-Chain Fatty Acids
SE	Sucrose-Equivalent
SG	Steviol Glycosides
SMD	Steered Molecular Dynamics
VMD	Visual Molecular Dynamics
VFT	Venus Fly Trap

PONTIFICIA UNIVERSIDAD CATOLICA DE CHILE
ESCUELA DE INGENIERIA

ORGANOLEPTICAL PROPERTIES OF NATURAL, NON-CALORIC SWEETENERS: MOLECULAR SIMULATION, MIXTURE OPTIMIZATION AND EXPERIMENTAL VALIDATION IN CARBONATED SOFT DRINKS

Thesis submitted to the Office of Research and Graduate Studies in partial fulfillment of the requirements for the Degree of Doctor in Engineering Sciences

WALDO ANDRÉS ACEVEDO CASTILLO

ABSTRACT

Sugar has historically played a leading role as a tabletop sweetener and in the preparation of various food products. However, at present, it has been determined that a significant number of chronic, non-communicable diseases are a consequence of the excessive consumption of sugar. These health trends are increasing awareness among consumers about the intake of sugary food and beverage encouraging them to shift their preferences towards products with less sugar and caloric content. Nowadays, the use of natural sweeteners in product formulations is becoming more and more frequent, with stevia extracts being the most popular. The term stevia, used to refer to steviol glycosides (SGs), are a suitable alternative to artificial sweeteners due to their sweetening capacity, similar to that of aspartame, and stability at low pH. Unfortunately, these compounds generate, in addition to their sweetening effect, unwanted sensory attributes such as bitterness, metallic, and licorice tastes, when added to foods and beverages.

The aim of the present study was to select optimal mixtures of natural, non-caloric sweeteners - highest sweetness and lowest bitterness - for carbonated soft drink using bioinformatics tools and sensory analysis.

We built three-dimensional models of the hT1R2-hT1R3 sweet taste receptor, as well as the hT2R4 and hT2R14 bitter taste receptors, using reference structure of class A and C

GPCR. Once these models were obtained, potential binding sites, as well as associated binding free energies, of natural, non-caloric sweeteners - from glycosylated terpenoids (GT) to sweet proteins - were predicted via molecular docking. The predicted binding free energies were correlated with the relative sweetness and bitterness previously reported in the literature.

Docking results showed that the binding free energy ($\Delta G_{binding}$) between receptor hT1R2-hT1R3 and sweeteners belonging to different families shows a strong correlation with their sweetness intensity for both, small sweeteners (r = -0.89) and sweet proteins (r= -0.96). Whereas $\Delta G_{binding}$ between the bitterness receptors and SG was negatively correlated with SG bitterness intensity, for both hT2R4 (r = −0.95) and hT2R14 (r = −0.89).

Furthermore, the binding mechanism mediated by hydrogen bonds of some GTs, including 10 active compounds of stevia, has also been identified on bitter taste receptors, because of the sugars present in these sweeteners. However, the affinity of SG for sweet taste receptors, as well as their differences in sweetness intensity, is due to their physicochemical properties *i.e.* a chemical structure that combines a hydrophobic scaffold functionalized by a number of hydrogen bond sites. On the contrary, the affinity for bitter taste receptors could be due to the steric characteristics of SG and their binding site architecture.

Finally, we selected optimal mixtures of natural, non-caloric sweeteners for carbonated soft drinks by sensory analysis. To this end, we determine equi-sweet of sucrose, stevia and tagatose, as well as analytical testing of different products, by using trained sensory panel and the canonical Scheffé´s equation for bitterness was calculated based on the three-component simplex lattice mixture design in soft drink matrix. Alternatively, a multi-objective decision model was applied to identify optimal combinations of sucrose, stevia, and tagatose, based on the thermodynamic properties of the sweetener-receptor and sweetener-sweetener interactions. The optimal mixtures predicted were similar to those obtained through DOE and sensory analysis, demonstrating the robustness of the model. Therefore, the most suitable combinations, depending on the sweetness/bitterness balance, were those containing 23 - 39 g/L sucrose, 0.19 – 0.34 g/L stevia and 34 - 42 g/L tagatose.

Furthermore, a reduction of almost 60% of sucrose can be achieved using both stevia and tagatose, keeping bitterness intensity low. If further reduction is desired, ternary mixtures with a higher proportion of tagatose are a good option to maintain a more sugar-like taste. This could result in a 79% reduction of total calories compared to a regular soft drink (pure sucrose).

Altogether, the results of this study and the tools hereby developed will help for developing new sweetener mixtures with other natural sweeteners, such as *Luo Han Guo* (also known as monk-fruit) or to reduce other unwanted attributes, besides bitterness.

Members of Doctoral Thesis Committee:

Eduardo Agosin T.
José Ricardo Pérez C.
Danilo González N.
Javier Sainz L.
Piero A. Temussi
Jorge Vásquez P.

Santiago, November, 2017

PONTIFICIA UNIVERSIDAD CATOLICA DE CHILE
ESCUELA DE INGENIERIA

PROPIEDADES ORGANOLÉPTICAS DE ENDULZANTES NATURALES, NO CALÓRICOS: SIMULACIÓN MOLECULAR, OPTIMIZACION DE MEZCLAS Y VALIDACION EXPERIMENTAL EN BEBIDAS CARBONATADAS

Tesis enviadas a la Dirección de Investigación y Postgrado en cumplimiento parcial de los requisitos para el grado de Doctor en Ciencias de la Ingeniería

WALDO ANDRÉS ACEVEDO CASTILLO

RESUMEN

El azúcar ha jugado históricamente un papel principal como edulcorante de la mesa y en la preparación de varios productos alimenticios. Sin embargo, en la actualidad, se ha determinado que un número significativo de enfermedades crónicas, no transmisibles son una consecuencia del consumo excesivo de azúcar. Estas tendencias de la salud están aumentando la conciencia entre los consumidores acerca de la ingesta de alimentos azucarados y bebidas que les estimula a cambiar sus preferencias hacia los productos con menos contenido de azúcar y calorías. Hoy en día, el uso de edulcorantes naturales en formulaciones de productos es cada vez más frecuente, siendo los extractos de stevia los más populares. El término stevia, usado para referirse a los glicósidos de esteviol (SGs), es una alternativa adecuada a los edulcorantes artificiales debido a su capacidad edulcorante, similar al aspartame, y estabilidad a bajo pH. Desafortunadamente, estos compuestos generan, además de su efecto edulcorante, atributos sensoriales no deseados tales como sabor amargo, metálico y regaliz, cuando se añaden a alimentos y bebidas.

El objetivo del presente estudio fue seleccionar mezclas óptimas de edulcorantes naturales, no calóricos - el más alto dulzor y el menor amargor - para bebidas carbonatadas usando herramientas bioinformáticas y análisis sensorial.

Construimos modelos tridimensionales del receptor de dulzor hT1R2-hT1R3, así como receptores de amargor hT2R4 y hT2R14, utilizando la estructura de referencia de GPCRs clase A y C. Una vez que se obtuvieron estos modelos, se predijeron los potenciales sitios de unión, así como las energías libres de unión asociadas, de edulcorantes naturales no calóricos - desde terpenoides glicosilados (GT) a proteínas dulces - mediante acoplamiento molecular. Las energías libres de unión calculadas se correlacionaron con el dulzor y amargor relativo previamente informados en la literatura.

Los resultados de acoplamiento mostraron que la energía libre de unión ($\Delta G_{interacción}$) entre el receptor hT1R2-hT1R3 y los edulcorantes pertenecientes a diferentes familias muestra una fuerte correlación con su intensidad de dulzor tanto para edulcorantes pequeños (r = -0.89) como proteínas dulces (r = -0.96). Mientras que el $\Delta G_{unión}$ entre los receptores de amargor y SG se correlacionó negativamente con la intensidad de amargor de SG, tanto para hT2R4 (r = -0.95) como hT2R14 (r = -0.89).

Además, el mecanismo de unión de algunos GTs, incluyendo los 10 compuestos activos de stevia, mediado por puentes de hidrógeno fue identificado tanto en los receptores de amargor como de dulzor, debido a los azúcares presentes en las estructuras de estos edulcorantes. Sin embargo, la afinidad de SG por los receptores de dulzor, así como sus diferencias en la intensidad de dulzor, se debe a sus propiedades físico-químicas, es decir, una estructura química que combina una plataforma hidrofóbica funcionalizada por un número de sitios de puentes de hidrógeno. Por el contrario, la afinidad por los receptores de amargor podría ser debido a las características estéricas de SG y su arquitectura de sitio de unión.

Finalmente, seleccionamos mezclas óptimas de edulcorantes naturales no calóricos para bebidas carbonatadas mediante análisis sensorial. Para ello, determinamos el dulzor equivalente de sacarosa, stevia y tagatosa, así como las pruebas analíticas de diferentes productos, mediante panel sensorial entrenado y se calculó la ecuación canónica de Scheffé para amargor basada en el diseño simplex-lattice de tres componentes en la matriz de bebidas. Alternativamente, se aplicó un modelo de decisión multi-objetivo para identificar combinaciones óptimas de sacarosa, stevia y tagatosa basadas en las propiedades termodinámicas de las interacciones edulcorante-receptor y edulcorante-edulcorante. Las

mezclas óptimas predichas fueron similares a las obtenidas a través de DOE y análisis sensorial, demostrando la robustez del modelo. Por lo tanto, las combinaciones más adecuadas, dependiendo del equilibrio dulzor/amargor, contiene 23 - 39 g/L sacarosa, 0.19 – 0.34 g/L stevia and 34 - 42 g/L tagatosa. Además, una reducción de casi 60% de sacarosa puede ser lograda usando tanto stevia como tagatosa, manteniendo baja la intensidad de amargor. Si se desea una reducción adicional, las mezclas ternarias con una alta proporción de tagatosa son una buena opción para mantener un sabor más similar al azúcar. Esto podría resultar en una reducción del 79% de las calorías totales en comparación con un refresco regular (sacarosa pura).

En conjunto, los resultados de este estudio y las herramientas desarrolladas ayudarán a desarrollar nuevas mezclas de edulcorantes con otros edulcorantes naturales como *Luo Han Guo* o también a reducir otros atributos no deseados, además del amargor.

Miembros de la Comisión de la Tesis Doctoral:

Eduardo Agosin T.
José Ricardo Pérez C.
Danilo González N.
Javier Sainz L.
Piero A. Temussi
Jorge Vásquez P.

Santiago, Noviembre, 2017

1. INTRODUCTION

1.1 Motivation

Sugar has historically played a leading role as a tabletop sweetener and in the preparation of various food products. However, at present, it has been determined that a significant number of chronic, noncommunicable diseases are a consequence of the excessive consumption of sugar (Malik et al., 2010). One way to prevent these diseases is by consuming non-caloric sweeteners in place of sucrose (Shankar et al. , 2013). There are numerous natural, plant-derived compounds that perform this function, among which steviol glycosides (SG), extracted from *Stevia rebaudiana*, are the most popular (Kinghora, Soejarto, & Inglett, 1986). Unfortunately, these compounds generate, in addition to their sweetening effect, unwanted sensory attributes such as bitterness, metallic, and licorice tastes, when added to foods and beverages (Rocha & Bolini, 2015). Therefore, the aim of this work was to develop a multi-objective decision model to identify optimal mixtures of natural sweeteners - highest sweetness and lowest bitterness - using bioinformatics tools and sensory evaluation.

1.2 Taste Receptors

1.2.1 Sweetness receptor

The human sweet taste receptor has been identified as a heterodimer of two class C G-protein coupled receptor (GPCR) subunits, i.e. hT1R2 and hT1R3 (human taste type 1 receptor 2 and 3) (Nelson et al., 2001; Li et al., 2002). In structural terms, the receptor contains 3 domains: a large extracellular region at the amino end, composed by the "Venus Fly Trap" (VFT) and cysteine-rich domain (CRD); and a typical seven-transmembrane helical domain (TMD) on the carboxyl end.

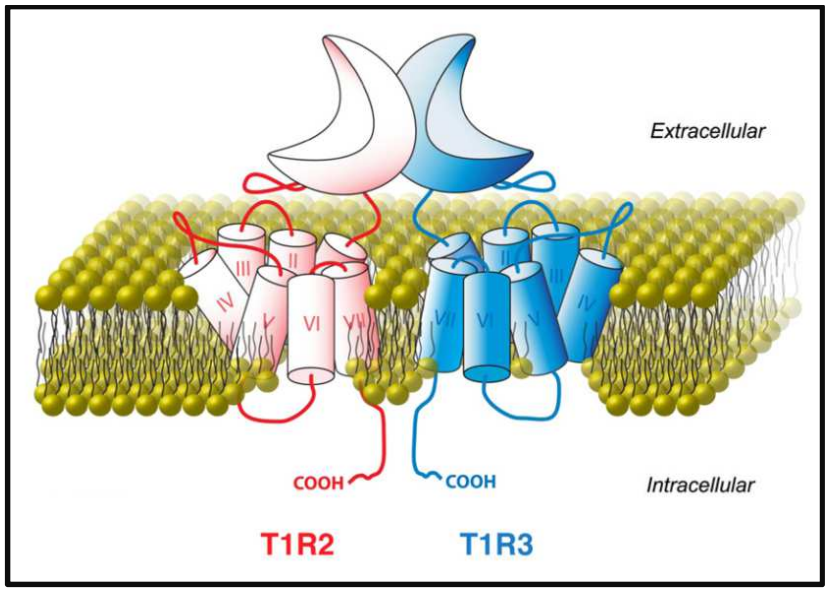

Figure 1-1: Representation of the sweet taste receptor (Adapted from Vigues et al., 2009)

The CRD of the hT1Rs are ~70-residues segments with 9 conserved cysteines. It is a unique domain of class C GPCR family located in the extracellular region connecting the VFT and TMD. Although the structure and function of the CRD is quite ambiguous, several studies have shown that the CRD plays a role in the allosteric coupling between the change in conformation of the VFT and TMD (Parmentier et al., 2002). Most recently, Jian et al. (2004) demonstrated that showed that tampering with the integrity of the CRD suppresses recognition of brazzein (Jiang et al., 2004).

Functional expression studies and molecular docking demonstrated that the hT1R2/hT1R3 receptor is activated by the interaction of the chemically diverse sweeteners with the VFT domain (Liu et al., 2012; Masuda et al., 2012). These molecules induce a conformational change in the receptor, which is transmitted to the cytoplasmic end to activate an intracellular G protein (Chun et al., 2012). G proteins - abbreviation for guanosine-5'-triphosphate (GTP) - binding proteins - are heterotrimeric complexes composed by alpha (α), beta (β) and gamma (γ) subunits. The activation mechanism of class C GPCR involves three sequential events: first, the agonist binds to the VFT domain and stabilizes the active conformation of the receptor; subsequently, the receptor-agonist interaction induces a

conformational change from VFT to transmembrane domain; and finally, the structural reorganization promotes the exchange of bound GDP for GTP on the G protein α-subunit that activates a cascade of further signaling events resulting in a change in cell function (Pin et al., 2004).

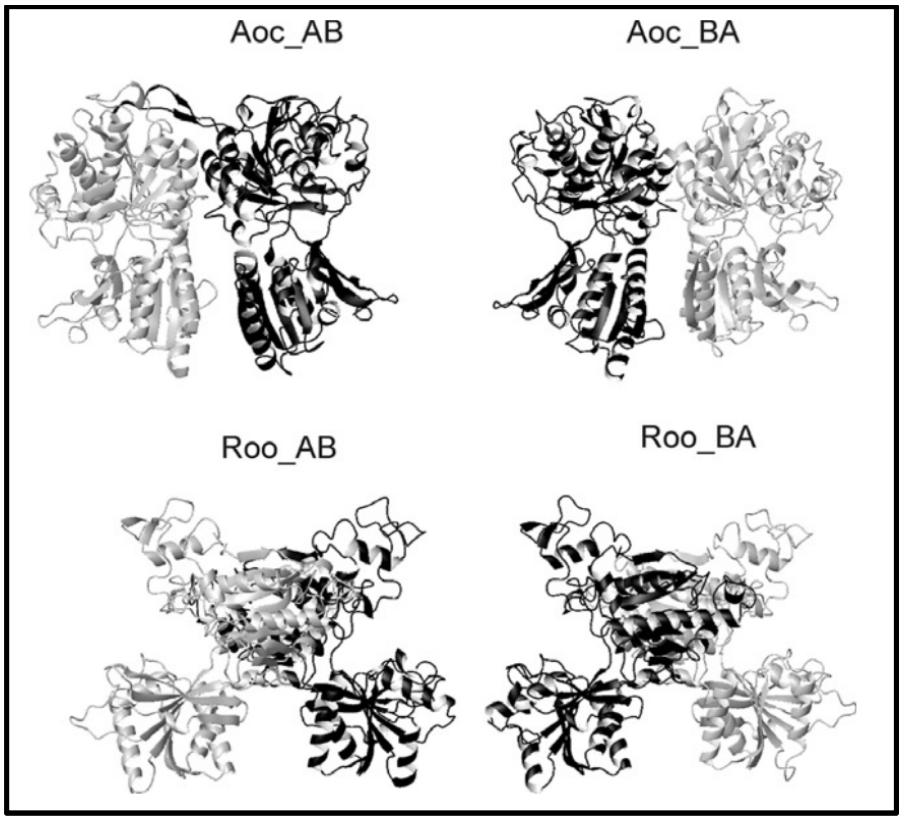

Figure 1-2: Molecular models of the four possible forms of the sweet receptor. Aoc_AB (hT1R2 closed/hT1R3 open), Aoc_BA (hT1R3 closed/hT1R2 open), Roo_AB (hT1R2 open/hT1R3 open) and Roo_BA (hT1R3 open/hT1R2 open). The models of hT1R2 and hT1R3 are represented as gray and black ribbons, respectively. Molecular models were generated using MOLMOL (Temussi, 2011)

Morini et al. (2005) built all possible VFT domain models of the hT1R2 and hT1R3 subunits using the X-ray crystal structure of the metabotropic glutamate receptor type I o mGLUR1 (PDB code: 1EWK and 1EWT). The mGLUR1 receptor was used as template for comparative modeling because i) it is member of the GPCR family; ii) the residues of the VFT domain cavity are conserved in both receptors; and iii) its activation mechanism is

similar to that of the sweetness receptor. Figure 1-2 illustrates the molecular models of the four possible forms of the sweet receptor. These models were used to show all possible sites of interaction both of small sweeteners and sweet proteins in the receptor (Morini, Bassoli, & Temussi, 2005).

1.2.2 Bitterness receptor

Transduction of bitter taste in humans is mediated by ~25 receptors of the hTAS2R gene family, also known as hT2R (Figure 1-3)(M. Behrens & Meyerhof, 2006). The hT2Rs are members of the large family of GPCRs. Due to low sequence similarity of T2Rs with class A GPCR, classification is somewhat ambiguous, but most analysis support the classification of T2Rs as class A GPCRs (Nordström, Sällman Almén, Edstam, Fredriksson, & Schiöth, 2011; DiPizio & Niv, 2014). The activation mechanism in this subfamily are poorly understood (Upadhyaya et al., 2010). In structural terms, hT2Rs contain between 290 and 333 amino acids, which are composed by a short extracellular domain at the amino end and a seven-transmembrane helical domain on the carboxyl end.

GLY28 and SER285 residues are highly conserved in transmembrane domains 1 and 7 of hT2Rs, according to amino acid sequence analysis and molecular modeling studies. These residues could play an important role in receptor activation mediated by the formation of hydrogen bonding between the residues. However, only GLY28 is conserved at the level of GPCR class A (Smith, 2010). Although the structure of hT2Rs receptors has not been solved, most of their 3D structures were predicted by comparative modeling, using as template the crystal structure of rhodopsin (member of class A GPCR) of different species. Despite limited sequence similarity, conserved residues in the transmembranal domain belong to binding sites for various compounds (Singh et al., 2011).

hT2R1 was the first modeled bitterness receptor for studying the mechanism of activation of the hT2Rs receptors (Upadhyaya et al., 2010). For this end, the crystal structure of opsin (PDB entry: 3DQB) was used as template, which shares a 22% sequence identity with hT2R1. Subsequently, the hT2R4 (Pydi, Bhullar, & Chelikani, 2012) and hT2R38 (Marchiori et al., 2013) receptors were modeled using bovine rhodopsin (PDB entry 1U19)

and squid (PDB entry: 2Z73) templates, respectively, sharing around 20% sequence identity with the corresponding bitter receptors.

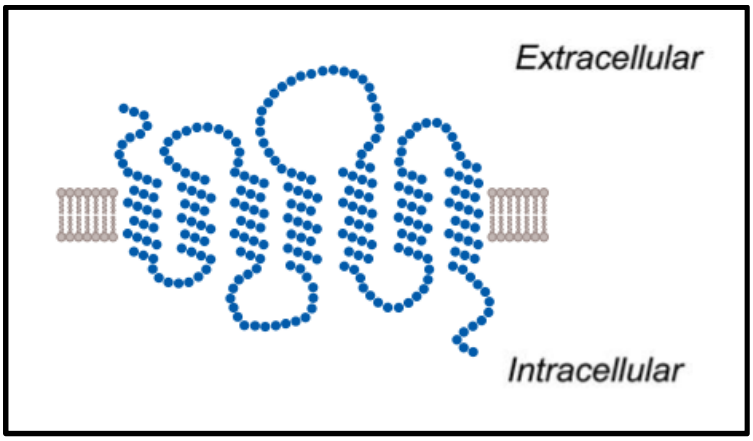

Figure 1-3: Representation of a bitter taste receptor (Adapted from Chandrashekar et al., 2006)

1.3 Natural, non-caloric sweeteners

Commercially available non-caloric sweeteners can be classified as natural and artificial. Among the latter, we find saccharin, cyclamate and aspartame, which have been widely used in food and beverage manufacturing because of their high sweetening power and sucrose-like taste (DuBois & Prakash, 2012). However, laboratory studies have determined that some of these sweeteners, such as saccharin and aspartame, have carcinogenic, teratogenic, neurotoxic and nephrotoxic potential in humans and therefore pose a potential health risk (National Cancer Institute, 2009). Therefore, the demand for natural, non-caloric sweeteners, such as stevia or monk fruit has increased significantly during the last decade. In particular, stevia, with its sweetening capacity of 300 fold higher than sucrose, is a product that has reached an important place in the family basket as a table top sweetener and for the preparation of various food products. Several active chemical principles – glycosylated diterpenoids - present in *Stevia rebaudiana* leaves are responsible for sweetness, among which the most important are stevioside, various rebaudiosides, steviolbioside, dulcosides and rubusoside. Unfortunately, these compounds generate, in addition to its sweetening effect, unwanted sensory attributes such as bitterness, metallic, and licorice tastes in foods and beverages. Recent *in vitro* studies in HEK 293 cells

revealed that SG specifically activate the hT2R4 and hT2R14 bitter taste receptors, triggering this mouth feel (Hellfritsch et al., 2012). Consequently, it is not uncommon to commercialize this product in combination with artificial sweeteners, such as sucralose, to reduce these off-flavour effects. Another alternative is to combine with other families of natural sweeteners, such as sweet proteins extracted from exotic fruits, which, at low concentration, enhance the sweetness and mask the undesirable attributes of stevia (Angelo & Lord, 2010). Both, low MW sweeteners and sweet proteins interact with the hT1R2/hT1R3 sweet receptor (Liu et al., 2012). Thus, the wide range of molecular sizes covered by these sweeteners, in addition to their chemical composition, are important features to consider at the moment of determining their binding mode to the receptor. Consequently, the characterization of the interaction of sweeteners with taste receptors at the molecular level will contribute to the understanding of the perceived taste of sweeteners in foods and beverages, allowing a better prediction and control of the resulting bitterness.

1.3.1 Low-molecular-weight sweeteners

Sensory studies and cell-based functional expression assays revealed that both natural and artificial low MW sweeteners simultaneously trigger a bitter taste from a certain concentration threshold, at which taste receptors are activated. Hellfritsch et al. (2012) carried out a comprehensive screening of 25 human bitter taste receptors, revealing that two receptors, hT2R4 and hT2R14, mediate the bitter off-taste of steviol glycosides; whereas hT2R31, hT2R43 and hT2R44 receptors mediate the bitter off-taste of saccharin and acesulfame-K (Kuhn et al., 2004; Pronin et al., 2007; Roudnitzky et al., 2011).

SG's potential binding sites on hT2R4 taste receptor were predicted by molecular docking (Singla & Jaitak, 2016). Results showed that rebaudioside A and stevioside lie in the same binding cavity of the receptor, composed by transmembrane regions with moderate participation from the extracellular region. In both cases, Phe 69, Phe 168, Phe 169, Ile 170, Glu 172, Met 259, Gly 260 and Lys 262 were responsible for this interaction.

On the other hand, high-throughput screening by cell-based functional bitter taste receptors expression assays allowed to identify a novel bitter taste receptor antagonist named

GIV3727 (Slack et al., 2010). This compound, identified as a negative allosteric modulator, NAM, inhibits the activation of hT2R31 and hT2R43 by saccharin and acesulfame K. Molecular modeling and site-directed mutagenesis studies suggested that two residues in helix seven were important for antagonist activity in hT2R43/31. Furthermore, human sensory trials showed that GIV3727 significantly reduced the bitterness associated with the two sulphonamide sweeteners, indicating that this T2R antagonist was active *in vivo*. Therefore, these results demonstrate that small molecule bitter receptor antagonists can effectively reduce the bitter taste of foods, beverages, and pharmaceuticals.

1.3.2 Sweet proteins

Another important family of natural, non-caloric sweeteners is constituted by some particular proteins which, most - discovered in the mid of the last century - are present in fruits of African trees. Five sweetening proteins, a flavor modifying protein and a protein having both functions are known so far. Among the sweetening proteins, we find thaumatin, monellin, mabinlin, brazzein and pentadin (Wintjens, et al., 2011). Taste-modifying proteins are miraculin and neoculin, which change the perception of sour to sweet taste.

Sweet proteins have, both structural and physico-chemical differences. They do not show sequential or structural similarity (Niccolai et al., 2001; Picone & Temussi, 2012), therefore they have virtually no homology, which makes it difficult to understand how they generate or modify sweetness. For example, monellin, unlike the others, does not contain disulfide bridges, which may explain its instability against changes in the temperature and pH (Table 1-1). Furthermore, most of these proteins are positively charged at neutral pH, with the exception of brazzein, which has an isoelectric point lower than 7 (Table 1-1).

The structure-activity relationship of thaumatin, as well as of monellin and brazzein, has been elucidated. Suspecting the critical role of positive charges, Kaneko and Kitabatake (2001) found that the charge-specific chemical modification of Lys 78, Lys 97, Lys 106, Lys 137, or Lys 187 residues by phosphopyridoxylation reduced sweetness significantly of thaumatin (Kaneko & Kitabatake, 2001). Combination of these results with those ensuing

from modifications of other charged residues led these authors to suggest the importance of charged residues of the protein for sweetness. Recently, Ohta et al. (2008) carried out a more systematic search for critical residues (Ohta, Masuda, Ide, & Kitabatake, 2008). For this purpose, they constructed several modified thaumatin proteins in which lysine or arginine residues were substituted by alanine. Four lysine residues (K49, K67, K106 and K163) and three arginine residues (R76, R79 and R82) were found to play significant roles in thaumatin sweetness, particularly K67 and R82. More recently, site-directed mutagenesis studies demonstrated that removal of the specific negative charge at Asp21 significantly enhances the sweetness intensity of thaumatin (Masuda et al., 2016).

Table 1-1: Properties of the sweet and taste-modifying proteins.

	Thaumatin [a]	Neoculin [b]	Brazzein [c]	Monellin [d]	Mabinlin [e]	Pentadin [f]	Miraculin [g]
Origin	*Thaumatococcus danielli* (Africa)	*Curculigo latifolia* (Malaysia)	*Pentadiplandra brazzeana* (Africa)	*Dioscorephyllum cumminisii* (Africa)	*Capparis masaikai* (China)	*Pentadiplandra brazzeana* (Africa)	*Richadella dulcifica* (Africa)
Amino acids	207	114/113	54	45/50	33/72	--	191
Class	all β	all β	α/β	α/β	Todo α		α/β
Active form	Monomer	Heterodimer	Monomer	Heterodimer	Heterodimer	--	Heterodimer
Variants	I, II	2 chains	--	2 chains	I, II, III, IV	--	--
M.W. [kDa]	22.2	12/13	6.5	10.7	12.4	12.0	98.4
Disulfide bridges	8	2	4	--	4	.--	4
Sweetness factor based on %w/v	3000	4000	2000	3000	--	500	--
Isoelectric point	12	8.6	5.4	9.3	11.3	9.1	7.7
Threshold [nM]	51	--	500	270	--	--	--

The data were extracted from [a] Van del Wel & Loeve, 2000; [b] Shirasuka et al., 2014; [c] F M Assadi-Porter; Aceti, & Markley, 2000; [d] Morris, Martenson, & Cagan, 1973; [e] Guan & Zheng, 2000; [f] Wel et al., 1989; and [g] Theerasilp & Kurihara, 1988

In structural terms, molecular docking results suggested that the sweet proteins could interact with a large cavity of the VFT domain of sweetness receptor according to 'wedge model' proposed by Temussi (2002), whereas low-molecular-weight sweeteners occupy the small cavities inside both subunits of the receptor (Piero Andrea Temussi, 2002)(Tancredi, Pastore, Salvadori, Esposito, & Temussi, 2004). Furthermore, mutagenesis studies have revealed that the CRD region of hT1R3 is also involved in the response to sweet protein, including brazzein, monellin and thaumatin (Jiang et al., 2004) (Masuda et al., 2013)

Therefore, sweet proteins bind to the sweetness receptor by structural and electrostatic complementarity. On one hand, the shape of the receptor binding cavity is wide and deep, forming a wedge-shaped surface capable of hosting large volume proteins, which was validated by molecular docking (Temussi, 2002). On the other hand, the binding site of the sweet proteins harbor charged residues complementary to those of the receptor, whose surface is predominantly negative. Therefore, the binding of the sweet protein to the receptor might also be mediated by electrostatic interactions (Esposito et al., 2006).

1.4 Optimal mixture of sweeteners

The proper combination of various sweeteners has been shown to be a more effective way of replacing sucrose in the preparation of various food product (Lawless, Science, & Hall, 1998). In fact, the mixture of certain sweeteners, both nutritious and non-nutritive, produces a synergistic effect on sweetness. In addition, it induces flavor enhancement, temporary sweetness profiles, and reduced costs of the sweetener system (Verdi & Hood, 1993).

At high concentrations, stevia exhibits unwanted attributes such as bitterness and licorice. For this reason, it is unlikely that stevia can be used as a single sweetener. However, this limitation is readily manipulable by blending with other sweeteners, in particular non-caloric ones. Among these, aspartame and potassium acesulfame, have been used in conjunction with stevia in the manufacture of beverages and table-top sweeteners. On the

other hand, natural sweeteners, such as thaumatin, have had an important impact both, in enhancing sweetness and masking off-taste of the stevia (Angelo & O. Lord, 2010).

Product optimization methods, such as design of experiments (DOEs), have been used to efficiently evaluate new ingredients and formulations. The mixture design method is a type of DOE that creates relationships between different mixtures in a product that must always equal 100% and provides information about ingredient. Choosing adequate sweeteners in the right proportion to achieve a good-tasting product is challenging due to the large number of possible combinations and the conflicting objectives, i.e. sweetness vs. bitterness, metallic, licorice, etc. Product formulations can be experimentally optimized to balance these objectives using statistical techniques, such as surface response and desirability function (Granato & de Araújo Calado, 2013).

1.5 Working hypothesis

The compounds responsible for sweetness present in *Stevia rebaudiana* simultaneously trigger a bitter taste from a certain concentration, due to the activation of the taste receptors hT2R4 and hT2R14. Bitter taste can be reduced by optimal mixtures of natural sweeteners using bioinformatics tools and sensory evaluation.

1.6 Objectives

The general objective of this thesis was to develop multi-objective decision models to identify optimum combinations of natural, non-caloric sweeteners - maximum sweetness, minimum bitterness - using bioinformatics tools.

For this purpose, the specific objectives were the following:

1 Construction of three-dimensional models for the sweet and bitter (hT2R4 and hT2R14) taste receptors, using comparative modeling techniques.

2 Characterization of the interaction of natural, non-caloric sweeteners - from glycosylated terpenoids to sweet proteins - with the sweetness and bitterness receptors, at the molecular level.

3 Development and validation of optimal mixtures of natural, non-caloric sweeteners for foods and beverages, using molecular simulation and sensory evaluation.

1.7 Approach

In this work, a multi-objective thermodynamically based decision model was developed to identify optimal mixtures of natural sweeteners in soft drink. The binding free energies of the different complexes were predicted and included as parameters of the multi-objective decision model. To this end, three-dimensional models of the hT1R2-hT1R3 sweetness receptor, as well as of the hT2R4 and hT2R14 bitterness receptors, were built using reference structure of class A and C GPCR. Once these models were obtained, potential binding sites and binding free energies and interactions of different sweeteners were estimated via molecular docking. The calculated binding free energies were correlated with the relative sweetness and bitterness previously reported in the literature.

Docking results showed that SGs have only one site for orthosteric binding to these receptors. The binding free energy ($\Delta G_{binding}$) between the receptor and SG was negatively correlated with SG bitterness intensity, for both hT2R4 ($r = -0.95$) and hT2R14 ($r = -0.89$). Bitterness intensity of SG resulted from the following features: (1) the presence of transmembrane regions in the binding cavity of hT2R4 and hT2R14, which favors the interactions with SG by hydrophobic contact, (2) the ability to form hydrogen bonds with amino acids at the binding pocket due to the presence of sugars at positions C-13 and C19, and (3) the difference in the total number and type of monosaccharides present in their structures. Furthermore, the architecture of the SG binding site, as well as the amino acid residues implicated in the interaction, is required for the activation of these bitter taste receptors. These results are presented in Chapter 2 entitled “Identifying the Interactions between Natural, Non-Caloric Sweeteners and the Human Sweet Receptor by Molecular Docking”.

On the other hand, the binding free energy ($\Delta G_{binding}$) between the sweetness receptor hT1R2-hT1R3 and sweeteners belonging to different families showed a strong correlation with their sweetness intensity for both, small sweeteners ($r = -0.89$) and sweet proteins ($r= -0.96$). Moreover, natural small sweeteners bind into the hT1R2-hT1R3 receptor through

hydrogen bonding and hydrophobic interactions, whereas sweet proteins bind predominantly via electrostatic interactions. In particular, the affinity of SGs for sweet taste receptors, as well as their differences in sweetness intensity, was due to their physical-chemical properties *i.e.* a chemical structure that combines a hydrophobic scaffold functionalized by a number of hydrogen bond sites. On the contrary, the affinity for bitter taste receptors could result from the steric characteristics of SGs and their binding site architecture.

These results are illustrated in the chapter 2: "Docking and Molecular Dynamics of Steviol Glycoside–Human Bitter Receptor Interactions" and chapter 3: "Identifying the Interactions between Natural, Non-Caloric Sweeteners and The Human Sweet Receptor by Molecular Docking".

Finally, a multi-objective decision model was applied to identify optimal combinations of sucrose, stevia, and tagatose based on the thermodynamic properties of the sweetener-receptor and sweetener-sweetener interactions. A reduction of almost 60% of sucrose can be achieved using both stevia and tagatose, keeping bitterness intensity low. Therefore, the most suitable combinations, depending on the sweetness/bitterness balance, were those containing 23 - 39 g/L sucrose, 0.19 – 0.34 g/L stevia and 34 - 42 g/L tagatose.

The results constitute the content of chapter 4: "Selecting Optimal Mixtures of Natural Sweeteners for Carbonated Soft Drinks through Multi-objective Decision Modeling and Sensory Validation".

2. DOCKING AND MOLECULAR DYNAMICS SIMULATIONS OF STEVIOL GLYCOSIDES – HUMAN BITTER RECEPTORS INTERACTIONS

Waldo Acevedo, Fernando González-Nilo, and Eduardo Agosin

Published in *Journal of Agricultural and Food Chemistry.* September 2016, Vol. 64, p. 7585 – 7596

Abstract

Stevia is one of the most sought after sweeteners by consumers due to its natural origin and minimum calorie content. Steviol glycosides (SG) are the main active compounds present in the leaves of *Stevia rebaudiana*, and are responsible for its sweetness. However, recent *in vitro* studies in HEK 293 cells revealed that SG specifically activate the hT2R4 and hT2R14 bitter taste receptors, triggering this mouth feel. The objective of the present study was to characterize the interaction of SG with these two receptors at molecular level. The results showed that SG have only one orthosteric binding site to these receptors. The binding free energy ($\Delta G_{binding}$) between receptor and SG was negatively correlated with SG bitterness intensity, for both hT2R4 (r=-0.95) and hT2R14 (r=-0.89). We also determined, by steered molecular dynamics (SMD) simulations, that the force required to extract stevioside from the receptors was greater than that required for rebaudioside A, in accordance with the ΔGs obtained by molecular docking. Finally, we identified the loop responsible for the activation by SG of both receptors. As a whole, these results contribute to a better understanding of the resulting off-flavor perception of these natural sweeteners in foods and beverages, allowing for better prediction – and control – of the resulting bitterness.

2.1 Introduction

Sugar has historically played a leading role as a tabletop sweetener and in the preparation of various food products. However, at present it has been determined that a significant number of chronic, noncommunicable diseases are a consequence of the excessive consumption of sugar (Malik et al., 2010). Among these diseases are cardiovascular

accidents, diabetes, and obesity, which claim the lives of 38 million people each year (World Health Organization, 2013).

One way to prevent these diseases is by consuming noncaloric sweeteners to replace sucrose (Shankar et al., 2013; Hu & Malik, 2010). There are numerous natural compounds derived from plants that perform this function, (Kinghora et al., 1986) where steviol glycosides (SG), extracted from *Stevia rebaudiana*, are the most popular. Among these glycosides, the most important are stevioside, various rebaudiosides, dulcosides, steviobioside, and rubusoside, which give the extract a sweetening activity about 300 times that of sucrose (Figure 2-1)(Prakash, Markosyan, & Bunders, 2014). The sweetening capacity – similar to aspartame – and stability of these active compounds transform them into an excellent alternative for the – at least partial – substitution of sugar in processed foods (Kroyer, 2010).

Unfortunately, these compounds generate, in addition to their sweetening effect, unwanted sensory attributes such as bitterness, metallic and licorice tastes in foods and beverages sweetened with Stevia (Rocha & Bolini, 2015). Recent *in vitro* studies in HEK 293 cells revealed that SG specifically activate the hT2R4 and hT2R14 bitter taste receptors, triggering this mouth feel (Hellfritsch et al., 2012). It is worthy to note that other artificial sweeteners, like saccharin and acesulfame-K, also induce a bitter taste, but this is due to the activation of hT2R43 and hT2R44 receptors instead (Kuhn et al., 2004). Humans have 25 taste receptors (hT2R type) responsible for the sensation of bitterness, which belong to a superfamily of G-protein coupled receptors (GPCR). Specifically, these receptors share partial sequence similarity with the GPCR Class A subfamily. However, the activation mechanisms of this subfamily are poorly understood (Pydi, Singh, Upadhyaya, Bhullar, & Chelikani, 2014). In structural terms, hT2R receptors have between 290 and 333 amino acids and are composed by 7 transmembrane segments, a short extracellular N-terminal domain, and an intracellular C-terminal domain (Adler et al., 2000; Meyerhof, 2005).

Functional studies in humans showed that hT2R receptors exhibit high selectivity for their ligands (Ji et al., 2014). On the one hand, the hT2R4 receptor has a limited degree of promiscuity (Meyerhof, Born, Brockhoff, & Behrens, 2011) and, on the other hand,

hT2R14 responds to a wide variety of natural and synthetic, structurally different bitter compounds, including alkaloids and medicinal drugs (Maik Behrens et al., 2004); while other receptors – such as hT2R16 and hT2R38 – are activated by a family of structurally related ligands that contain β-glucopyranoside and isothiocyanate (Bufe et al., 2002; Bernd Bufe et al., 2005). Thus, the architecture of the ligand-binding site, as well as the amino acid residues implicated in the interaction, are required for the activation of these bitter taste receptors (Brockhoff et al., 2010).

GLY28 and SER285 residues are highly conserved in transmembrane domains 1 and 7 of hT2R receptors (Pydi et al., 2012). These residues could play an important role in receptor activation, mediated by the formation of hydrogen bonds between residues. However, only GLY28 is conserved in Class A GPCRs (Smith, 2010). Moreover, most hT2R structural models have been constructed by comparative modeling, using the crystal structure of rhodopsin (a member of the GPCR Class A family) from different species as a template (Pydi et al., 2012; Upadhyaya et al., 2010; Marchiori et al., 2013). Despite the limited sequence similarity, the conserved residues act as binding sites for various compounds. The first modeled structure developed to study the activation mechanism of hT2R receptors, was hT2R1(Upadhyaya et al., 2010). Opsin (PDB ID: 3DQB), which has 22% sequence identity with hT2R1, was used as template. Subsequently, the hT2R4 and hT2R38 receptors were modeled, using bovine (PDB ID: 1U19) and squid (PDB ID: 2Z73) rhodopsin as templates, respectively, which have about 20% sequence identity with each receptor (Pydi et al., 2012; Marchiori et al., 2013).

Kubota and Kubo were the first to propose that the chemical basis of bitterness, based on the structure of diterpenes isolated from the Rabdosia plant, could be represented by a three-point attachment model, resulting from the presence of a proton donor group AH-, a proton acceptor group B- and a third binding site X- that interacts with the hydrophobic site on the receptor (Kubota & Kubo, 1969). More recently, Nofre and Tinti developed the Multipoint Attachment Model (Nofre & Tinti, 1996), a more elaborated theory for the taste of any molecule, including simple sugars and artificial sweeteners. This model assumes the presence of at least eight fundamental recognition points or sites, namely, B-, AH-, XH-,

G1- ,G2- ,G3- , G4- and D- that interact with a receptor through three types of elementary interactions, *i.e.* ionic, H-bonding and steric interactions.

The objective of the present study was to develop a model capable of predicting the bitterness intensity of the main sweetening compounds extracted from *Stevia rebaudiana*, by molecular simulation. To this end, we built a model for hT2R4 and hT2R14 bitter taste receptors, using as reference structures, bovine and squid rhodopsin, respectively. Then, we identified the corresponding binding sites by both hydrophobic interactions and hydrogen bonding and we calculated the binding free energy associated with SG. The calculated binding free energies were correlated with the SG relative bitterness previously reported in the literature (Shankar et al., 2013). Finally, we simulated, by steered molecular dynamics (SMD), the unbinding process of the ligands and the conformational changes of the binding sites of the modeled bitter taste receptors.

2.2 Materials and methods

2.2.1 Template selection

The amino acid sequences of hT2R4, hT2R14 and hT2R1 bitter taste receptors were retrieved from the NCBI (Accession: EAW83983, EAW96222, and EAX08075, respectively). Squid rhodopsin (PDB ID: 2Z73) was selected as a template to model hT2R14, since the latter does not have homolog proteins with a known structure. To this end, we used the PGenTHREADER method (Lobley, Sadowski, & Jones, 2009), based on the technique of protein fold recognition, which allows for the detection of templates for three-dimensional (3D) structural prediction of this protein family with more certainty. Bovine rhodopsin (PDB ID: 1U19) and opsin (PDB ID: 3DQB) were used as templates to model hT2R4 and hT2R1, respectively, in accordance to that reported in the literature (Upadhyaya et al., 2010; Pydi et al., 2012).

2.2.2 Modeling of bitter taste receptors

We built comparative models for hT2R4, hT2R14 and hT2R1 using the crystal structure of the protein templates mentioned above. The hT2R1 receptor was used as a negative control. Models were built using the SWISS-MODEL server (SIB Swiss Institute of

Bioinformatics and the Biozentrum & der Universität Basel, 2003; Biasini et al., 2014). The resulting models were subjected to cycles of energy minimization until convergence and equilibration for 20 ps, in order to relax the conformation of side chains and avoid conformational tension generated by the homology model. All calculations were performed using the programs NAMD (NAnoscaled Molecular Dynamics; v 2.9) and CHARMM force field (Phillips et al., 2005;Vanommeslaeghe et al., 2010). Subsequently, we assessed the stereochemical quality of the models using Ramachandran plot (RAMPAGE), PROCHECK (Overall quality factor) and ERRAT (Overall quality factor). The models were visualized and rendered using Visual Molecular Dynamics (VMD 1.9)(Lovell et al., 2003;·Humphrey, Dalke, & Schulten, 1996).

2.2.3 Ligand preparation

The 3D structure of the active ingredients of stevia were obtained from the PubChem database (National Center for Biotechnology Information, 2004) as sdf file format (Figure 2-1). The program OpenBabel 2.3.1 was employed to convert ligand representations to mol2 format and visually checked to correct structural errors.

Table 2-1: Chemical structure of steviol glycosides[a]

Compound	R_1	R_2
Stevioside (1)	$\beta-glc-$	$\beta-glc-\beta-glc-$
Rebaudioside A (2)	$\beta-glc-$	$(\beta-glc)_2-\beta-glc-$
Rebaudioside B (3)	H –	$(\beta-glc)_2-\beta-glc-$
Rebaudioside C (4)	$\beta-glc-$	$(\beta-glc)_2-\alpha-rha-$
Rebaudioside D (5)	$\beta-glc-\beta-glc-$	$(\beta-glc)_2-\beta-glc-$
Rebaudioside E (6)	$\beta-glc-\beta-glc-$	$\beta-glc-\beta-glc-$
Rebaudioside F (7)	$\beta-glc-$	$(\beta-glc)_2-\alpha-xyl-$
Steviolbioside (8)	H –	$\beta-glc-\beta-glc-$
Dulcoside A (9)	$\beta-glc-$	$\beta-glc-\alpha-rha-$
Rubusoside (10)	$\beta-glc-$	$\beta-glc-$

[a] R_1 and R_2 referred to in Figure 2-1. Glc, D-glucopyranosyl; rha, L-rhamnopyranosyl; xyl, D-xylopyranosyl.

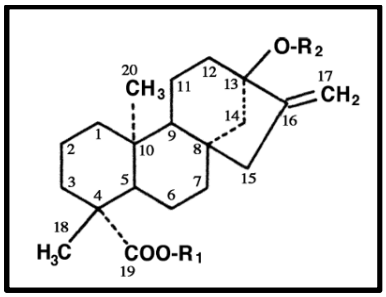

Figure 2-1: Chemical structure of steviol glycosides (SG) 1 - 10 (R_1 and R_2 referred to in Table 2-1).

2.2.4 Molecular docking of "sweeteners – bitter taste receptors"

Binding sites, as well as the associated free energies ($\Delta G_{binding}$) of the different sweeteners with both, the hT2R4 and hT2R14 receptors, were predicted using the program Autodock Vina (Trott & Olson, 2009; Serio, 2014). Protein and ligand preparation was carried out using Autodock Tools 1.5.6 (Morris et al., 2009). Gasteiger partial charges were assigned to the atoms of ligands. The AutoTors option was used to define rotatable bonds in the sweeteners. The Lamarckian genetic algorithm was employed for all docking calculations. The visual inspection of the results was carried out using the MGL Tools package. We selected a volume of 60x60x60 grid points, enough to cover each receptor. In Autodock Vina (Trott & Olson, 2009), the binding free energies - $\Delta G_{binding}$ - were estimated by the sum of inter- and intra-molecular contributions that approximate the thermodynamic stability of the ligand with the receptor.

$$\Delta G_{binding} = w_1 \Delta G_{gaussian} + w_2 \Delta G_{repulsion} + w_3 \Delta G_{hbond} + w_4 \Delta G_{hydrophobic} + w_5 \Delta G_{torsional} \quad (2.1)$$

Where $\Delta G_{gaussian}$ is the attractive term for dispersion, $\Delta G_{repulsion}$ is the repulsive term, ΔG_{hbond} describes interactions by hydrogen bonds, $\Delta G_{hydrophobic}$ depicts hydrophobic interactions and $\Delta G_{torsional}$ corresponds to the number of rotatable bonds. The value of the weights was calculated by minimizing the difference between interaction affinities (pK_d), predicted and measured, using a set of 1300 complexes from the ligand-protein database (LPDB), and a nonlinear optimization algorithm (Serio et al., 2014). LPDB contains data of high-resolution, ligand-protein complexes and known experimental binding affinities (Brooks, 2001).

Subsequently, we carried out redocking simulations on the previously predicted binding sites, both to validate binding free energies ($\Delta G_{binding}$) and the bioactive conformation of the ligands. Finally, we correlated the $\Delta G_{binding}$ calculated with the relative bitterness of the evaluated sweeteners. The relative bitterness values for SG were obtained from Hellfritsch et al. (Hellfritsch et al., 2012). It is worthy to note that the SwissDock docking server (Grosdidier et al., 2011) yielded significantly lower correlations than those obtained by Autodock Vina.

2.2.5 Mathematical modeling of the relationship between relative bitterness and the interaction parameter

The experimental ligand-receptor binding free energy is described by:

$$\Delta G = RT \times \ln(K_d) \quad (2.2)$$

Where R is the gas constant equivalent to 1.98721 [cal/K*mol], T is the temperature in Kelvin (K), and K_d is the dissociation constant. The relative bitterness (RB) of the different active compounds was obtained from the literature based on 1 mM of rubusoside (Hellfritsch et al., 2012). Thus, we express the RB values as relative K_d values:

$$K_d = \frac{K_d(\text{rubusoside})}{RB}$$

From eq 2.2, we obtain a linear relationship for RB:

$$\ln(RB) = \ln(K_d) - {}^{1}/_{RT} \times \Delta G \quad (2.3)$$

2.2.6 Analysis of protein-ligand interaction

The residues responsible for hydrogen bonding and hydrophobic interactions with SG were identified and visualized with the program LigPlot+ (Wallace et al., 1995). LigPlot+ is a graphic system that generates multiple two-dimensional (2D) diagrams of protein-ligand interactions. These analyses were carried out from 3D coordinates from lower energy poses of receptor-ligand complexes. Hydrogen bonds were identified by geometric criteria between hydrogen (H), the donor (D) and the acceptor (A). The H-A and D-A distances should be less than 2.7 Å and 3.3 Å, respectively. The D-H-A and H-A-AA angles should be greater than 90°, where AA is the atom bound to the acceptor from the amino acid. The distance and angle geometric criteria were established based on crystal structures of

protein-ligand complexes (Rezácová et al., 2008). We estimated the hydrophobic interactions of ligands at the binding site between pairs of carbon atoms whose minimum and maximum contact distance was 2.9 and 3.9 Å, respectively. Finally, intramolecular interactions are represented schematically in 2D from 3D coordinates of the protein-ligand complex.

2.2.7 Molecular dynamics simulations

Based on receptor docked conformations for stevioside and rebaudioside A, we run Conventional Molecular Dynamics (CMD) simulations using NAMD (NAnoscaled Molecular Dynamics; v 2.9) (Phillips et al., 2005). The latter allowed to relax the collision between atoms to obtain a more stable complex conformation. These SG were employed as references, considering that they are the most quantitatively important SG present in *Stevia rebaudiana* (Espinoza et al., 2014). We applied periodic boundary conditions to the system to obtain consistent behavior. We assigned a distance cutoff of electrostatic interaction of 12, which is sufficient to achieve reasonable results from the molecular dynamics calculations (Loncharich & Brooks, 1989). The particle mesh Ewald method was employed for electrostatic interactions in periodic boundary conditions with grid dimensions of 1.0 Å. The files generated for the ligand-protein complexes using the VMD 1.9 software were first inserted into a POPC lipid bilayer using VMD's "membrane" plugin (Sommer, 2013).

Then, simulations were carried out using the parameter file CHARMM 22 (Chemistry at HARvard Macromolecular Mechanics) for proteins and lipids. The energy of each system was minimized, using the Powell algorithm at constant temperature (310 K), followed by equilibration with the Langevin dynamics (Adcock & McCammon, 2006) to control the kinetic energy, temperature, and/or pressure of the system. The Langevin dynamics method follows the equation:

$$m_i \frac{d^2 x_i}{t^2} = F\{x_i(t)\} - \gamma_i m_i \frac{dx_i}{dt} + R_i(t) \quad (2.4)$$

Where F is the force, γ is the damping coefficient, m is the mass and R(t) is the frictional force.

The predicted models were refined by minimization for 2000 steps, keeping the backbone fixed the first 1000 steps, and equilibration for 18 ps. Later, ligand parameterization was accomplished using the ACPYPE web server (Fogh et al., 2005; Nilges et al., 2008). Parameterized ligands were inserted into the binding site of the protein and saved as a ligand-protein complex using VMD. Finally, the different complexes inserted in lipid membrane were minimized for 1000 steps (Supplementary figure 2-2) and then equilibrated for 10 ns in order to relax the conformation of the ligand, as well as the lateral chains of the residues of the receptor. Each equilibration trajectory was saved at 5 ps for further analysis. After the simulations, the RMSD values of alpha carbon atoms (Cα) in the receptors were calculated, using the initial respective structures as reference points in the MD trajectories; and the root mean square fluctuation (RMSF) was executed to compare the conformation of free and SG-bound proteins. The analyzed trajectories were plotted using GNUPLOT.

2.2.8 Steered molecular dynamics simulations

After the different complexes were minimized and equilibrated by CMD, we performed SMD simulations to study the unbinding process of the ligands, as well as the conformational changes of the binding sites of the modeled bitter taste receptors. To do this, the equilibrated ligand-receptor complexes were driven at constant velocity (cv), using the approach implemented in NAMD (Phillips et al., 2005). The ligands were extracted from the binding site at a constant velocity of 0.005 Å/ps by applying an external force variable to its center of mass. The force exerted on the ligand was defined as:

$$F = k\,(vt - x) \tag{2.5}$$

Where k is the spring constant (k = 7 Kcal/mol*Å) of the contraint, v is the pulling velocity (v = 0.005 Å/ps), t represents time (in ps), and x is the position of the ligand at time t. Force was applied to carbon 1 (C-1) of the aglycone part of stevioside and rebaudioside A. SMD simulations were run for 20 ps at 300 K. Unbinding directions were calculated using Tcl/Tk scripts and the information of residues was stored as a reference file. Trajectories were saved every 10 steps. Each simulation was repeated 6 times. All graphical analyses were performed using VMD 1.9 software.

2.3 Results

2.3.1 Modeling of taste receptors responsible for the bitterness of stevia

The template for the comparative modeling of hT2R14 was selected using PGenTHREADER, based on the percentage of identity and p-value. Squid rhodopsin (PDB ID: 2Z73) showed a sequence identity of 18.7% and a p-value of 2e-04 with respect to hT2R14. Meanwhile, bovine rhodopsin (PDB ID: 1U19) and opsin (PDB ID: 3DQB) showed a sequence identity of 21.6% and 20.3% with respect to hT2R4 and hT2R1, respectively; and a p-value of 6e-04, similar for both receptors. These results indicate that these transmembrane proteins - 2Z73, 1U19 and 3DQB - which belong to the class A GPCR family, are appropriate templates for predicting the 3D structure of hT2R4, hT2R14 and hT2R1 (Figure 2-2). Figure 2-2 (a to c) illustrates the loops in the extracellular regions and seven transmembrane domains, which were relaxed by molecular simulations to refine their structures.

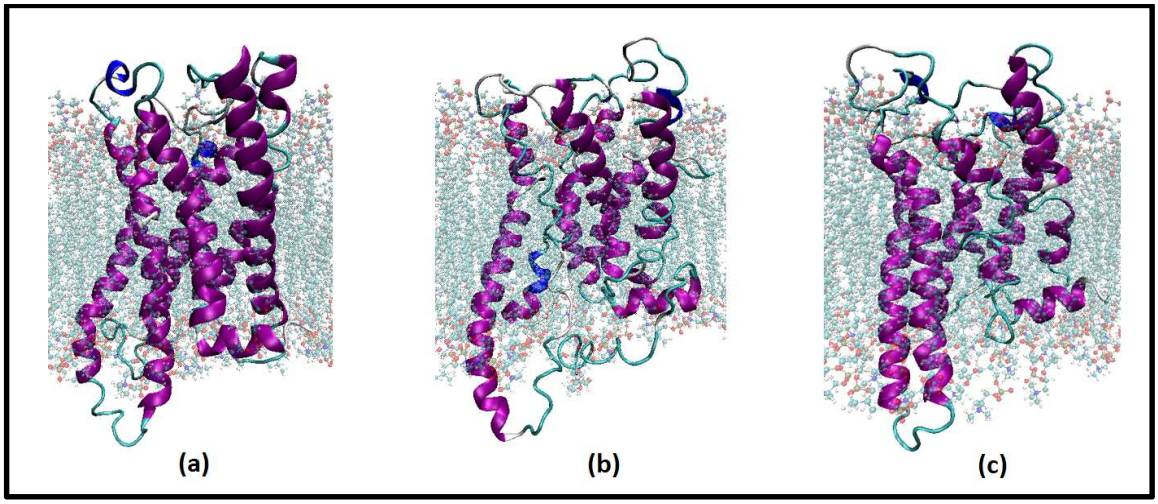

Figure 2-2: Comparative models of hT2R4 (a), hT2R14 (b) receptors, and hT2R1 (c) used as a negative control, generated by SWISS-MODEL.

We compared the structures of our homology model, generated using a single template, with the fragment modeling approach (GPCR-SSFE Database), using a suite of structure alignment techniques (TopMatch webserver) (Worth, Kreuchwig, Kleinau, & Krause, 2011; Sippl & Wiederstein, 2008). Results indicated that the structures of transmembranal

regions were similar, with a root-mean-square error superposition of 2.86 and 2.19 Å for hT2R4 and hT2R14, respectively.

Ramachandran plots (Supplementary figure 2-1) evidenced that 92.2% of the residues are in favoured regions, 4.8% in allowed regions, and 3.0% in outlier regions for hT2R4; 83.8% of the residues are in favoured regions, 12.4% in allowed regions, and 3.8% in outlier regions for hT2R14 and 83.3%, 9.0%, and 7.6%, respectively for hT2R1. PROCHECK analyses of the hT2R4, hT2R4 and hT2R1 models yielded overall average G factors of -1.08, -1.22 and -1.27, respectively. Overall quality factors were 81.395, 66.809 and 69.585 for hT2R4, hT2R4 and hT2R1, respectively.

2.3.2 Molecular docking and binding site characterization

Molecular docking showed that the calculated binding free energies ($\Delta G_{binding}$) negatively correlated with SG bitterness intensity (Hellfritsch et al., 2012) (Figure 2-3). The correlation coefficient for the 10 evaluated SG with hT2R4 and hT2R14 was -0.95 and -0.89, respectively. On the other hand, we found a poor correlation with hT2R1 (R = -0.50).

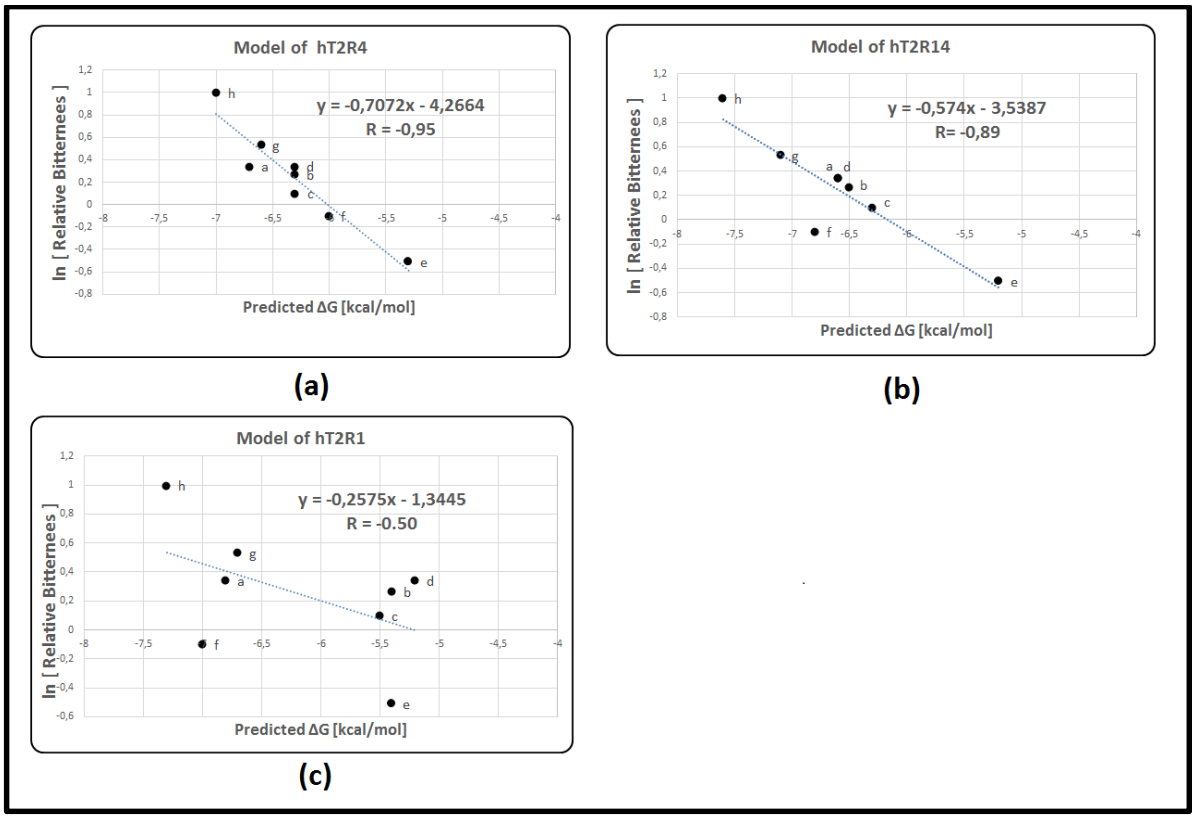

Figure 2-3: Relationship between relative bitterness and binding free energy of SG with bitter taste receptors. Steviol glycosides (SG) were inserted into the binding sites of hT2R4 (a), hT2R14 (b) receptors, and hT2R1 (c), used as a negative control. Data correspond to: (a) stevioside; (b) reb A; (c) reb B; (d) reb C; (e) reb D; (f) steviolbioside; (g) dulcoside A; and (h) rubusoside. The relative bitterness data for SG were obtained from the study by Hellfritsch et al (Hellfritsch et al., 2012) [3].

Rubusoside, the bitterest SG, has a lower $\Delta G_{binding}$ than rebaudioside D, for both receptors (Figure 2-3a and 3b); this could result from their different structural characteristics, as rubusoside and rebaudioside D contain 2 and 5 glucose residues, respectively. On the other hand, those SG that contain rhamnose, *e.g.* dulcoside A and rebaudioside C, have lower ΔGs for hT2R14.

Table 2-2 identifies those amino acids responsible for hydrogen bonding and hydrophobic interactions in hT2R4 and hT2R14 with SGs. The fact that 43 and 75%, of the aminoacidic residues responsible for these interactions in the receptors are polar suggests that the hydrophilic nature of the pocket favors the binding of these sweeteners with the bitter taste receptors.

Table 2-2: Binding free energy and binding sites of steviol glycosides (SG) for hT2R4 and hT2R14 bitter taste receptors.

Compound[a]	$\Delta G_{binding}$ for hT2R4 (Kcal/mol)	$\Delta G_{binding}$ for hT2R14 (Kcal/mol)	Binding site in hT2R4	Binding site in hT2R14	Relative bitterness at 1 mM[b]	xlogP[c]
1	-6.7	-6.6	Leu 61, Asn 65, Thr 66, Phe 69, Asn 73, Glu 75, Val 78, Phe 84	Ser 155, Ile 156, Asn 157, Ser 167, Asp 168, Ser 170, Arg 174, Tyr 240, Ser 246, Phe 247, Glu 258	1.4	-1.2
2	-6.3	-6.5	Asn 65, Thr 66, Leu 80, Phe 84	Ser 167, Asp 168, Ser 170, Tyr 240, Ser 246, Phe 247	1.3	-2.8
3	-6.3	-6.3	Asn 65, Thr 66, Phe 84, Ser 77	Ser 155, Ile 156, Lys 163, Asp 168, Arg 174	1.1	-1.0
4	-6.3	-6.6	Asn 65, Thr 66, Leu 80, Phe 84	Ser 167, Asp 168, Ser 170, Tyr 240, Ser 246, Phe 247	1.4	-2.3
5	-5.3	-5.2	Val 78, Leu 80, Ser 81	Arg 160, Ser 169, Thr 173	0.6	-4.4
6	-6.3	-7.2	Thr 66, Glu 75, Val 78, Leu 80	Ser 155, Asn 157, Gly 158, Ser 246, Glu 258	-	-2.8
7	-6.5	-6.5	Asn 65, Thr 66, Asn 73, Glu 75, Ser 77, Val 78	Ser 167, Asp 168, Ser 170, Tyr 240, Ser 246, Phe 247	-	-2.7
8	-6.0	-6.8	Thr 66, Glu 75, Ser 77	Asn 86, Ile 152, Ile 156, Arg 160, Asp 168, Arg 174	0.9	0.6
9	-6.6	-7.1	Asn 65, Thr 66, Phe 69, Asn 73, Glu 75, Ser 77	Ser 155, Ile 156, Asn 157, Arg 160, Ser 167, Asp 168, Tyr 240, Ser 246, Phe 247	1.7	-0.7
10	-7.0	-7.6	Leu 61, Phe 69, Asn 65, Thr 66, Asn 73, Ser 77, Val 78, Phe 83, Phe 84	Ser 155, Asn 157, Arg 160, Ser 167, Asp 168, Ser 169, Tyr 240	2.7	0.4

[a]Compound number refers to structures given in Figure 2-1 and Table 2-1. [b]Relative bitterness values extracted from Hellfritch et al. (2012) (Hellfritsch et al., 2012). [c] Values extracted from the PubChem database (National Center for Biotechnology Information, 2004).

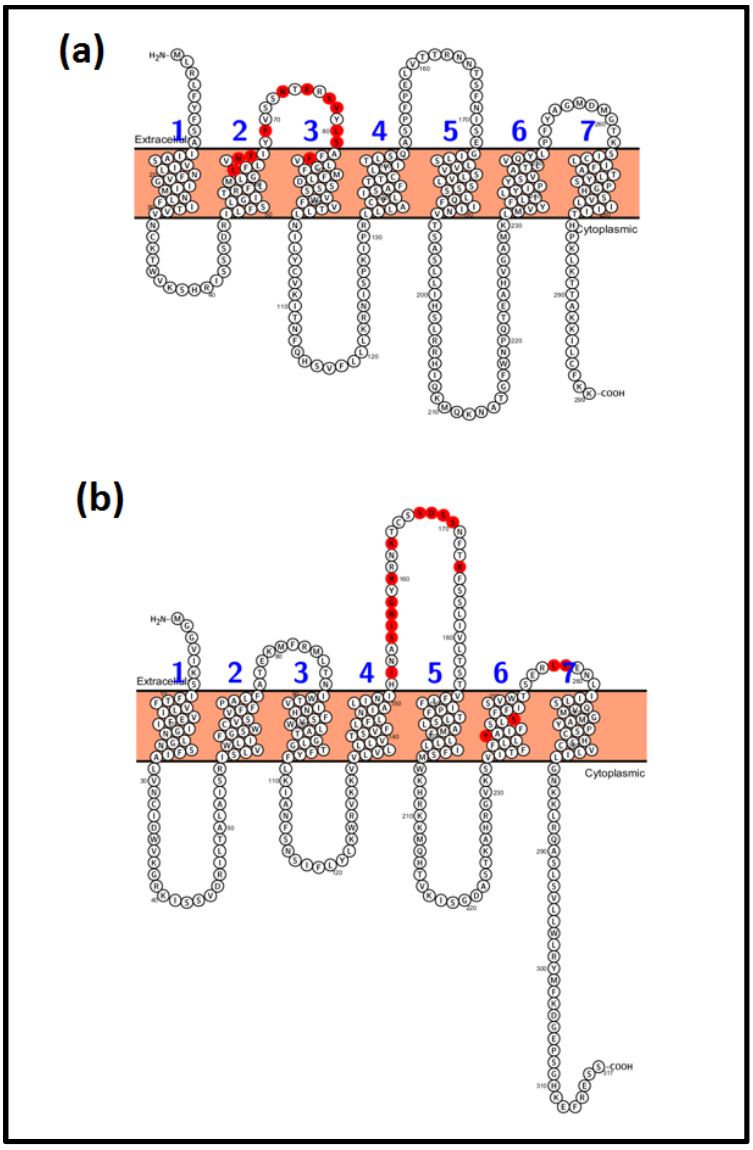

Figure 2-4: Two-dimensional representation of hT2R4 (a) and hT2R14 (b) amino acid sequence. The potential binding sites of SG are indicated by red circles.

Figures 2-4 and 2-5 depict the potential binding sites of SG and the pose of docked stevioside in the receptors, respectively. The binding cavity in these receptors was mainly composed by transmembrane regions – with moderate participation from the extracellular region – which interact with monosacharides bound to the C-13 and C-19 of SG (Figure 2-1). The surface of the hT2R4 and hT2R14 binding cavity is 2017 and 3430 $Å^2$, respectively.

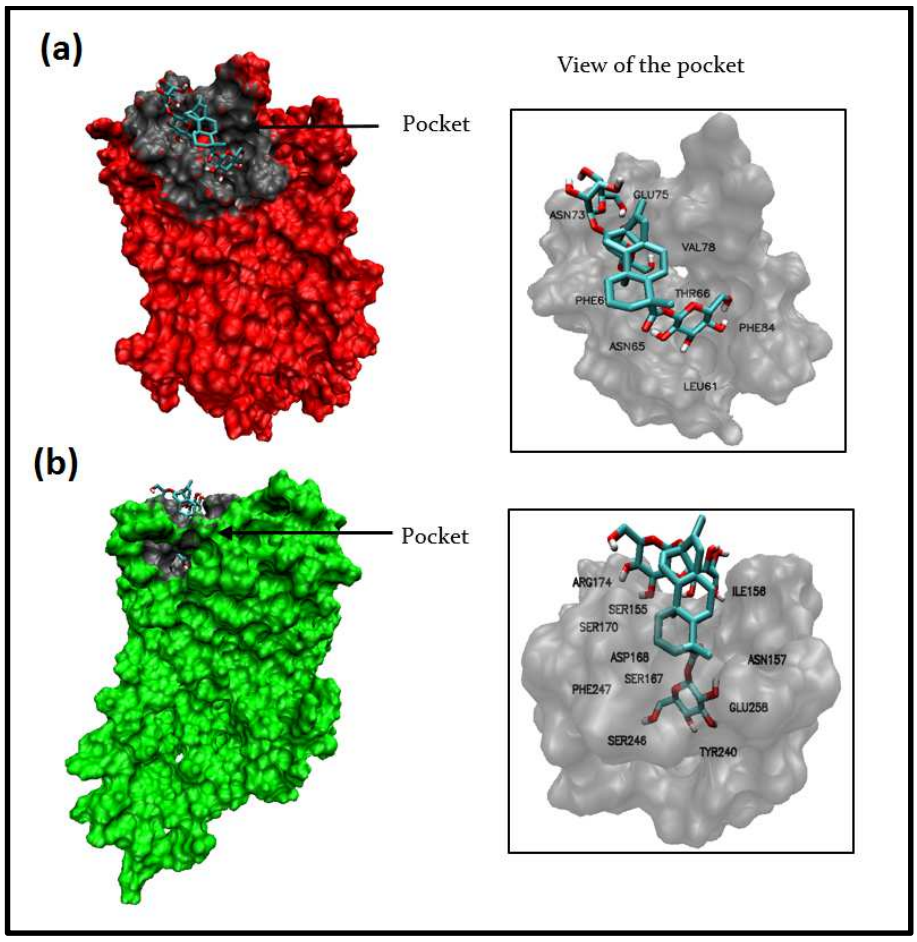

Figure 2-5: Snapshots of VMD showing the potential binding site and pose of docked stevioside on hT2R4 (a) and hT2R14 (b).

Docking of different complexes allowed to identify the most representative modes of SG binding to the bitter taste receptors (Figures 2-6 and 2-7). SG differ both in their orientation and conformation, selectively interacting with specific residues at the binding site. In addition, the interactions of SG with the binding pocket of bitter taste receptors are governed by both hydrogen bonding and hydrophobic interactions (Mayank & Vikas, 2015). On the one hand, oxygen and nitrogen atoms from residues of the binding pocket interact with the OH groups of monosaccharides bound at positions C-13 and C-19 of SG by hydrogen bonds. On the other, the carbons of the aglycone part of SG and of apolar residues at the binding site interact with each other through hydrophobic interactions.

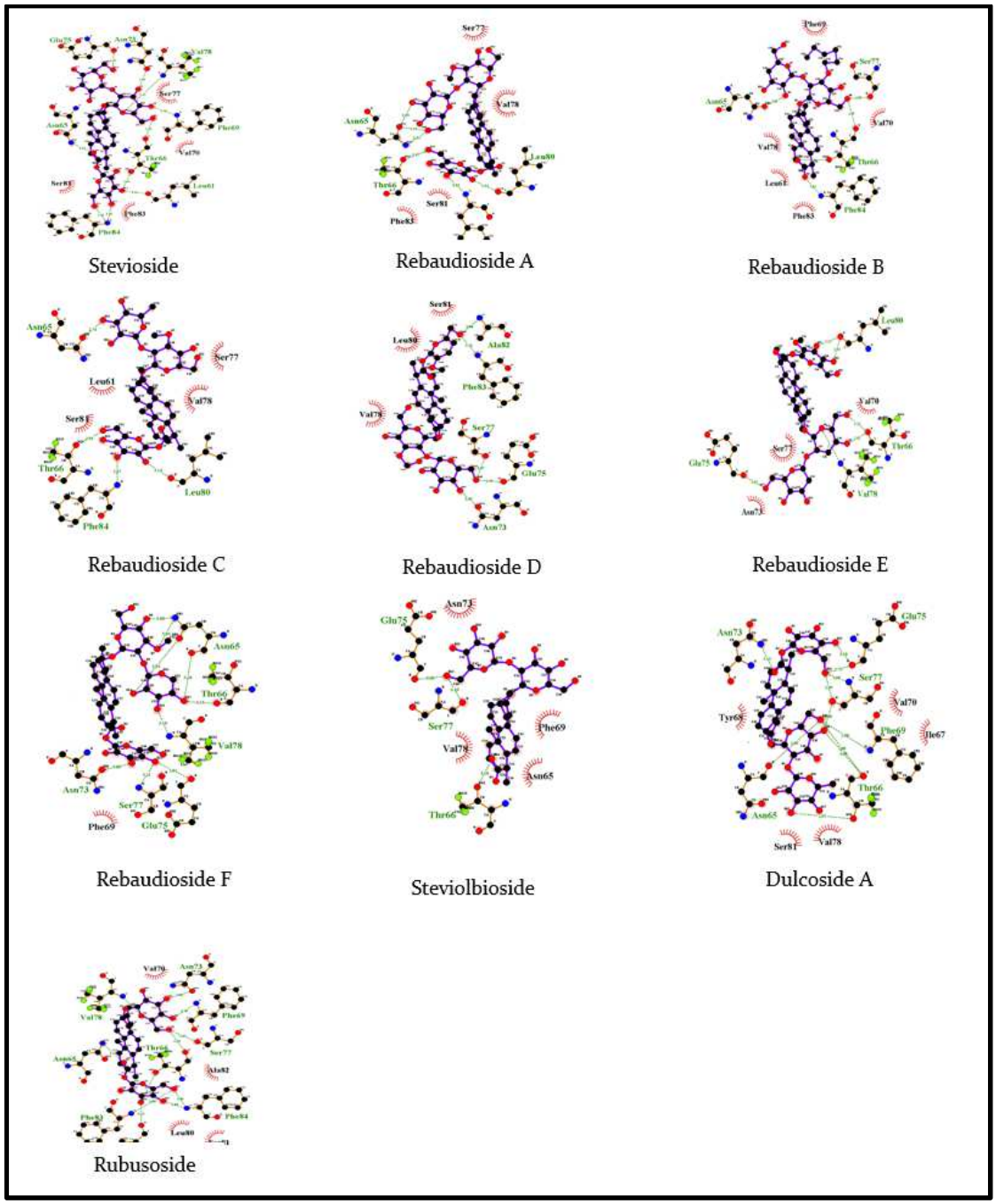

Figure 2-6: Binding pattern of SG with the hT2R4 bitter taste receptor. The amino acids responsible for the hydrogen bonds and hydrophobic interactions are represented by three letter codes in green and black, respectively. Carbon, oxygen and nitrogen atoms are indicated by closed black, red and blue circles, respectively.

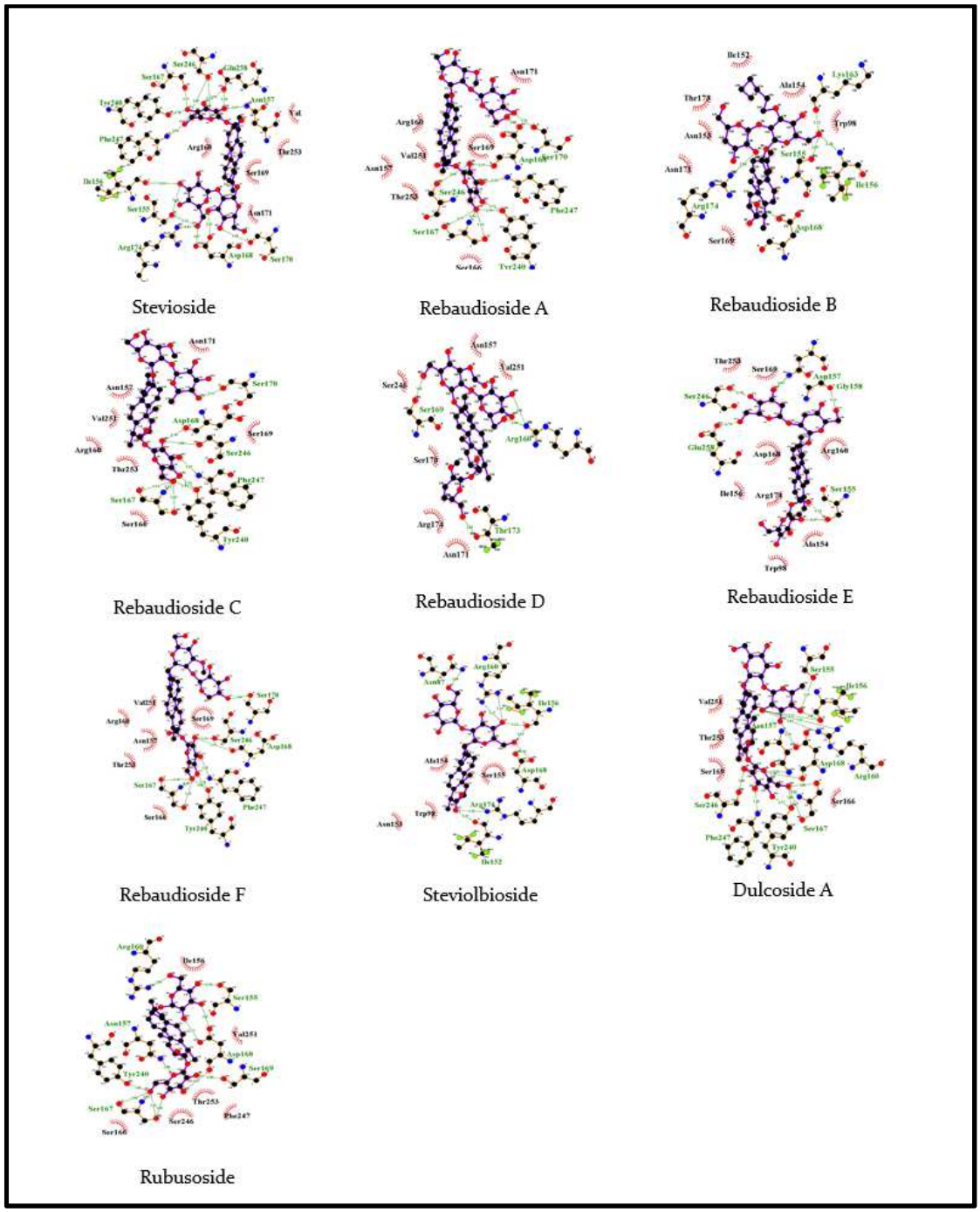

Figure 2-7: Binding pattern of SG with the hT2R14 bitter taste receptor. The amino acids responsible for the hydrogen bonds and hydrophobic interactions are represented by three letter codes in green and black, respectively. Carbon, oxygen and nitrogen atoms are indicated by closed black, red and blue circles, respectively.

2.3.3 Ligand-receptor molecular dynamics simulations

Figure 2-8 shows all the conformations of the hT2R4 and hT2R14 receptors bound to stevioside or to rebaudioside A after 10 ns of equilibration. RMSD values of the receptor bound to the ligand were between 3.0 and 4.0 Å (Supplementary figure 2-3). On the other hand, RMSD values of the ligand bound to the receptor were between 2.0 and 3.0 Å (Supplementary figure 2-4). Accordingly, it can be inferred that the overall conformations of receptors, as well as of ligands, were stable.

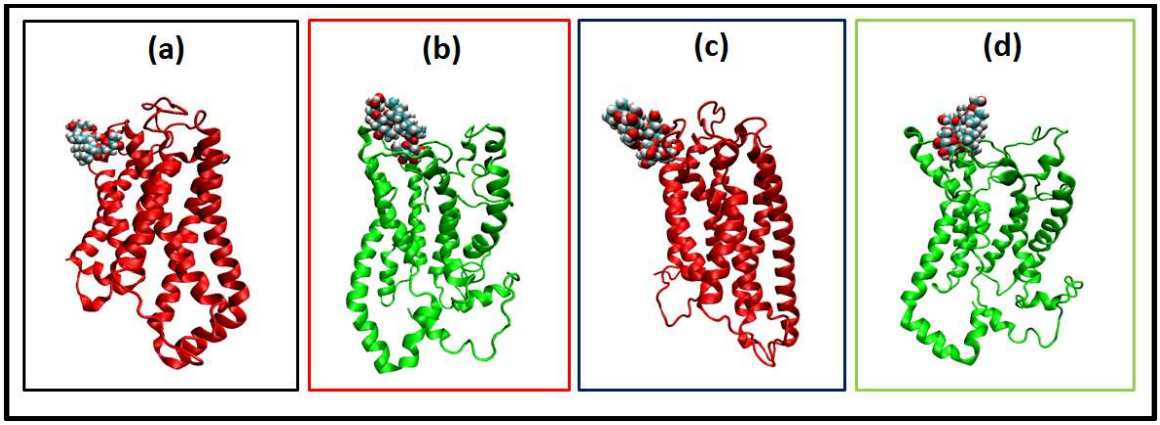

Figure 2-8: Snapshots from Visual Molecular Dynamics showing the stevioside (c and d) and rebaudioside A (e and f) poses on hT2R4 (red color) and hT2R14 (green color) bitter taste receptors.

RMSD calculations allowed to estimate the global stability of the conformations, but do not consider the local region of proteins, particularly the binding site. Therefore, we decided to analyze some physical parameters for this purpose, including the number of hydrogen bonds and RMSF. The results evidenced that, on average, the number of hydrogen bonds of both ligands with binding site residues is between 3 and 4 (Supplementary figure 2-5), and fluctuations are less than 1.5% of RMSF (Figure 2-9). In general, the conformations of the different protein-ligand complexes were stable (Figures 2-8a and b).

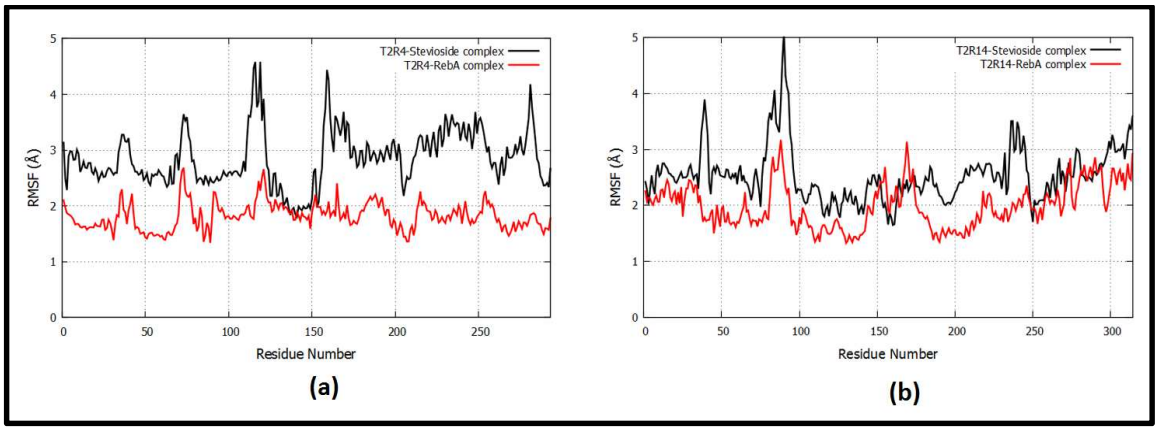

Figure 2-9: Root mean square fluctuation value at Cα carbon of hT2R4 (a) and hT2R14 (b) residues bound to stevioside (black line) and rebaudioside A (red line).

2.3.4 Steered molecular dynamics simulations

After inspection of the SG binding sites on the receptors, and a comparative analysis of SG-hT2R interactions, we run SMD simulations at constant velocity to extract SG – stevioside and rebaudioside A – from the binding site in order to better understand the different affinities of both ligands. Stevioside and rebaudioside A were stabilized, during the unbinding process, at 3 and 1 ps for hT2R4 and hT2R14, respectively. Moreover, the force peak employed to extract stevioside from the binding site was greater than the one required for rebaudioside A, with values of 3747 and 2057 pN; and 1647 and 1279 pN for hT2R4 and hT2R14, respectively (Figure 2-10).

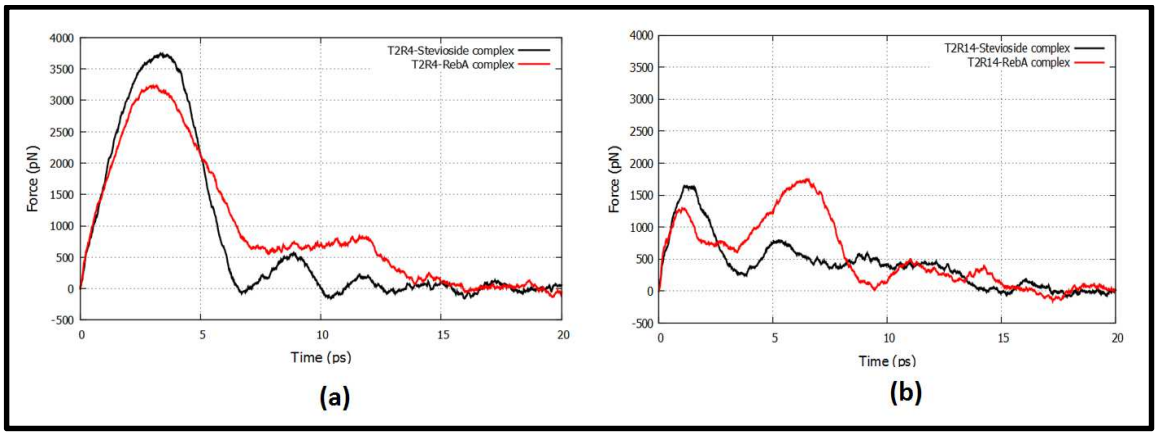

Figure 2-10: Evolution of the pulling force exerted on stevioside (black line) and rebaudioside A (red line) during unbinding from hT2R4 and hT2R14 pockets.

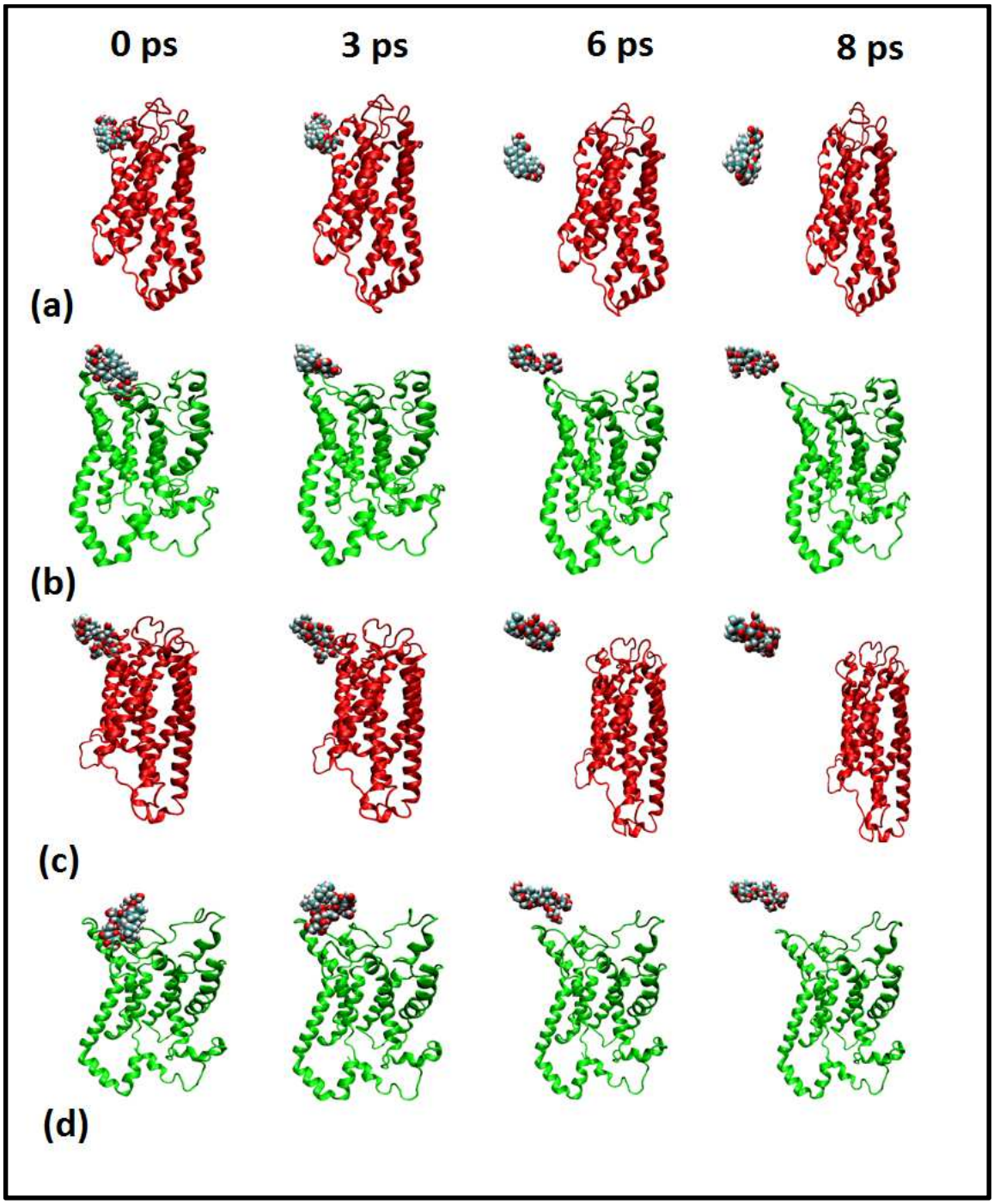

Figure 2-11: Images of the stevioside (a and b) and rebaudioside A (c and d) unbinding process from the hT2R4 (red color) and hT2R14 (green color) binding sites during 8 ps simulations.

Figure 2-11 illustrates the different phases of the unbinding process. After equilibration inside the binding pocket, the D-glucopyranosyl C-19 hydroxyl group of stevioside and rebaudioside A disentangles from the Tyr 68 – Ser 81 extracellular loop of hT2R4, and the His 151 – Thr 184 of hT2R14, making its way to the binding pocket entrance. RMSF values indicate that these extracellular loops are highly flexible during ligand unbinding. In particular, Ser 71 and Ser 72 residues for hT2R4 - and Ser 155 and Ser 170 for hT2R14 - correspond to peaks of RMSF fluctuations. Furthermore, hT2R4 experiences bigger conformational changes than hT2R14 in the dissociation of the ligand (Supplementary figure 2-6).

2.4 Discussion

Hellfritch et al. proposed that the bitter taste of stevia is promoted by the structural characteristics of SG - e.g. the sugar content in their structures - and the nature of the SG binding cavity of hT2R4 and hT2R14 receptors (Hellfritsch et al., 2012). In the present study, we predicted the 3D structure of the hT2R4 and hT2R14 bitter taste receptors, and elucidated the interaction patterns with SG.

Even though Worth et al. suggested that building comparative models of GPCR using transmembrane fragments from multiple templates might lead to more accurate results than homology modeling, using a single template (Worth et al., 2011), we found out that both approaches were very similar (Supplementary figure 2-7). The latter confirms that homology modelling using a single template is an appropiate tecnique to build this type of receptors.

The resulting models share the same structural pattern – seven transmembrane helices and the presence of loops in both, the extracellular and intracellular regions – similar to other previously modeled bitter taste receptors (Upadhyaya et al., 2010; Pydi et al., 2012; Marchiori et al., 2013). Unlike sweet taste receptors, these proteins have a small extracellular region – around 60 amino acid residues; thus, it is likely that these sweeteners bind to both, the extracellular and the transmembrane regions.

Previous studies have shown that the most divergent sequences of hT2Rs are the extracellular loops, which affect the selectivity of various bitter taste receptors, such as

hT2R3, hT2R7, hT2R10, hT2R13 and hT2R61 (Ji et al., 2014; Pronin et al., 2004). Moreover, the intracellular loops play a critical role in the activation of these receptors (Pydi et al., 2014), as the conformational change in these regions allows for the formation of bridges between transmembrane domains, stabilizing the inactive state of the receptor.

We determined, by molecular docking, that the calculated binding free energies ($\Delta G_{binding}$) negatively correlate with the bitterness intensity of different SG. This strong correlation confirms the potential binding sites predicted for the SG to hT2R4 and hT2R14. Furthermore, the poor correlation obtained for hT2R1 suggests that SG only bind to hT2R4 and hT2R14. Indeed, the binding site identified on hT2R1 is not appropriate to accommodate this type of sweeteners.

It is possible that the SG binding site identified on hT2R1 was mainly composed by transmembrane regions, while the binding pocket of hT2R4 and hT2R14 included both, extracellular regions and a moderate participation of the transmembrane regions; thus, receptor activation by these sweeteners – similar to other water soluble molecules, such as phenylthiocarbamide, quinine and caffeine – might start with a marked intervention of the extracellular regions (Floriano et al., 2006).

In addition, our docking results confirm previous sensory studies reporting that rubusoside is the bitterest SG, and rebaudioside D is the least bitter (Hellfritsch et al., 2012). Therefore, this suggests that the affinity of SG to bitter taste receptors, as well as the differences in bitterness intensity and the reported activation thresholds (Hellfritsch et al., 2012), could be due to the steric characteristics of SG and their binding site architecture (Brockhoff et al., 2010).

The SG with more sugars have less affinity for bitter taste receptors, since the size of the receptor binding cavity is limited. In fact, the surface of the hT2R14 binding cavity is greater than that of hT2R4, allowing larger SG to adequately bind. This characteristic could explain the capacity of hT2R14, as well as hT2R10 and hT2R46, to respond to a wide variety of different bitter compounds (Maik Behrens et al., 2004; Meyerhof et al., 2010).

Furthermore, the high affinity of rhamnose-containing SG, rebaudioside C and dulcoside A, to hT2R14 does not result only from the total amount of monosaccharides, but also from the type of sugars present in their structure. This confirms the results of Hellfritsch et al. in that the activation threshold of hT2R14 by rhamnose-containing SG are lower than for other SG (Hellfritsch et al., 2012).

Regarding potential SG binding sites on these receptors, besides those recently identified in hT2R4 by Singla & Jaitak, 2016, *i.e.* Phe 69, Phe 168, Phe 169, Ile 170, Glu 172, Met 259, Gly 260 and Lys 262, we showed that SG lies in the same binding cavity sharing a set of amino acids, including Asn 65, Thr 66, Val 78, Phe 84 for hT2R4; and Ser 167, Asp 168, Ser 246 for hT2R14. Activation of these receptors by SG may result from the stimulation of residues, such as Val 78 and Phe 84 for hT2R4; and Ser 167 and Asp 168 for hT2R14, at a first, extracellular binding site by monosaccharides at the C-13 position; and the allosteric modulation of a second, transmembraneous binding site by the monosaccharidic moieties of SG. This multipoint stimulation model has also been suggested for sweet taste receptors but, unlike bitter taste receptors, the sugars at the C-13 and C-19 positions only stimulate residues at the extracellular region (Mayank & Vikas, 2015).

In addition, SG interactions with the binding pockets of the hT2R4 and hT2R14 bitter receptors are governed by hydrogen bonding and hydrophobic interactions. The binding mechanism of SG mediated by hydrogen bonds has also been identified on sweet taste receptors (Mayank & Vikas, 2015; Shallenberger & Acre, 1967), due to the sugars present in these sweeteners. On the other hand, the hydrophobic interactions between aminoacidic residues and both components of SG could further promote their stability at the binding site. Moreover, SG could simultaneously trigger sweetness and bitterness due to the polarization of their sugars and their proximity - probably 3 - 4 Å - to the binding sites of sweet and bitter taste receptors (Birch & Mylvaganam, 1976).

The analysis of the SG unbinding process by SMD unravelled the difference in ligand affinity between both receptors. Indeed, the peak applied force for stevioside was greater than for rebaudioside A, as stevioside forms more hydrogen bonds with the residues of both receptors (Figures 2-6 and 2-7). Moreover, we propose that the extracellular loops Tyr

68 – Ser 81 on hT2R4, and His 151 – Thr 184 on hT2R14 are responsible for anchoring stevioside and rebaudioside A to their respective binding sites. Furthermore, the SG coupling process possibly induces some changes in the structure of both receptors, allowing for the formation of hydrogen bonds between the transmembrane regions and, thus, stabilizing the active conformations of the receptors (Singh et al., 2011; Tan et al., 2012).

In conclusion, in this work we constructed a comparative model for the hT2R4 and hT2R14 receptors using the 3D structure of 1U19 and 2Z73, respectively, which was subsequently validated using a Ramachandran plot. Furthermore, we predicted the intensity of bitterness of the active compounds in stevia, from their binding free energy ($\Delta G_{binding}$) with the modeled bitter taste receptors. Calculated ΔGs negatively correlated with reported bitterness of SG, that is, the more negative the $\Delta G_{binding}$ between the sweetener and the receptor, the greater the bitterness intensity.

Finally, bitterness intensity of SGs resulted from the following features: 1) the presence of transmembrane regions at the binding cavity of hT2R4, and hT2R14, which favors the interactions with SG by hydrophobic contact; 2) the ability to form hydrogen bonds with amino acids at the binding pocket due to the presence of sugars at the C-13 and C19 positions; and 3) the difference in the total number and type of monosaccharides present in their structures.

Therefore, the binding model of SG with hT2R4 and hT2R14 taste receptors developed here could be useful to propose strategies to reduce unwanted attributes, such as bitterness, from this type of sweeteners.

3.6 Acknowledgments

We are grateful to Javier Sainz, Prodalysa Inc. for recommendations and suggestions during the course of this work; to Francisco Saitúa and Martín Cárcamo for their constructive comments on the manuscript; and to the anonymous referees who provided valuable feedback to improve the final manuscript. Waldo Acevedo was supported by a doctoral fellowship from the Chilean National Council of Scientific and Technological Research (CONICYT).

3. IDENTIFYING THE INTERACTIONS BETWEEN NATURAL, NON CALORIC SWEETENERS AND THE HUMAN SWEET RECEPTOR BY MOLECULAR DOCKING

Waldo Acevedo, César A. Ramírez-Sarmiento, and Eduardo Agosin

Submitted to *Journal of Food Chemistry,* Manuscript ID: FOODCHEM-S-17-0923.

Abstract

Natural sweeteners, such as stevia, thaumatin and monellin, exert their sweet taste by specifically binding to sweet taste receptors. However, the molecular basis of their sweetening power remains to be ascertained. In the present study, we characterized the interaction of natural, non-caloric sweeteners - from glycosylated terpenoids (GTs) to sweet proteins - with the sweetness receptor, at the molecular level. The binding free energy between hT1R2-hT1R3 and sweeteners of different families shows a strong correlation with their sweetness intensity for both, small sweeteners (r = -0.89) and sweet proteins (r= -0.96). The correlation is further improved and generalized throughout all families of sweeteners evaluated, when EC_{50} values are used instead of relative intensities. Altogether, these results contribute to a better understanding of the sweetness perception of these sweeteners, and promote the use of simple docking studies for better prediction – and management – of resulting sweetness in foods and beverages.

3.1 Introduction

Chronic, non-communicable diseases are the leading cause of death worldwide, claiming the lives of more than 38 million people each year (World Health Organization, 2013). These include cardiovascular accidents, diabetes and obesity, mainly resulting from excessive sugar consumption (Malik et al., 2010). A measure of prevention of these types of diseases has been the commercial development of non-caloric sweeteners to replace sucrose (Shankar et al., 2013; Hu & Malik, 2010).

Commercially available non-caloric sweeteners can be classified as natural and artificial. Among the latter are saccharin, cyclamate and aspartame, among others, which have been

widely used in food manufacturing because of their high sweetening power and similar taste to sucrose (DuBois & Prakash, 2012). On the other hand, the demand for non-caloric sweeteners of natural origin, such as stevia and monk fruit (*Luo Han Guo*), both glycosylated isoprenoids, has significantly increased. In particular, stevia, with a sweetening power 300 times greater than sugar, is a product that has reached an important place in the family shopping basket as a tabletop sweetener and additive for the production of various food products (Prakash et al., 2014). Furthermore, we also find sweet proteins, including brazzein, monellin and thaumatin, with the latter being the most commercially demanded due to a sweetening power 3000 times greater than sugar on a weight basis, as well as its ability for masking off-taste and improving the taste profile of foods and beverages (Kant, 2005).

Natural – and artificial – sweeteners can activate the sweet taste receptor (Prakash et al., 2014). This taste receptor is a heterodimer belonging to the class C family of G-protein coupled receptors (GPCRs) and is composed of the hT1R2 and hT1R3 subunits. In structural terms, the receptor contains 3 domains: an important N-terminal extracellular region, composed of the "Venus Fly Trap" (VFT) domain and a cysteine-rich domain (CRD); and a C-terminal transmembrane domain. Although the three-dimensional structure of the sweetness receptor has not been elucidated yet, it is still possible to build comparative models to study the structure-activity relationship of sweeteners. In fact, three-dimensional models of the sweetness receptor have already been built, using the crystal structure of the metabotropic glutamate receptor 1 (or mGluR1) (Temussi, 2002). This receptor was used as template for comparative modeling because i) it belongs to the GPCR family; ii) the residues of the VFT domain cavity are conserved in both receptors; and iii) its activation mechanism is similar to that of the sweet taste receptor (J.-P. Pin, Galvez, & Prézeau, 2003).

Functional expression studies of the taste receptor and molecular docking demonstrated that the heterodimer hT1R2/hT1R3 is activated by most sweeteners upon binding to the receptor's VFT domain (Liu et al., 2012; Masuda et al., 2012). Given the structural similarity that steviol glycosides (SGs) have with traditional sweeteners – like sugar – it is

assumed that they interact with the same binding site (Zhang et al., 2010). These observations provide an excellent scenario for understanding the molecular basis of the differences in sweetness perception.

The first attempts to understand the structure-taste relationships of these molecules were made by identifying groups of atoms and interactions responsible for the sweet taste properties of several molecules. More recently, Nofre and Tinti developed the Multipoint Attachment Model (MPA) (Nofre & Tinti, 1996), a more elaborated theory for the taste of any molecule, including simple sugars and artificial sweeteners. This model assumes the presence of at least eight fundamental recognition points or sites, namely B, AH, XH, G1, G2, G3, G4, and D, that bind to a receptor through elementary ionic, hydrogen bonding and steric interactions. Morini et al. employed the MPA model as a guide in constructing a pseudoreceptor model based on a training set of 24 compounds, including simple sugars and artificial sweeteners (Bassoli et al., 2002). With this strategy, sweetness intensity was correlated with the binding affinity of sweeteners into the receptor, obtaining a correlation coefficient of 0.985 between calculated binding energies and experimentally measured sweetness intensities.

In a previous study, we demonstrated that the binding free energies ($\Delta G_{binding}$) of several SGs with the hT2R4 and hT2R14 bitter taste receptors, calculated through simpler and computationally inexpensive molecular docking simulations, have high negative correlations with the reported bitterness of these molecules, with correlation coefficients between 0.89-0.95 (Acevedo et al., 2016). Furthermore, interactions of SGs with the binding pockets of these bitter taste receptors could be represented by the MPA model (Nofre & Tinti, 1996), with their interaction points within the binding site being governed by hydrogen bonding and hydrophobic interactions.

Here, we extend our model to predict the sweetening capacity of different families of natural sweeteners - from glycosylated terpenoids, e.g. stevia or monk fruit, to sweet proteins, e.g. monellin or thaumatin - using molecular simulations. To this end, we built a comparative model of the hT1R2 and hT1R3 subunits using the metabotropic glutamate receptor as a template. Once these models were obtained, we identified the potential

binding sites and estimated the binding free energies and interactions of 29 different sweeteners via molecular docking. The calculated binding free energies were successfully correlated with their relative sweetness reported in the literature. Altogether, our results provide a simple framework for computationally predicting the sweetness perception of natural and artificial sweeteners.

3.2 Materials and methods

3.2.1 Template selection

The amino acid sequences of the homologous hT1R2 and hT1R3 receptor subunits, including both the VFT domain and the CRD, were retrieved from UniProtKB (Access Code: Q8TE23 and Q7RTX0, respectively). The template was selected based on the e-value of the BLAST search and its sequence identity with both hT1R2 and hT1R3. Based on these criteria, the metabotropic glutamate receptor 3 o mGluR3 (PDB: 2E4U), which belongs to the class C family of GPCRs, was used as a template to model hT1R2 and hT1R3.

3.2.2 Modeling of sweet taste receptor

We built comparative models for the hT1R2 and hT1R3 subunits, using the SWISS-MODEL tool of the EXPASY server and chain A from the crystal structure of 2E4U as template (SIB Swiss Institute of Bioinformatics and the Biozentrum & der Universität Basel, 2003). Subsequently, we assessed the stereochemical quality of the models using Ramachandran plot (RAMPAGE), PROCHECK (Overall quality factor) and QMEAN (Lovell et al., 2003). These models were visualized and rendered using the Visual Molecular Dynamics 1.9 (VMD) software (Humphrey et al., 1996). Subsequently, we built a hT1R2-hT1R3 heterodimeric complex model (Supplementary figure 3-3), based on the crystal structure of the mGluR3 dimer published by Muto et al (Muto et al., 2007).

The resulting model of the heterodimeric complex was subjected to cycles of energy minimization until convergence and equilibration for 10 nanoseconds, to relax the conformation of side chains and prevent conformational tension generated by the

homology model. All calculations were performed using NAMD (NAnoscaled Molecular Dynamics, version 2.9). Then, structural superposition of the starting and final conformations using TopMatch was carried out (Sippl & Wiederstein, 2012).

3.2.3 Preparation of ligands

Sweeteners from different families were used as ligands: six simple sugars (glucose, galactose, fructose, xylose, sucrose and tagatose), three artificial sweeteners (sucralose, saccharin, and aspartame) and several natural sweeteners (different isomers of monatin, glycyrrhizin, mogroside V, active compounds of stevia and sweet proteins) (Figure 3-1). The three-dimensional structure of these compounds was obtained from the PubChem database in SDF file format, except for sweet proteins thaumatin, brazzein, monellin and neoculin, whose structures were extracted from the Protein Data Bank using the PDB IDs: 1THW, 1BRZ, 1FA3 and 2D04, respectively. Non-protein ligands were converted into mol2 format using the program OpenBabel v2.3.1 and visually checked to correct structural errors (O'Boyle et al., 2011).

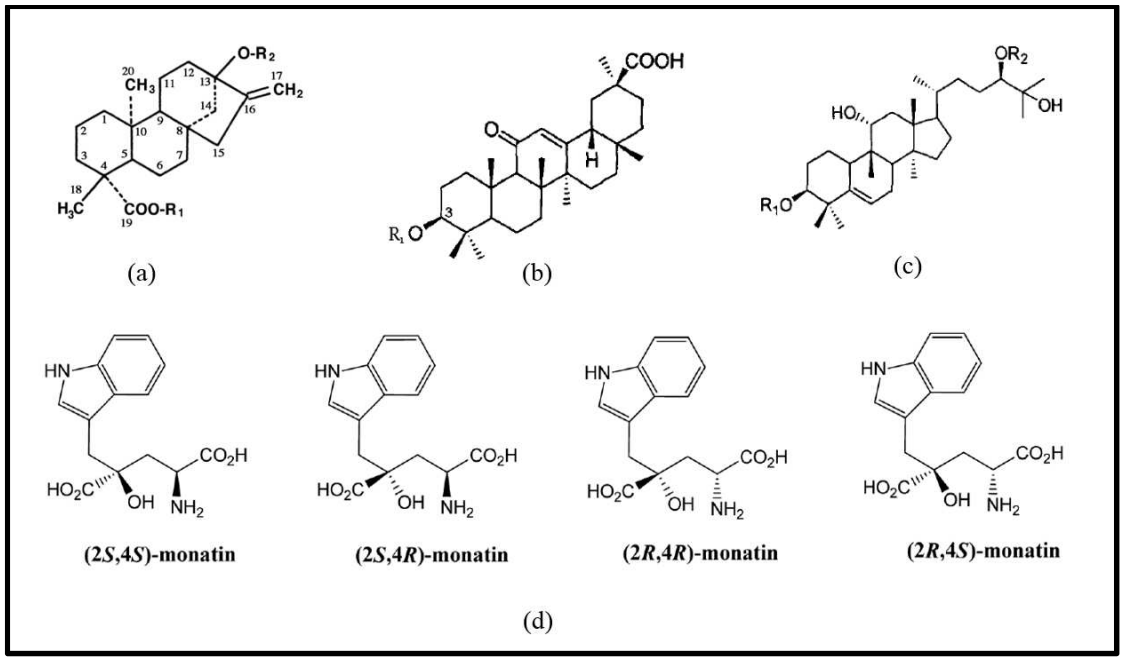

Figure 3-1: Chemical structures of (a) steviol glycosides (SG), (b) glycyrrhizin, (c) mogroside V and (d) four stereoisomers of monatin. R_1 and R_2 referred to in Table 3-1.

Table 3-1: Chemical structure of glycosylated terpenoids[a]

compound	R_1	R_2
Glycyrrhizin (n)	$\beta-glcA-\beta-glcA$	
Mogroside V (o)	$\beta-glc-\beta-glc$	$(\beta-glc)_2-\beta-glc-$
Stevioside (p)	$\beta-glc-$	$\beta-glc-\beta-glc-$
Rebaudioside A (q)	$\beta-glc-$	$(\beta-glc)_2-\beta-glc-$
Rebaudioside B (r)	$H-$	$(\beta-glc)_2-\beta-glc-$
Rebaudioside C (s)	$\beta-glc-$	$(\beta-glc)_2-\alpha-rha-$
Rebaudioside D (t)	$\beta-glc-\beta-glc-$	$(\beta-glc)_2-\beta-glc-$
Rebaudioside E (u)	$\beta-glc-\beta-glc-$	$\beta-glc-\beta-glc-$
Rebaudioside F (v)	$\beta-glc-$	$(\beta-glc)_2-\alpha-xyl-$
Steviolbioside (w)	$H-$	$\beta-glc-\beta-glc-$
Dulcoside A (x)	$\beta-glc-$	$\beta-glc-\alpha-rha-$
Rubusoside (y)	$\beta-glc-$	$\beta-glc-$

[a] Compounds n, o and p - y are referred to in Figure 3-1b, 3-1c and 3-1a, respectively. Glc, D-glucopyranosyl; rha, L-rhamnopyranosyl; xyl, D-xylopyranosyl; GlcA, glucopyranosiduronic acid

3.2.4 Molecular docking of "sweetener – sweet taste receptor"

We first identified the binding interface between hT1R2-hT1R3 heterodimeric complex and the sweet proteins, using the ClusPro 2.0 docking protein-protein web server (Comeau at al., 2004). The best docking poses were selected based on the lowest energy value and visualized using VMD software (Humphrey et al., 1996). Calculation of the electrostatic potential on the contact surface was performed using the APBS software (Mirzadeh, Theillard, Helgadóttir, Boy, & Gibou, 2013). Subsequently, we used the PRODIGY web server to predict $\Delta G_{binding}$ of different protein-protein complexes based on their structural properties of the complexes (Xue at al., 2016; Vangone & Bonvin, 2015), as follows:

$$\Delta G_{binding} = w_1 IC_{charged/charged} + w_2 IC_{charged/apolar} + w_3 IC_{polar/polar} - w_4 IC_{polar/apolar} + w_5 NIS_{apolar} - w_6 NIS_{charged} - 15.9433 \quad (3.1)$$

Where $ICs_{x/y}$ is the number of Interfacial Contacts found at the interface between Interactor 1 and Interactor 2. Two residues are defined in contact if any of their heavy atoms are within a distance of 5.5 Å and further classified according to the polar/apolar/charged nature of the interacting residues (*i.e.* $ICs_{charged/apolar}$ is the number of ICs between charged and apolar residues).

Moreover, thaumatin was mutated by replacing the amino acid Asp for Asn at position 21 using the "Mutate Residue" plugin of VMD 1.9, based on previous mutagenesis studies that demonstrated that this replacement significantly enhances the sweetness intensity of thaumatin (Masuda et al., 2016). Then, we identified the binding site of mutated thaumatin on the sweet taste receptor using the ClusPro 2.0 web server. Finally, we calculated the $\Delta G_{binding}$ of mutated thaumatin onto the receptor using the PRODIGY web server.

In the case of non-protein sweeteners, their binding sites within hT1R2-hT1R3 receptor and associated $\Delta G_{binding}$ were predicted using the Autodock Vina software, as previously described (Acevedo et al., 2016). In keeping with the predictive power of our strategy, molecular docking was performed inside a volume of 90 x 30 x 30 grid points that comprises the whole sweetness receptor.

We correlated the calculated $\Delta G_{binding}$ with the relative sweetness of all the evaluated sweeteners, which were obtained from the literature at 5% (w/v) sucrose. The relative sweetness values for simple sugars, artificial sweeteners, SGs and thaumatin were obtained from various sources, *i.e.* the Canadian Sugar Institute, 2015; Shankar et al., 2013; Amino, Kawahara, Mori, Hirasawa, & Sakata, 2016; and Kinghorn, Chin, Pan, & Ohio, 2010; respectively.

We also correlated the calculated $\Delta G_{binding}$ with reported half maximal effective concentrations (EC_{50}), namely an indirect measure of affinity between a ligand and a receptor based on a dose-dependent response. We employed EC_{50} values available for 9 out of 29 sweeteners analyzed in this work, which were obtained using cell-based fluorescence measurements of calcium responses after exposure to these sweeteners (Masuda et al., 2012; Assadi-Porter et al., 2010; Ohta, Masuda, Tani, & Kitabatake, 2011). It is worth noting that all this reported EC_{50} values were obtained using similar experimental set-ups, matching in terms of i) the type of cell line (HEK293), culture medium (GlutaMAX) and temperature (37 ºC); and ii) the transient co-transfection of hT1R2 and hT1R3 and the incubation time before measurement (48 h).

3.3 Results

3.3.1 Modeling of sweet taste receptor

The template for comparative modeling of hT1R2 and hT1R3 was selected based on both sequence identity and e-value after using BLAST. Chain A of the metabotropic glutamate receptor mGluR3 (PDB: 2E4U) showed a sequence identity of 27% and 26% and an e-value of 2e-41 and 5e-43 against hT1R2 and hT1R3, respectively. This chain comprises the active conformation of the receptor 2E4U whose structure is bound to glutamate, thus constituting an appropriate template to predict the three dimensional structure of the VFT domain and the CRD of hT1R2 (Supplementary figure 3-2a) and hT1R3 (Supplementary figure 3-2b).

Ramachandran plots indicate that 82.8% of the residues are in favored regions, 10.7% in allowed regions and 6.5% in outlier regions for hT1R2; whereas 87.1% of the residues are in favored regions, 8.0% in allowed regions, and 4.9% in outlier regions for hT1R3 (Supplementary figure 3-1). PROCHECK analyses of the hT1R2 and hT1R3 models yielded overall average G factors of -0.67 and -0.49, respectively, which suggest that the conformations both of main and side chain of the models are good. The value of normalized QMEAN score for the hT1R2 and hT1R3 subunits was 0.44 and 0.49, respectively, pointing that the resulting models were close enough to a set of experimental protein structures from the PDB database. Therefore, the above analysis provides solid evidence that the predicted 3D structure of hT1R2 and hT1R3 is of good quality. Furthermore, structural superposition of the starting and final conformations using TopMatch demonstrated the absence of significant structural changes (Supplementary figure 3-4), as evidenced by root-mean-square error superposition value of 4.04 Å and 78% sequence identity in the equivalent regions between original and refined protein structures.

3.3.2 Analysis of molecular docking

As illustrated in Figure 3-2, the calculated $\Delta G_{binding}$ negatively correlated with the sweetness intensities reported for sweeteners belonging to different families. The correlation coefficient r for the 25 small sweeteners and 4 sweet proteins with hT1R2-hT1R3 were -0.89 and -0.96, respectively. It is also noticeable that GTs (Figure 2,

compounds o to y) have a lower $\Delta G_{binding}$ for the receptor than other non-protein sweeteners, with mogroside V having the lowest $\Delta G_{binding}$. In particular for SGs (Figure 3-2, compounds p to x), rebaudioside A (compound q; Table S1) showed the lowest $\Delta G_{binding}$ and rebaudioside C (compound s; Table S1) the highest one, against hT1R2-hT1R3, when compared to all other SGs. This result should be related to the chemical features of these sweeteners. Stevioside (compound p; Figure 3-2), although lacking one glucose moiety when compared to rebaudiosides, follows rebaudioside A as the SG with highest affinity to hT1R2 and hT1R3 (Supplementary table 1-1). Moreover, SGs containing rhamnose – dulcoside A and rebaudioside C – are among the SGs with higher $\Delta G_{binding}$ for hT1R2-hT1R3; and lower $\Delta G_{binding}$ for bitterness receptors hT2R4 and hT2R14 (Acevedo et al., 2016), suggesting that this moiety might allow a good discrimination between bitter and sweet tastes. Regarding protein sweeteners, Figure 3-2 evidences that neoculin has a lower $\Delta G_{binding}$ for hT1R2-hT1R3 complex, followed by thaumatin, monellin and brazzein.

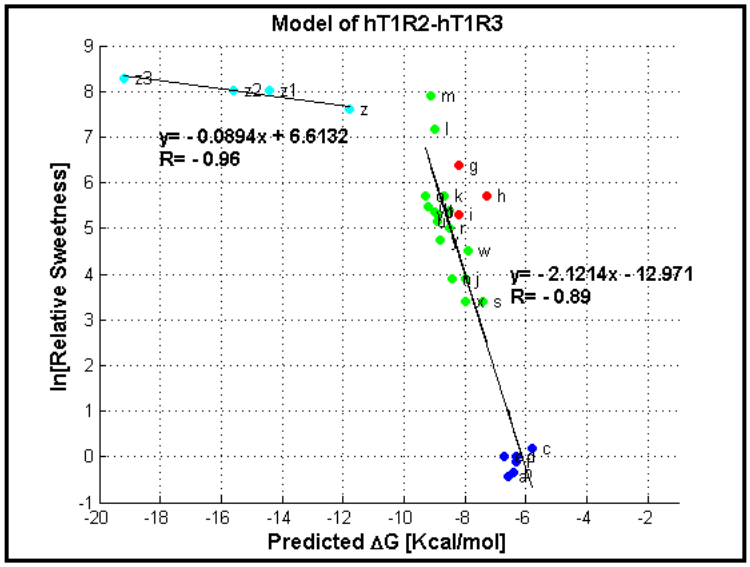

Figure 3-2: Relationship between relative sweetness of sweeteners and $\Delta G_{binding}$ calculated from molecular docking onto the hT1R2- hT1R3 sweet receptor. The data corresponds to: (a) glucose, (b) galactose, (c) fructose, (d) xylose, (e) sucrose, (f) tagatose, (g) sucralose, (h) saccharin, (i) aspartame, (j) monatin 2S4,S, (k) monatin 2S4,R, (l) monatin 2R4,S, (m) monatin 2R4,R, (n) glycyrrhizic acid, (o) mogroside V, (p) stevioside, (q) reb A, (r) reb B, (s) reb C, (t) reb D, (u) reb E, (v) reb F, (w) steviolbioside, (x) dulcoside A, (y) rubusoside, (z) thaumatin, (z1) brazzein, (z2) monellin and (z3) neoculin. Relative sweetness data of sweeteners were obtained from the Canadian Sugar Institute,(Canadian Sugar Institute, 2015) Shankar et al.,(Shankar et al., 2013) Amino at al.,(Amino et al., 2016) and Kinghorn et al.,(Kinghorn et al., 2010)

Our analysis also shows a poor correlation against relative sweetness for monatin 2R,4S and 2R,4R, as well as for sucralose and saccharine (Figure 3-2, compounds a to m). Moreover, we had to separate our analyses between protein sweeteners and non-protein ones, due to the impossibility to obtain good correlations when considering them altogether. A possible explanation for this is the lack of discrimination within both groups of non-GTs sweeteners when using relative sweetness as a quantifiable measurement, rather than a poor behavior of our computational analysis. To further support this idea, we opted to correlate the calculated $\Delta G_{binding}$ against the reported half maximal effective concentrations (EC_{50}) that were estimated from cell-based fluorescence measurements of calcium responses after exposure to 9 of the 29 sweeteners analyzed in this work (Masuda et al., 2012; Assadi-Porter et al., 2010; Ohta, Masuda, Tani, & Kitabatake, 2011).

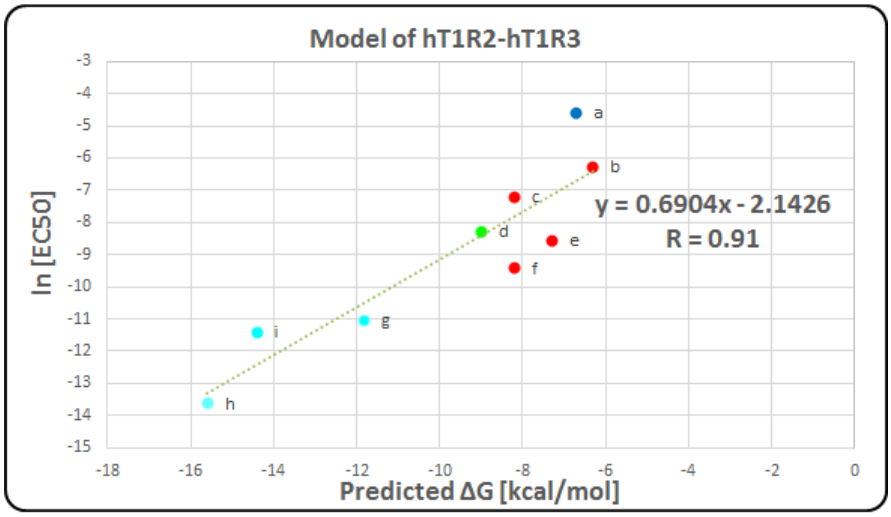

Figure 3-3: Relationship between half maximal effective concentrations (EC_{50}) of sweeteners and $\Delta G_{binding}$ calculated from molecular docking onto the sweet receptor. The data corresponds to: (a) glucose, (b) cyclamate, (c) aspartame, (d) stevioside, (e) saccharin, (f) sucralose, (g) brazzein, (h) thaumatin and (i) monellin. EC50 data was taken from Masuda et al.,(K. Masuda et al., 2012) Assadi-Porter et al. (Assadi-Porter et al., 2010) and Otha et al. (Ohta et al., 2011a)

As shown in Figure 3-3, there is a significant improvement in the correlation throughout all types of sweeteners when apparent binding affinities rather than sweetness potency are used as the experimental variable. It is worth mentioning that EC_{50} data sets obtained from

the literature are comparable, because similar experimental procedures and conditions were employed, i.e. both, sweet taste receptor and Gα16-gust44 protein, were expressed in HEK293 cells.

These results suggest that the use of computationally derived calculations of binding affinities alongside sweetness intensities and cell-based determinations of EC_{50} could potentially enable the rational design of novel sweeteners with improved features and lower effective concentrations. Consistent with this idea, the calculated $\Delta G_{binding}$ of engineered thaumatin - modified at Asp21 with Asn - is lower than native thaumatin ($\Delta G_{binding}$ = -21.1 Kcal/mol), equivalent to almost 5,000 times sweeter than sucrose (calculated from the equation shown in Figure 3-2), in line with experimental evidence on the effect of this mutation in increasing sweetness intensity of thaumatin (Masuda et al., 2016).

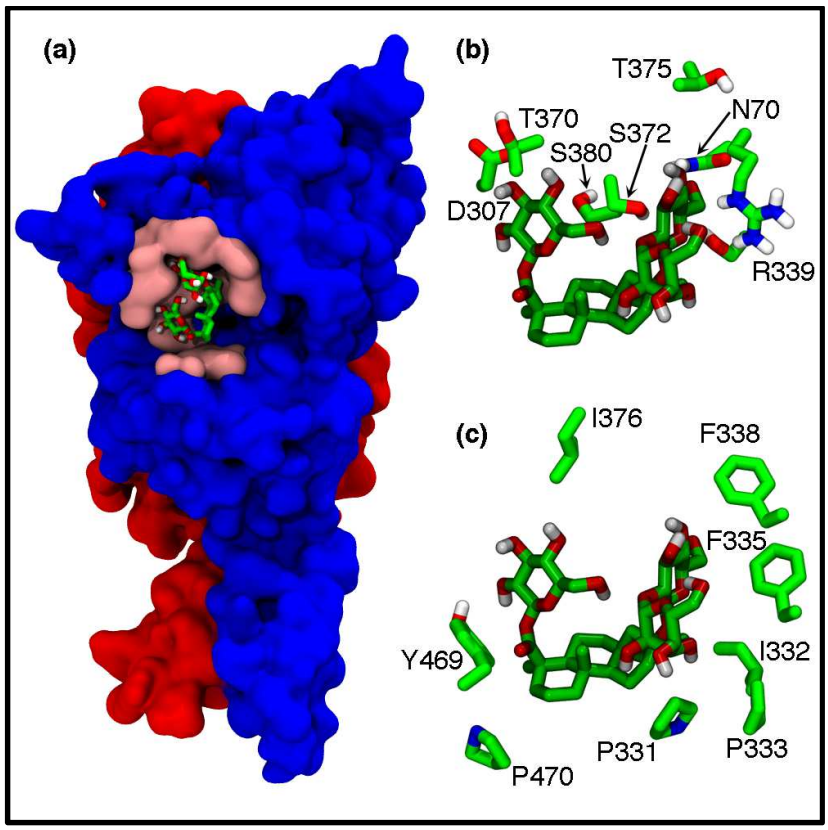

Figure 3-4: Visualization of the potential binding site and docking pose of stevioside into the hT1R2 subunit. A detailed inspection of the binding site within hT1R2 shows the amino acids responsible for the interaction with stevioside through (a) hydrogen bond and (b) hydrophobic contacts.

Since there is good correlation between experimental sweetness measurements and calculated $\Delta G_{binding}$, Figure 3-4 and Supplementary figure 3-5 depict the potential binding sites of different small sweeteners and poses of docked stevioside within the sweet taste receptor, respectively. All these sweeteners bind to small binding cavities of hT1R2 as well as hT1R3. Furthermore, Table S1 identifies those amino acids responsible for hydrogen bonding and hydrophobic interactions for hT1R2 and hT1R3 with small sweeteners as well as sweet proteins. In particular, the fact that 54.3% and 51.8% of the amino acids responsible for hydrogen bonding and hydrophobic interactions with simple sugars and GTs are polar, strongly suggests that the hydrophilic nature of the binding pocket favors the binding of these sweeteners within the sweet taste receptor. The docking of the different complexes allowed us to identify the most representative modes of binding for GTs to the sweetness receptor (Supplementary figure 3-5). They differ both in orientation and conformation, by selectively interacting with specific binding site residues. In fact, the conformation is set to the shape and size of the pocket, for both hT1R2 and hT1R3. Thus, stimulation of a specific set of residues with different physicochemical properties could partly explain the characteristic sweetness intensities of these sweeteners.

Figure 3-5 depicts the potential binding sites and poses of sweet proteins on hT1R2-hT1R3 receptor. As expected, all the evaluated sweet proteins bind to the same binding site on the receptor, which is constituted by a cavity wide and deep enough to allow accommodation of these high molecular weight sweeteners. The surface area of this binding cavity is around 1845 Å, whereas the binding surface for small non-protein sweeteners is around 700 Å (see Supplementary table 1-1). Furthermore, a comparison of the electrostatic surface of all the evaluated sweet proteins as well as the hT1R2-hT1R3 receptor shows that the electrostatic potential of the binding interface of these sweeteners is mainly positive, whereas the receptor has a negatively charged binding cavity (Supplementary figure 3-6). This observation suggests that the dominant feature in receptor-sweet protein binding is the electrostatic surface potential.

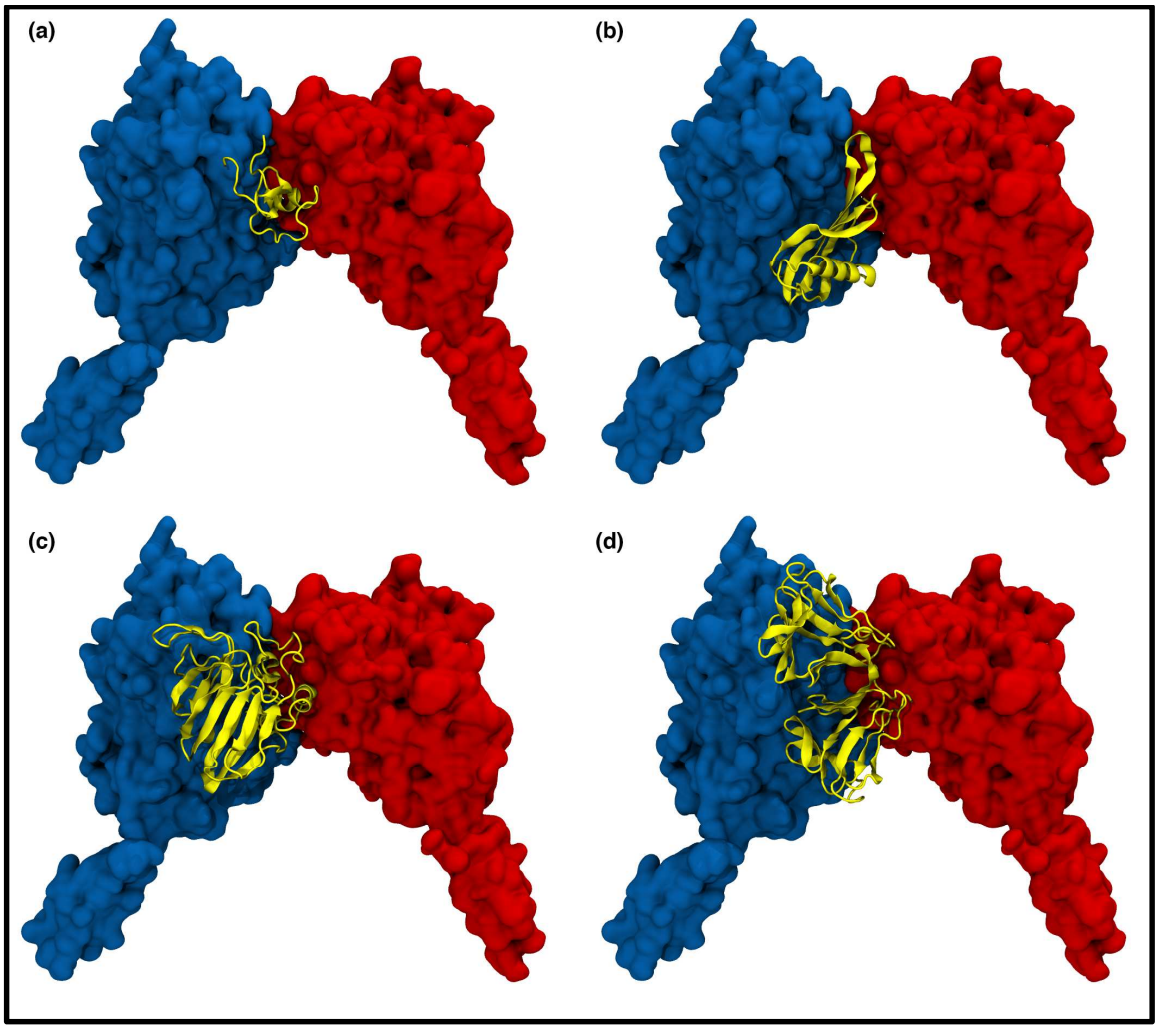

Figure 3-5: Visualization of the structures, potential binding site and docking poses of (a) brazzein, (b) monellin, (c) thaumatin and (d) neoculin into the sweet receptor hT1R2-hT1R3.

3.4 Discussion

The structure of the sweet receptor's extracellular region consists of multiple loops and cavities, which could play an important role in ligand recognition similar to other GPCR receptors, such as bitter taste receptors (Singh et al., 2011). In this study, we demonstrated that the $\Delta G_{binding}$ derived computationally for several sweeteners using molecular docking onto the sweetness receptor hT1R2-hT1R3 are negatively correlated with the sweetness intensity; that is, the more negative the $\Delta G_{binding}$ between sweetener and receptor, the

greater the sweetness intensity (Hellfritsch et al., 2012). Furthermore, the presence of cavities in both subunits to which different families of sweeteners bind preferentially in our computational analysis, suggests that the receptor contains more than one binding site (Cui et al., 2006). In fact, low molecular weight sweeteners bind to small cavities of hT1R2, as well as hT1R3, subunits; whereas sweet proteins could interact with the sweet receptors according to a mechanism termed the 'wedge model' in which they bind to large external cavity conformed by both subunits (Temussi, 2002; Picone & Temussi, 2012). The strong correlation obtained between either sweetness intensity or EC_{50} and our calculated binding affinities confirms this observation, thus indicating that the mechanism of activation of sweet proteins is different from that used by small sweeteners (Temussi, 2006; Xu et al., 2004).

Regarding the potential binding sites on the sweet taste receptors of the evaluated GTs, we showed that all of them bind into the same cavity and share a set of amino acids. Besides those previously identified for stevioside in hT1R2 VFT domain by Zhang et al., 2010, these include Ala305, Ser329 and Glu382 that are involved in hydrogen bond interactions for hT1R2; whereas the carbons of sugars, as well as the terpene moiety, bind via hydrophobic interactions. Furthermore, the GTs have lower $\Delta G_{binding}$ than simple sugars due to the number of glucose moieties present in their structures, probably playing an important role in stabilizing the closed conformation of the VFT domain of the receptor. These findings confirm the results obtained by Cherón et al. 2016, using a QSAR model for sweetness prediction, indicating that the high sweetening power of GTs is due to a limited number of hydrogen bond sites with a moderate molecular weight (Chéron et al., 2016).

The binding mechanism mediated by hydrogen bonds of some GTs, including 10 active compounds of stevia, has also been identified on bitter taste receptors, because of the sugars present in these sweeteners. However, the affinity of SG for sweet taste receptors, as well as their differences in sweetness intensity, is due to their physical-chemical properties *i.e.* a chemical structure that combines a hydrophobic scaffold functionalized by a number of hydrogen bond sites. On the contrary, the affinity for bitter taste receptors

could be due to the steric characteristics of SG and their binding site architecture (Acevedo et al., 2016).

We also showed that all the sweet proteins evaluated herein bind to a wide cavity, formed by both subunits, by selectively interacting with specific binding site residues belonging to the VFT domain. For example, brazzein interacts with Val111, Ser129, Asn 152, Ser155 of hT1R2 and Lys155, Phe159, Arg177, Asp419 of hT1R3, whereas thaumatin interact with Gln109, Leu 156, Lys 174 of hT1R2 and Phe159, Ser158, Arg177, Glu178 (see Table S1 for more details). By contrast, Jiang et al. proposed, based on functional expression studies, that the CRD of hT1R3 forms a single and additional binding site for sweet proteins (Jiang et al., 2004). Moreover, we demonstrated the key role of electrostatic interactions in the interaction of sweet proteins with the sweet receptor, besides the structural complementarity described by the 'wedge model', which could potentially explain the high sweetening power of this type of sweeteners (Esposito et al., 2006). In fact, the calculated $\Delta G_{binding}$ for an engineered thaumatin obtained by neutralizing a negative charge provided by Asp at position 21 with Asn is lower than that of the native thaumatin, in line with the experimental evidence (Masuda et al., 2016); and confirming that engineering of the electrostatic interaction surface is a potential tool to increase the sweetening power of this and other sweet proteins.

3.5 Conclusions

In conclusion, our work provides a molecular rationale for the differences in sweetness intensity of different types of tastants, which can be summarized in the following features: 1) the importance of the electrostatic potential in the interaction of sweet proteins and sweet taste receptor; 2) the ability of GTs to form hydrogen bonds with amino acids at the binding pocket due to the presence of sugars in their structures; 3) the establishment of hydrophobic interactions between the receptor and GTs, which could help to stabilize the closed conformation of the receptor VFT domain. Moreover, the strong correlation between our computational estimations and the binding affinities estimated at half maximal effective concentration (EC_{50}), through cell-based calcium responses upon exposure to

tastants, strengthens the idea of using molecular docking for designing and predicting the sweet taste of novel sweeteners.

3.6 Acknowledgments

We are grateful to Javier Sainz, from Prodalysa Inc. and to Dr. Danilo Gonzalez, from University Andrés Bello, in Santiago, Chile, for recommendations and suggestions during the course of this work. Waldo Acevedo was supported by a doctoral fellowship from the Chilean National Council of Scientific and Technological Research (CONICYT) [grant number 21130688 to W.A.].

4. SELECTING OPTIMAL MIXTURES OF NATURAL SWEETENERS FOR CARBONATED SOFT DRINKS THROUGH MULTI-OBJECTIVE DECISION MODELING AND SENSORY VALIDATION

Waldo Acevedo, Chloé Capitaine, Ricardo Rodríguez, Ingrid Araya, Fernando González-Nilo, José R. Pérez-Correa and Eduardo Agosin

Submitted to Food Quality and Preference *Journal.* Manuscript ID: FQAP_2017_5

Abstract

Current demand of low-calorie beverages has significantly raised as a result of consumer concerns on the negative effects of refined sugars present in carbonated soft drinks. Consequently, natural sweeteners, and their mixtures, are being increasingly employed for these product developments. The objective of this study was to develop a methodology to optimize mixtures of natural, non-caloric sweeteners – with the highest sweetness and the lowest bitterness - for carbonated soft drinks. To this end, and with the aid of a trained sensory panel, we first determined the most suitable mixtures of tagatose, sucrose and stevia in a soft drink matrix, using a three-component simplex lattice mixture design. Then, a multi-objective decision model was applied to identify optimal combinations of these sweeteners, based on the thermodynamic properties of the sweetener-receptor and sweetener-sweetener interactions. Both, sucrose and tagatose, were able to reduce stevia´s bitterness. However, an increase of bitterness intensity was found above 0.23 g/L of stevia (sucrose equivalency or SE > 5). Both, sensory analysis and multi-objective decision modeling identified similar optimal mixtures, corresponding to 23 - 39 g/L sucrose, 0.19 - 0.34 g/L stevia and 34 - 42 g/L tagatose were determined, depending on the desired sweetness/bitterness balance. Within this constrained area, a reduction of almost 60% of sucrose can be achieved in both approaches, keeping bitterness intensity low. In conclusion, the multi-objective, thermodynamically-based decision model developed in this study is an efficient tool for formulating optimal mixtures of natural sweeteners for low calorie carbonated soft drinks.

4.1 Introduction

The consumption of carbonated sugary drinks has been a constant matter of concern to public health due to the negative contribution of refined sugars and calories to diet. In recent decades, the intake of these beverages has increased considerably around the world. From 1997 to 2010, average annual consumption of soft drinks worldwide increased by 20%, mainly sugar-sweetened carbonated drinks (Basu at al., 2013). This increase has been related with rising rates of obesity and other health outcomes, like type 2 diabetes mellitus and cardiovascular diseases (Basu et al. 2013; Vartanian et al. 2007; Malik et al. 2010). These health trends are increasing awareness among consumers about the intake of carbonated sugary drinks, encouraging them to shift their preferences towards products with less sugar and caloric content. In order to meet this demand, beverages sweetened with a large variety of non-caloric artificial sweeteners, like potassium acesulfame and Aspartame™, have been developed by the industry as healthier alternatives. Their sweetening power at very low concentrations and their limited caloric contribution made these compounds an excellent alternative to replace sugar. However, consumer's reports and studies with animals have claimed that the consumption of these high-intensity, artificial sweeteners may have an effect on health in the long-term (Bradstock et al. 1986; Soffritti et al. 2006). More recently, Suez et al (2014) demonstrated that consumption of commonly used non-caloric artificial sweeteners formulations drive the development of glucose intolerance through induction of compositional and functional alterations to the intestinal microbiota (Suez et al., 2014). Nowadays, the use of natural sweeteners in product formulations is becoming more and more frequent, with stevia extracts being the most popular. The term "stevia" is used to refer to steviol glycosides (SGs), a group of ten sweet-tasting compounds which are extracted from the leaves of the *Stevia rebaudiana* grass (Kinghora et al., 1986). SGs are a suitable alternative to artificial sweeteners in the preparation of various food products, due to their sweetness strength and stability at low pH. Different formulations of steviol glycosides, as well as purified fractions of stevia leaves, are present in the market, with particular chemical and sensory profiles (Espinoza et al., 2014). However, SGs have limitations in mimicking sucrose sweetness temporal

profiling; furthermore, these compounds generate undesirable sensory attributes such as bitterness, metallic, and licorice tastes in foods and beverages (Kappes et al. 2006; Prakash et al. 2008; Schiffman et al. 1995).

Recent *in vitro* studies in HEK 293 cells revealed that SG specifically activate the hT2R4 and hT2R14 bitter taste receptors above a given concentration, triggering a bitter mouthfeel (Hellfritsch et al., 2012). Furthermore, molecular docking studies showed that interactions of SGs with the binding pockets of these bitter receptors and other sweet receptors, could be represented by the MultiPoint Attachment model (MPA) (Nofre & Tinti, 1996), whose interaction points within the binding site are being governed by hydrogen bonding and hydrophobic interactions (Acevedo et al., 2016).

In order to overcome these limitations of SGs, one or more sweeteners are usually mixed with stevia extracts to obtain a more balanced product. Sweetness synergies, stability, as well as improvements in flavor and temporal taste profiling can be achieved with the right combination of sweeteners (Carakostas et al., 2012). Furthermore, the addition of bulk-sweeteners to high-intensity sweeteners could improve mouthfeel, mask off-tastes and increase sweetness perception (Andersen & Vigh, 2002). For example, D-tagatose, a natural low-caloric sweetener, has been mixed with stevia to prepare a reduced-caloric beverage to achieve a taste substantially similar to the full-calorie beverage (Lee et al., 2010).

Choosing adequate sweeteners, in the right proportion, to achieve a good-tasting product is challenging due to the large number of possible combinations and the conflicting objectives of sweetness against bitterness, metallic, licorice, etc. Product formulations can be experimentally optimized to balance these objectives using statistical techniques such as surface response and desirability function; however, these techniques are costly and time consuming.

The objective of this study was to develop a methodology to select optimal mixtures of natural, non-caloric sweeteners for preparing carbonated soft drinks with the lowest caloric content, while maintaining the tastiness – high sweetness and low bitterness - of full caloric ones. To this end, we first determined equi-sweet concentrations of sucrose, stevia

and tagatose, as well as ternary mixtures of these sweeteners taking advantage of a trained sensory panel. Bitterness was also determined for the same mixtures using three-component simplex lattice mixture design. The resulting experimental data was fitted to a canonical Scheffé´s equation for bitterness. Then, we developed a multi-objective thermodynamically based decision model to identify optimal mixtures of natural sweeteners in these soft drinks. The interaction energies between sweeteners, as well as between sweetener-receptor, were predicted and included as parameters of the multi-objective decision model. Finally, a multi-objective optimization problem (MOP) was solved using the Generalized Reduced Gradient (GRG) Non-linear code within EXCEL. Pareto-optimal fronts were obtained, indicating the options towards products with lowest sugar, caloric content and cost.

4.2 Materials and methods

4.2.1 Experimental design of optimal mixtures by sensory analysis

4.2.1.1 Reference soft drink matrix and sweeteners

A standard soft drink matrix was employed in every sample: 1.5 g/L of citric acid monohydrate (Merck, Germany), 0.6 g/L lemon-lime flavoring (Givaudan, Switzerland) and carbonated water with 3 volumes of food-grade CO_2 (Indura, Chile). Purified water (Agua Purificada ByP, Chile) was carbonated with three volumes of CO_2 using a Zahm & Nagel 9000 Pilot Plant carbonation and filling equipment (Buffalo, USA). The sweeteners employed were sucrose (Merck, Germany), D-tagatose (CJ Cheiljedang, South Korea) and water-purified stevia (Stevia Clear^{TM}, Steviol Glycosides > 95%, Prodalysa, Chile). The sweeteners were weighted and mixed with the other components in glass bottles, which were filled with carbonated water up to 360 mL. All the samples were stored at 5°C until analysis.

4.2.1.2 Selection and training of the panel

Fourteen female panelists, aged 40-50 years old, were selected from a panel previously trained for sensory evaluation under ISO Norms (ISO, 2012) (Centro de Aromas y

Sabores, DICTUC, Santiago, Chile). The panelists followed a two-month specific training on sweeteners.

The panel was introduced to the main descriptors of sweeteners, using the following reference standards: sucrose for sweetness (Merck, Germany), caffeine for bitterness (Sigma Aldrich, U.S.A.), glycyrrhizin acid ammonium salt for licorice (Sigma Aldrich, U.S.A.) and ferrous sulphate for metallic (Sigma Aldrich, U.S.A.). Plenary sessions were performed to discuss about the selected attributes and the use of a 14-points scale to evaluate response intensity. In these sessions, three concentrations of each descriptor (low, medium and high) were given to establish a reference within the scale**.** Once the panel was capable to recognize basic attributes, reference solutions were assessed in individual booths using CompuSense 5.3 software (CompuSense Inc., Canada). To reinforce the use of the scale for sweetness, the CompuSense Feedback Calibration Method® was employed to assess sucrose samples. This method gives an immediate feedback to the judge comparing its scores with the established range values set, for each product attribute (Findlay, Castura, & Lesschaeve, 2007). Panel performances were assessed in order to validate consensus (agreement between panelists), repeatability and discrimination capacity (aptitude of panelists to discriminate samples of different aromatic intensities) of the panelists and the whole panel (Pineau et al., 2007).

4.2.1.3 Sweetness equivalence determination

As a weight-based Simplex Lattice design was not applicable here, due to the differences among sweetness intensity of sucrose, tagatose and stevia. Regression lines were fitted and equi-sweet concentrations for each sweetener were determined with a six-point sweetness Concentration–Response curve as illustrated in Figure 3-2.

For this purpose, the panel was asked to rank different aqueous solutions for sweetness, bitterness, licorice and metallic tastes using a linear 14-point scale displayed on a computer screen in each cabin (Portmann & Kilcast, 1996). Sucrose and tagatose were not expected to show high intensities of attributes other than sweetness, but all attributes were included to avoid any halo dumping effect (Schifferstein, 1996). Analyses were carried out in duplicate in individual sensory booths, illuminated with white light. Samples were

presented at room temperature in 20-mL plastic cups, marked with 3-digit random numbers. To minimize the carry-over effect, panelists were asked to rinse their palate for 5 minutes between samples with water and salt-free rice crackers (Jumbo, Chile). Samples were randomized for each session.

Since panelists were trained to assess sweetness intensity based on a sucrose-referenced scale, this correspondence of sucrose concentration and sweetness rating confirms the reliability of the scaling methodology employed in this study.

4.2.1.4 Experimental design and mixture samples

A three-component Simplex Lattice mixture design (Gorman & Hinman, 1962) was conducted to investigate the maximum achievable replacement of sucrose (X_1) by non-caloric natural sweeteners in a carbonated soft drink matrix. The mixture components consisted of sucrose (X_1), stevia (X_2) and tagatose (X_3). A 15-point lattice was used with a quadratic model (Figure 3-3). One reference point was included in the center, yielding 16 points in total. The employed sweetener concentrations were based on equi-sweet values calculated from the sweetness-concentration curves (Figure 3-2). A sweetness value of 10, on a fourteen-point scale, was established as the "unity". This means, at least theoretically, that each mixture must be as sweet as a 10% w/v sucrose solution (10 sucrose equivalency). As the variables were independent, component proportions were expressed as fractions of the mixture and the sum ($X_1 + X_2 + X_3$) equals one (Gorman & Hinman, 1962). The response values were sweetness, bitterness, metallic, and licorice.

4.2.1.5 Data analysis

Data from the Simplex Lattice points was used to calculate the Scheffé´s canonical cubic equation for three components:

$$Y = \beta_1 X_1 + \beta_2 X_2 + \beta_3 X_3 + \beta_{12} X_1 X_2 + \beta_{13} X_1 X_3 + \beta_{23} X_2 X_3 + \beta_{123} X_1 X_2 X_3 \quad (4.1)$$

where Y is the value given for the attribute´s intensity of each sample (sweetness for example), β is the parameter estimate for each linear and interaction term of the prediction model; and X_1, X_2 and X_3 represent the sweetness proportion of sucrose, stevia and tagatose in each mixture, respectively (Gorman & Hinman, 1962). The significance and

the fit of each model was assessed through an Analysis of Variance (ANOVA), at 5% significance level ($p \leq 0.05$), using the R statistical software. Triangular response surface plots were constructed based in the Scheffé´s canonical cubic equation fitted to the sensory data, using QualityTools™ package (Roth, 2012). R statistical software package was employed to analyze the results of the descriptive sensory evaluation.

4.2.2 Determination of Optimal mixtures by multi-objective optimization

4.2.2.1 Preparation of ligand

The 3D structures of sucrose, D-tagatose, stevioside and rebaudioside A were obtained from the PubChem database (National Center for Biotechnology Information, 2004) in sdf file format, using the PubChem CIDs 5988, 92092, 442089 and 6918840, respectively (Figure 4-1). Stevioside and rebaudioside A were included in this study because they are the most abundant species in stevia extracts (Espinoza et al., 2014). OpenBabel version 2.3.1 was employed to convert ligand representations to mol2 format and to visually check them for correct structural errors.

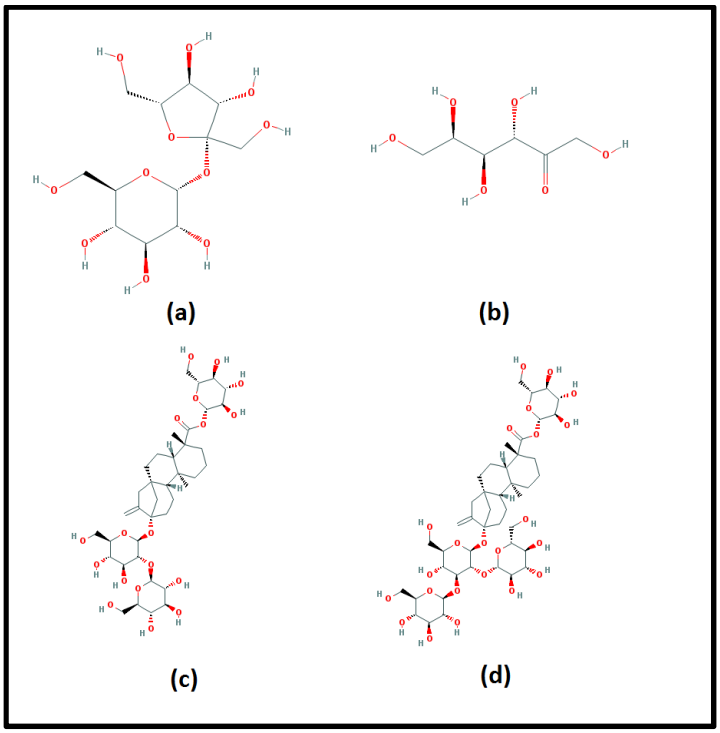

Figure 4-1: Chemical structures of (a) sucrose, (b) D-tagatose, (c) stevioside and (d) rebaudioside A**.**

4.2.2.2 Binary and ternary interaction energy of sweeteners

Binary interaction energies ($\Delta E_{interaction}$) were calculated using an algorithm that creates N configurations of two molecules (Supplementary figure 4-1). The sampling algorithm is based on the Euler angles formed between the pair of molecules (Fan et al. 1992; Avila-Salas et al. 2012). Thereby, we generated 100.000 random pair configurations to explore the whole surface of the base molecule. Then, we calculated the energies using PM6 semi-empirical quantum mechanics methods through Molecular Orbital PACkage (MOPAC) that was parallelized using MPI libraries to distribute the tasks in different nodes (Stewart 2013; James J. P. Stewart 2016). The resulting binary interaction energies of the 100.000 conformations were further processed to calculate the total interaction energy, as follows:

$$\Delta E_{interaction} = E_{complex} - (E_{molA} + E_{molB}) \quad (4.2)$$

where $E_{complex}$ corresponds to the energy of the pair between the couple of molecules, and E_{molA} and E_{molB} correspond to the energy of each molecule isolated.

Subsequently, the ternary interaction energies were calculated as previously described from the most stable configurations of pairs of sweeteners. The different complexes were hierarchized by interaction energies and visualized using Visual Molecular Dynamics (VMD version 1.9) (Humphrey et al., 1996).

4.2.2.3 Sweetener-receptor interactions

Binding free energies ($\Delta G_{binding}$) of evaluated sweeteners, including sucrose, tagatose, stevioside and rebaudioside A, with hT1R2-hT1R3 sweet receptor was obtained as follows. We built comparative models for the hT1R2 and hT1R3 subunits, using the SWISS-MODEL of the EXPASY server (SIB Swiss Institute of Bioinformatics and the Biozentrum and der Universität Basel 2003; Schweden et al. 2003; Biasini et al. 2014) and chain A from the crystal structure of metabotropic glutamate receptor subtype 3 o mGluR3 (PDB entry 2E4U) as template. Subsequently, we built a hT1R2-hT1R3 heterodimeric complex model (Supplementary figure 3-3), based on the mGluR3 dimer published by Muto et al (Muto et al., 2007). Our models differ from those reported in the literature, because we extended the heterodimeric complex model to predict the binding free energies of several natural sweeteners, including sucrose, tagatose, stevioside and rebaudioside A,

by molecular docking (Cui et al. 2006; Masuda et al. 2012; Maillet et al. 2015). The binding sites, as well as associated binding free energies ($\Delta G_{binding}$), of the sweeteners with the hT1R2-hT1R3 receptor were predicted using the Autodock Vina software, as previously described (Acevedo et al., 2016). In keeping with the predictive power of our strategy, molecular docking was performed inside a volume of 90 x 30 x 30 grid points that comprises the whole sweetness receptor.

Binding free energies ($\Delta G_{binding}$) of the sweeteners with hT2R4 and hT2R14 bitter receptors were obtained from Acevedo et al. 2016. Finally, the $\Delta G_{binding}$ of sucrose and tagatose, with the bitter receptors was set to zero, because these sugars elicit only sweet taste and no off-flavours (Fujimaru, Park, & Lim, 2012).

All these values of interaction energies were used as parameters for the multi-objective decision model. These results are presented in Table 4-1 and 4-2.

4.2.2.4 Multi-objective optimization

We developed a multi-objective decision model to identify the optimal mixture of natural sweeteners - i.e. maximum sweetness and minimum bitterness - based on the thermodynamic properties of sweetener-receptor and sweetener-sweetener complexes.

The interactions of the different complexes are included in the following equations:

$$f_1 = \beta_{11}X_1 + \beta_{12}X_2 + \beta_{13}X_3 + \beta_{14}X_1X_2 + \beta_{15}X_1X_3 + \beta_{16}X_2X_3 + \beta_{17}X_1X_2X_3 \quad (4.3)$$

$$f_2 = \beta_{21}X_1 + \beta_{22}X_2 + \beta_{23}X_3 + \beta_{14}X_1X_2 + \beta_{15}X_1X_3 + \beta_{16}X_2X_3 + \beta_{17}X_1X_2X_3 \quad (4.4)$$

$$f_3 = \beta_{31}X_1 + \beta_{32}X_2 + \beta_{33}X_3 + \beta_{14}X_1X_2 + \beta_{15}X_1X_3 + \beta_{16}X_2X_3 + \beta_{17}X_1X_2X_3 \quad (4.5)$$

Where f_1 corresponds to the objective function for sweetness, and f_2 and f_3 for bitterness, i.e. the interaction of the sweeteners with hT2R4 and hT2R14 bitter taste receptors, respectively. X_1, X_2 and X_3 represent the sweetness fraction of sucrose, stevioside (or rebaudioside A) and tagatose for each mixture, respectively. β_{ij} is the estimated parameter for each linear and interaction term of the prediction model, where the first three parameters of the functions f1, f2 and f3 correspond to the interaction between receptor and sweetener (Table 4-1) and the rest correspond to the binary and ternary interactions (Table 4-2).

Then, we considered the following multi-objective cost function:

$$\mathrm{F(X)} = \ w_1 \cdot f_1 \ - \ w_2 \cdot f_2 \ - \ w_3 \cdot f_3 \ ; \quad \text{with} \ \ w_j \ \geq 0 \ \text{and} \ \sum_1^N w_j = 1 \qquad (4.6)$$

The weight (wj's) indicates the relative importance the Decision Maker (DM) attaches to objective j and must be specified for each of the k objectives *a priori*. Finally, considering $w_2 = w_3$, assuming that the bitterness response is the same for the interactions of a sweetener with hT2R4 and hT2R14, and applying the weighting method (Wang & Rangaiah, 2017) to solve the multi-objective optimization problem, we get:

$$\mathrm{Max}\, F(X) = w \cdot \frac{f_1}{\min(f_1)} - (1 - \ w) \cdot \frac{f_2 + f_3}{\min(f_2) + \min(f_3)}; \ \text{with} \ \ 0 \leq \ w \ \leq 1 \qquad (4.7)$$

The objectives $\frac{f_1}{\min(f_1)}$ and $\frac{f_2 + f_3}{\min(f_2) + \min(f_3)}$ were named f1-norm and f2-norm, corresponding to the normalized functions for sweetness and bitterness, respectively.

We solved the multi-objective maximization problem, using the Generalized Reduced Gradient (GRG) Non-linear code within EXCEL (Equation 4.7). In general, multi-objective optimization provides many optimal solutions, known as non-dominated solutions or Pareto-optimal front, except when the objectives are not conflicting for which only one unique solution exists (Ngatchou et al. , 2005). Therefore, we selected an optimal solution from the Pareto-optimal front based on maximum sweetness and minimum bitterness.

4.3 Results

4.3.1 Concentration - sweetness response for sucrose, tagatose and stevia sweeteners

Our results confirm previous results that sweetness intensity increases linearly with sucrose and tagatose concentrations (Figures 4-2a and 4-2b) (Fujimaru et al. 2012; Choi and Chung 2014). However, tagatose is less sweet than sucrose (slope of 0.84). However, tagatose is less sweet than sucrose (slope of 0.84). On the contrary, a logarithmic function fit the data for stevia sweetness (Figure 4-2c), confirming that the shape of the concentration-response functions for high intensity sweeteners is not linear (Choi and Chung 2014; DuBois et al. 1991). As for sweetness, the intensity rating for bitterness is higher as the concentration of

stevia increases. These results are consistent with previous works (Prakash et al. 2008; Schiffman et al. 1995).

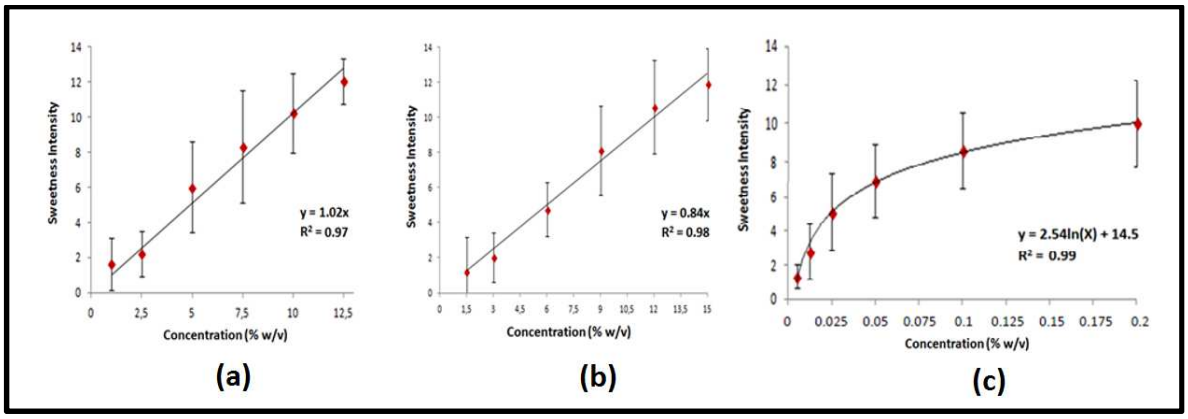

Figure 4-2: Concentration-response curves for (a) sucrose, (b) tagatose and (c) stevia in purified water. The y-axis shows sweetness intensity (SI) on a scale of fourteen points. The x-axis indicates the concentration of each sample in g/100mL for (a) Sucrose, SI = 1.02*C, R^2 = 0.974 (b) Tagatose, SI = 0.84*C, R^2 = 0.98; and (c) Stevia, SI = 2.54*ln(C) + 14.5, R^2 = 0.9747.

4.3.2 Sweeteners mixture design for a soft drink matrix

The average sensory intensities for sweetness, bitterness, metallic and licorice for the 16 tested samples are illustrated in Figure 4-3 (see also Table S1). Sweetness intensity was lower than expected, considering that all samples were prepared to achieve a sweetness intensity of 10, according to the equi-sweet curves (Figure 4-2). Previous studies have reported that carbonation suppress the perception of sweetness (Cowart 1998; Hewson et al. 2009; Di Salle et al. 2013), which could explain these differences. On the other hand, the average values for sweetness were very similar between samples, which is consistent with the proposed experimental design. The latter varied between 5.64 and 7.81, with an overall average of 6.78. No substantial synergies between sweeteners were found. Furthermore, there was a sharp increase in bitterness intensity when the proportion of stevia was superior to 50%. It is worth mentioning here that stevia concentration of samples 4 and 5 is relatively high (0.615 and 1.636 g/L, respectively), which may lead to a saturation in the perception of bitterness, and therefore a misleading evaluation. This was also the case for the sample with the highest bitterness (value of 7.31). These results are

consistent with previous works, which indicate that the bitter attribute becomes noticeable at relatively high sucrose-equivalent (SE) levels of stevia (SE>6) (Heikel et al. 2012; Schiffman et al. 2003; Waldrop and Ross 2014). Furthermore, bitterness remains low and relatively constant in sucrose-tagatose blends (samples 1, 6, 10, 13 and 15).

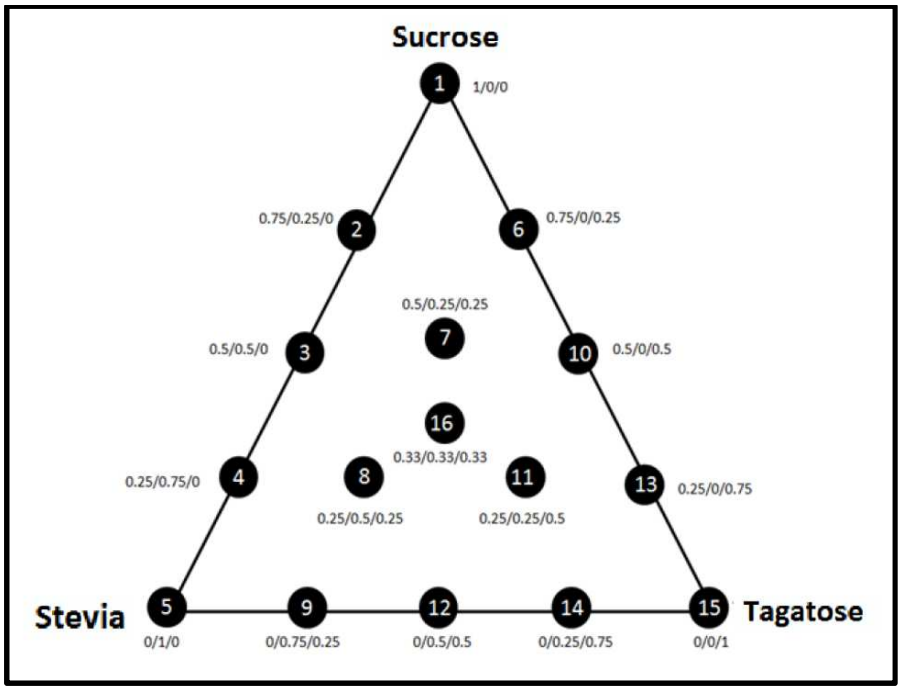

Figure 4-3: Graphical representation of the equi-sweetness of the 16 samples evaluated in the simplex in soft drink matrix. All samples are represented with a black circle with the number inside. The proportion of sweetness of each component is under the corresponding sample (sucrose/stevia/tagatose).

4.3.3 Mathematical model and contour plots

The canonical Scheffé´s equation for bitterness was:

$$Y = 6.33X_2 + 1.23X_3 - 9.53X_1X_2 - 10.57X_2X_3 \quad (4.8)$$

Stevia (X_2 in the equation) was the single component that contributed to a greater extent to this equation, whereas the contribution of pure sucrose (X_1) was not significant; therefore, this variable was removed from the equation. Furthermore, ternary interactions neither contribute significantly to the bitterness equation. Bitterness intensity decreased when

stevia was mixed with sucrose or tagatose. More details of the model can be found in Table S2.

The bitterness model was employed to generate the respective contour plots (Figure 4-4). As expected, bitterness increases along the sweetness proportion of stevia. Therefore, bitterness for both binary and ternary mixtures remains relatively constant, at a same proportion of stevia. For example, similar bitterness intensities were predicted for the following sucrose/stevia/tagatose mixtures: (0.30/0.70/0); (0.15/0.70/0.15) and (0/0.70/0.30). Therefore, sucrose and tagatose exert both a similar effect in suppressing stevia bitterness. As mentioned above, the latter results from the fact that pure stevia contributed more than tagatose to bitterness in the Scheffe´s model and, therefore, the intensity of this attribute increases near the stevia vertex.

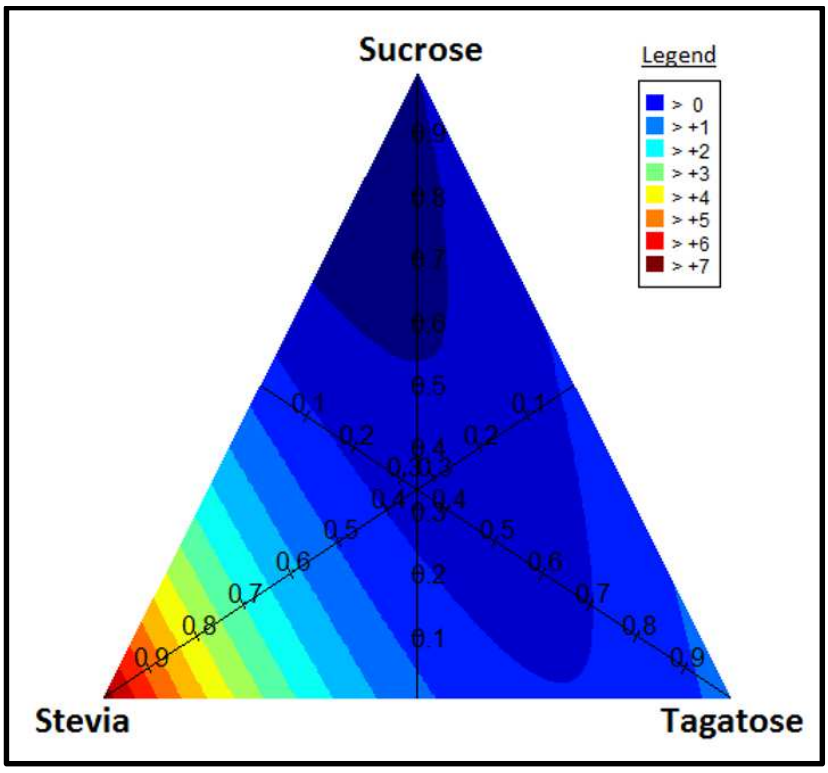

Figure 4-4: Contour plots for bitterness in carbonated soft drink. Each vertex represents a pure compound and the projected line represents the proportion of the respective compound in the mixture. Intensities of both attributes are indicated by colors.

Four checkpoints were assessed to determine the suitability of Scheffé's model for bitterness (Supplementary figure 4-2). Differences between observed and calculated values for bitterness (Table S3) were not perceptible, and can be tolerated considering the length of the scale. Furthermore, the panelists were asked for selecting the sample that tasted better, and most of them pointed sample 1 (0.3 sucrose, 0.45 stevia and 0.25 tagatose). Therefore, the surrounding area of this sample (within the contour plot) seems promising to further tests, considering the low intensity of undesirable off-tastes (Figure 4-4). These results indicate that the predictive power of the model is reasonable.

Considering cost and health issues, the amount of tagatose in the final product should be limited to 15 g per serving (35% of sweetness); indeed, an ileostomy study suggested that 15 g of D-tagatose added to diet daily is effective to control commonly occurring functional gastrointestinal disorders like irritable bowel syndrome (Normén et al..

Altogether, these results suggest that the optimal zone must be constrained to equi-sweet fractions of stevia comprised between 0.45 and 0.6; and tagatose fractions lower than 0.35 (Figure 4-6). Even though stevia does not contribute to the energetic content of the final product (Supplementary figure 4-7), bitterness limits its addition. Arbitrarily, the maximum sucrose fraction was set at 0.4, to achieve a reduction of at least 60% of sucrose.

4.3.4 Analysis of molecular interactions

We first compared the structure of the molecular models of the sweeteners sucrose, tagatose, stevioside and rebaudioside A, extracted from PubMed database, with their geometry optimized by PM3 semi-empirical quantum mechanics (Supplementary figure 4-3), to evaluate potential different conformational ensembles, as described for aspartame (Toniolo & Temussi 2016). Results showed that the structures were similar with root-mean-square error superposition values of 0.574, 0.368, 1.927 and 1.266 Å for sucrose, tagatose, stevioside and rebaudioside A, respectively.

Table 4-1: Binding free energy of selected sweeteners for sweet and bitter taste receptors

Number	Compound	$\Delta G_{binding}$ for hT1R2-hT1R3 (Kcal/mol) [a]	$\Delta G_{binding}$ for hT2R4 (Kcal/mol) [b]	$\Delta G_{binding}$ for hT2R14 (Kcal/mol) [b]
1	Sucrose	-6.7 (β_{11})	0 (β_{21})	0 (β_{31})
2	Tagatose	-6.3 (β_{13})	0 (β_{23})	0 (β_{33})
3	Stevioside	-9.0 (β_{12})	-6.7 (β_{22})	-6.6 (β_{32})
4	Rebaudioside A	-9.2 (β_{12})	-6.3 (β_{22})	-6.5 (β_{32})

The binding free energy were obtained from Acevedo et al., 2016 [b] and Acevedo et al., 2017 (In preparation) [a]
β_{ij} correspond to parameter of the multi-objective model

Table 1 shows the $\Delta G_{binding}$ values of sweeteners evaluated with hT1R2-hT1R3 sweet receptor, as well as hT2R4 and hT2R14 bitter receptors. Stevioside and rebaudioside A have lower $\Delta G_{binding}$ values with hT1R2-hT1R3 sweet taste receptor due to their physical-chemical properties, *i.e.* a chemical structure that combines a hydrophobic scaffold functionalized by hydrogen bond sites. Hence, $\Delta G_{binding}$ values of stevioside and rebaudioside A contribute more than sucrose and tagatose in the function for sweetness (equation 4.3). On the other hand, only $\Delta G_{binding}$ values of stevioside and rebaudioside A for both, hT2R4 and hT2R14, significantly contribute to bitterness (equations 4.4 and 4.5).
Figure 3-4 depicts the potential binding sites and poses of docked stevioside within the sweet taste receptor. Detailed inspection of the binding site within hT1R2 shows that the interaction between responsible amino acids and stevioside is carried out through hydrogen bonds and hydrophobic contacts. All the tested sweeteners bind to small binding cavities of hT1R2, as well as hT1R3.
Table 4-2 shows the binary and ternary interaction energies of sweeteners, as well as the associated best configuration (see also Supplementary figure 4-4). The interactions were included in the model because the sweeteners interact with each other before they bind to the taste receptors. The tagatose-rebA complex has the lowest $\Delta E_{interaction}$ because this pair of molecules could bind by higher number of hydrogen bonds than the rest of the complexes. Therefore, the combination of tagatose and rebaudioside A contributes more in the equation for both, sweetness and bitterness, than the rest of the interactions.

Table 4-2: Binary and ternary interaction energies (kcal/mol) of selected sweeteners (SUC: sucrose, TAG: tagatose, STE: stevioside, REB: rebaudioside A)

Interaction	Interaction energy (kcal/mol)
SUC-STE	-8.21 (β_{14})
SUC-REB	-9.09 (β_{14})
SUC-TAG	-8.81 (β_{15})
TAG-STE	-9.41 (β_{16})
TAG-REB	-11.18 (β_{16})
SUC-STE-TAG	-5.90 (β_{17})
SUC-REB-TAG	-9.27 (β_{17})
β_{ij} correspond to parameter of the multi-objective model SUC: sucrose, TAG: tagatose, STE: stevioside, REB: rebaudioside A.	

It is noteworthy that the multi-objective decision model without the contributions of the interactions between sweeteners yielded inconsistent results (Supplementary figure 4-5), *i.e.* only two extreme solutions (1/0/0 and 0/1/0) for combinations of sucrose-stevioside-tagatose, as well as for sucrose-rebA-tagatose. On the other hand, when both, binary and ternary interactions were included in the multi-objective model, results were consistent with experimental values.

4.3.5 Identification of optimal mixtures by multi-objective optimization

Supplementary figure 4-6 shows f1-norms and f2-norms, as well as the proportion of each component in the mixture, by incremental weight change. The intensity of off-tastes remains low in those samples where sucrose or tagatose predominate (in terms of sweetness), for weight values lower than 0.70. However, there was an abrupt rise of bitterness intensity as the proportion of both stevioside and rebaudioside A increases from 0.71 to 1.0 weight values.

Figure 4-5 illustrates the Pareto-optimal curve for the combinations of sucrose-stevioside-tagatose and sucrose-rebA-tagatose. The intensity of both, sweetness and bitterness, increases proportionally. Potential solutions from Pareto-optimal front for both combinations are shown in Table S4.

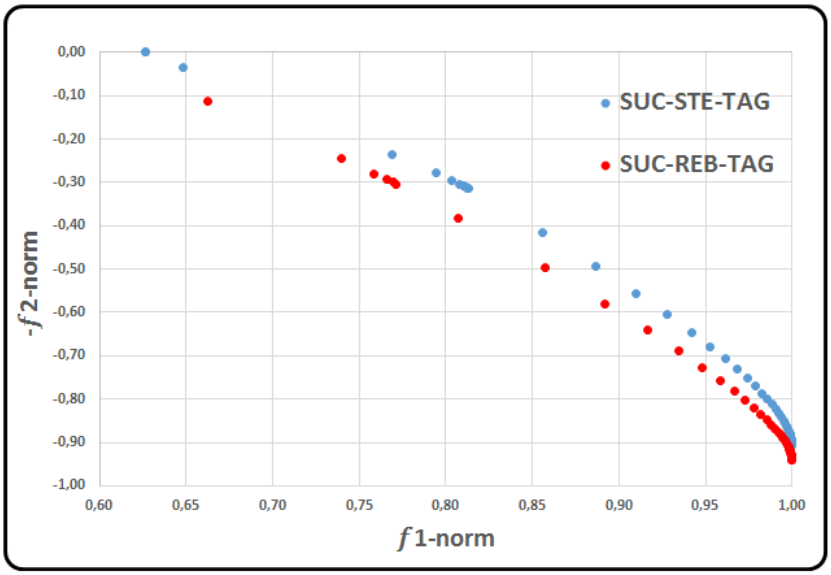

Figure 4-5: Pareto-optimal curve for the combinations of (a) sucrose-stevioside-tagatose and (b) sucrose-rebA-tagatose. f1-norm and f2-norm correspond to normalized functions for sweetness and bitterness, respectively.

Figure 4-6 shows the proposed optimal zone when all these constraints are incorporated: on one side, a minimum sucrose, stevioside and tagatose relative fractions of 0.24/0.45/0.26 and a maximum of 0.28/0.50/0.28, respectively; on the other, a minimum sucrose, rebaudioside A and tagatose proportion of 0.23/0.45/0.28 and a maximum of 0.26/0.50/0.29, respectively. The sweeteners proportions of these samples were calculated to achieve the minimum bitterness and maximum sweetness. Given these results, the optimal combinations of sucrose-stevioside-tagatose (27 g/L, 0.19 g/L, 34 g/L) and sucrose-rebA-tagatose (25 g/L, 0.19 g/L, 36 g/L) found by the multi-objective decision model are within the suitable zone experimentally identified by sensory optimization (Figure 4-6).

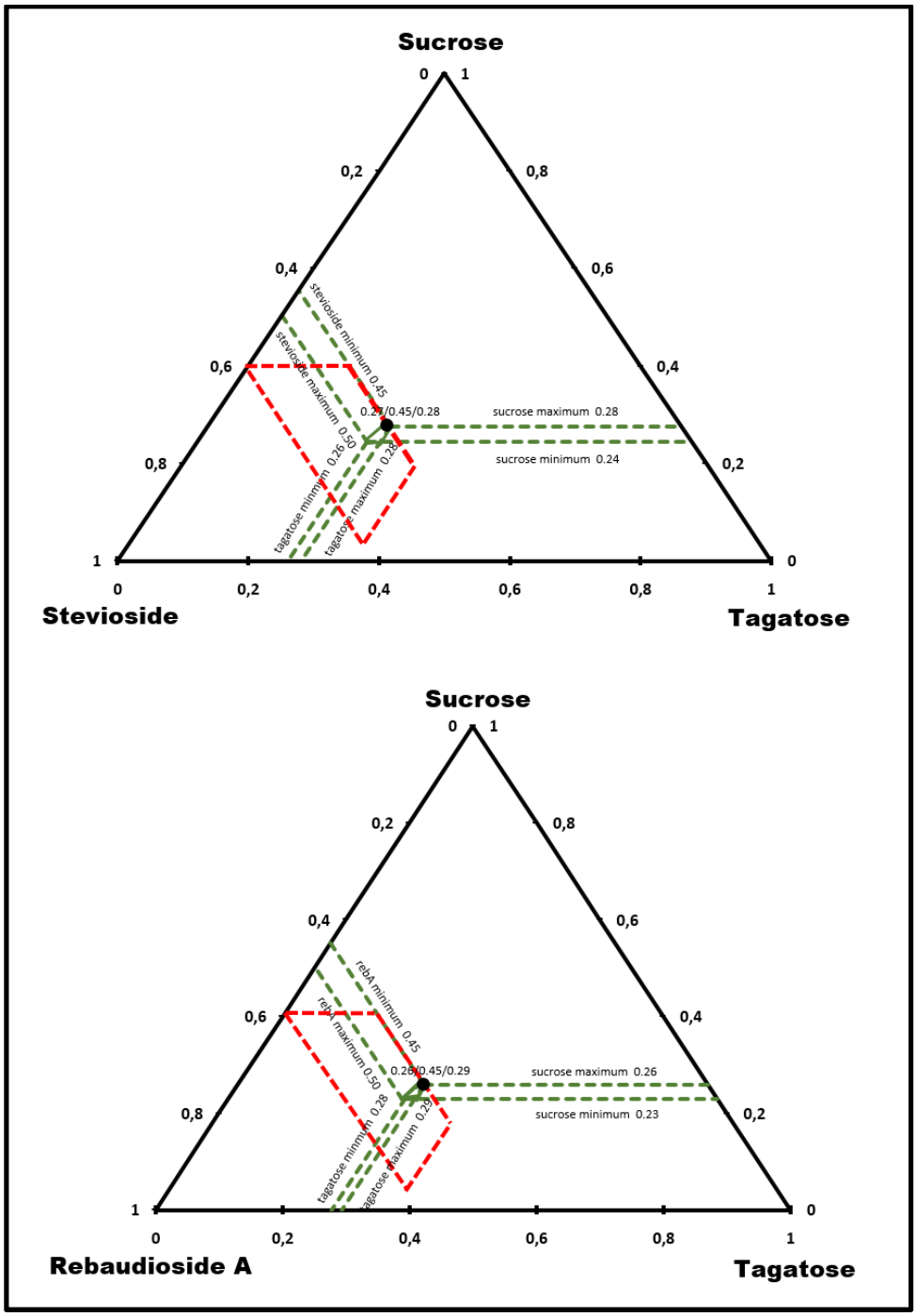

Figure 4-6: Optimal zones for the mixtures of (a) sucrose-stevioside-tagatose and (b) sucrose-rebA-tagatose identified by multi-objective optimization (green dotted line) and sensory optimization (red dotted line). Optimal combination of sweeteners in the carbonated soft drink are represented with a black circle inside the proposed optimal area.

4.4 Discussion

In this study we developed a multi-objective thermodynamically-based decision model to identify optimal mixtures of natural sweeteners. This model could be used as an alternative tool for product formulations of carbonated soft drinks, in addition to DOE and statistical techniques, such as surface response and desirability function (Granato & de Araújo Calado, 2013).

The interactions between sweeteners were found to be critical for model optimization. Indeed, these contributions describe the resulting organoleptic properties of the mixture, including sweetness synergy and masking undesirable tastes (Lawless et al. 1998; Andersen et al. 2002; Liao et al. 2015), substantially improving the predictive power of the multi-objective decision model. These results support the hypothesis that the sweeteners could interact with each other around the binding sites of the taste receptors. Indeed, the interactions between the sweeteners, i.e. sucrose, tagatose and stevia, are mainly governed by hydrogen bonding because of the hydroxyl groups present in their structures (Deshmukh, Bartolotti, & Gadre, 2008). These interactions could further promote their stability at the binding site.

The interaction of tagatose with both, stevioside and rebaudioside A, are energetically more stable than the rest of the evaluated complexes (Table 4-2). When combined with one or more high-intensity sweeteners, tagatose is able to improve the sensory characteristics of the sweetened product, such as mouthfeel, flavor and aftertaste (Andersen & Vigh, 2002). The use of tagatose as food ingredient is not only interesting for its flavor-enhancer properties, but also for its nutritional and physiological properties. Indeed, tagatose has been considered a prebiotic, based on the promotion of specific beneficial bacteria and the increase of short-chain fatty acids (SCFAs), due to its fermentation by colonic bacteria (Bertelsen, Jensen, & Buemann, 1999). Furthermore, tagatose does not affect plasma insulin and glucose levels in either normal or diabetic individuals, and even blunts the rise in plasma glucose when taken before an administration of oral glucose (Donner, Wilber, & Ostrowski, 1999). This property makes tagatose a desirable sugar substitute in food products for diabetics.

Despite the reduction of bitterness is crucial for the acceptability of the final product, the cost of ingredients and calories per serving can be used as supplementary factors when selecting sweetener combinations. In terms of cost, sucrose is the less expensive ingredient, whereas stevia is the most expensive (US$ 0.45 and US$ 150 per kg, respectively). However, due to the minimal amount of stevia used in each sample, the limiting ingredient in terms of cost is tagatose, with a sale price of US$ 10/kg (see Supplementary figure 4-8). Besides the cost, human tolerance to tagatose is an important issue to consider. Indeed, even though previous works have shown that tagatose is well tolerated by most subjects, gastrointestinal symptoms, such as flatulence, laxation, diarrhea and bloating were observed in some individuals at 30 g or higher doses. Hence, the intake of tagatose per eating occasion should not exceed this limit as a way to prevent commonly occurring functional gastrointestinal disorders like irritable bowel syndrome, a very common disorder among the population (Normén et al. 2001; Buemann et al. 1999). Considering cost and health issues, the amount of tagatose in the final product should be limited to 15 g per serving (35% of sweetness). Within these limits, the amount of tagatose added to the final mixture is key for reducing the proportion of sucrose and, therefore, the amount of calories per serving, maintaining a more "sugar like" taste profile (Supplementary figure 4-8).

As mentioned before, cost and heat energy are determinant factors to find an optimal product formula in terms of sweetness and bitterness intensity. A set of Pareto optimal solutions shows that, within the proposed optimal area, the optimal combinations of sucrose-stevioside-tagatose and sucrose-rebA-tagatose correspond to relative fractions of 0.27/0.45/0.28 and 0.26/0.45/0.29, respectively (Supplementary table 4-4). However, the cost of production and the amount of tagatose makes these mixtures less suitable. When price and calories reduction are incorporated, then relative fractions of 0.24/0.50/0.26 and 0.23/0.50/0.27 would be more appealing.

4.5 Conclusions

In conclusion, in this work, we demonstrated that a multi-objective decision model could be successfully employed to identify optimal mixtures of natural sweeteners - highest

sweetness and lowest bitterness - based on the interaction energies of sweetener-receptor and sweetener-sweetener complexes. The optimal mixtures predicted by multi-objective thermodynamic modeling were similar to those obtained through DOE and sensory analysis, demonstrating the robustness of the developed model. Therefore, the most suitable combinations, depending on the sweetness/bitterness balance, were those containing 23 - 39 g/L sucrose, 0.19 - 0.34 g/L stevia and 34 - 42 g/L tagatose.

Experimental sensory optimization validated the results predicted by the multi-objective decision model. A reduction of almost 60% of sucrose can be achieved using both stevia and tagatose, keeping bitterness intensity low. If further reduction is desired, ternary mixtures with a higher proportion of tagatose are a good option to maintain a more sugar-like taste. This could result in a 79% reduction of total calories compared to a regular soft drink (pure sucrose). However, if an economically feasible product is required, the reduction of the amount of tagatose would be mandatory.

Finally, multi-objective optimization will be a useful tool for developing new sweetener mixtures with other natural sweeteners, such as *Luo Han Guo* (also known as monk-fruit) or to reduce other unwanted attributes besides bitterness.

4.6 Acknowledgments

We are grateful to Professor Piero Andrea Temussi, from University of Naples, for his valuable comments that contributed significantly to improve the final manuscript; to Javier Sainz, from Prodalysa Inc. in Santiago, Chile, for his recommendations and suggestions during the course of this work; to Felipe Bravo, from Center for Bioinformatics and Integrative at University Andrés Bello, Santiago, for theoretical calculations of ternary interaction energy of sweeteners.

5. CONCLUSIONS

In this study, we constructed a comparative model for the hT1R2-hT1R3 sweetness receptor, as well as the hT2R4 and hT2R14 bitterness receptors, using reference structure of class A and C GPCR, which were subsequently validated using Ramachandran Plot. The construction of these three-dimensional models were useful to study the organoleptical properties of natural, non-caloric sweeteners - from glycosylated terpenoids to sweet proteins – at molecular level.

We predicted the intensity of bitterness of the active compounds in stevia from their binding free energy ($\Delta G_{binding}$) with the modeled bitter taste receptors. Calculated ΔG values negatively correlated with the reported bitterness of SG; that is, the more negative the $\Delta G_{binding}$ between the sweetener and the receptor, the greater the bitterness intensity.

Furthermore, bitterness intensity of SGs resulted from the following features: 1) the presence of transmembrane regions at the binding cavity of hT2R4 and hT2R14, which favors the interactions with SG by hydrophobic contact; 2) the ability to form hydrogen bonds with amino acids at the binding pocket due to the presence of sugars at the C-13 and C19 positions; and 3) the difference in the total number and type of monosaccharides present in their structures.

Our work provides a molecular rationale for the differences in sweetness intensity of different types of tastants, which can be summarized in the following features: 1) the importance of the electrostatic potential in the interaction of sweet proteins and sweet taste receptor; 2) the ability of GT to form hydrogen bonds with amino acids at the binding pocket due to the presence of sugars in their structures; 3) the establishment of hydrophobic interactions between the receptor and GTs, which could help to stabilize the closed conformation of the receptor VFD. Moreover, the strong correlation between our computational estimations and the binding affinities estimated at half maximal effective concentration (EC50), through cell-based calcium responses upon exposure to tastants, strengthens the idea of using molecular docking for designing and predicting the sweet taste of novel sweeteners.

Therefore, the affinity of SG for sweet taste receptors, as well as their differences in sweetness intensity, is due to their physical-chemical properties *i.e.* a chemical structure that combines a hydrophobic scaffold functionalized by a number of hydrogen bond sites. On the contrary, the affinity for bitter taste receptors could be due to the steric characteristics of SG and their binding site architecture.

Finally, we demonstrated that a multi-objective decision model could be successfully employed to identify optimal mixtures of natural sweeteners - maximum sweetness and minimum bitterness - based on the interaction energies of sweetener-receptor and sweetener-sweetener complexes predicted by molecular docking and quantum mechanics methods, respectively. The optimal mixtures predicted were similar to those obtained through DOE and sensory analysis, demonstrating the robustness of the model. Therefore, the most suitable combinations, depending on the sweetness/bitterness balance, were those containing 23 - 39 g/L sucrose, 0.19 – 0.34 g/L stevia and 34 - 42 g/L tagatose. Experimental sensory optimization validated the results predicted by the multi-objective decision model. A reduction of almost 60% of sucrose can be achieved using both stevia and tagatose, keeping bitterness intensity low. If further reduction is desired, ternary mixtures with a higher proportion of tagatose are a good option to maintain a more sugar-like taste. This could result in a 79% reduction of total calories compared to a regular soft drink (pure sucrose). However, if an economically feasible product is required, the reduction of the amount of tagatose would be mandatory. Finally, multi-objective optimization will be a useful tool for developing new sweetener mixtures with other natural sweeteners, such as *Luo Han Guo* (also known as monk-fruit) or to reduce other unwanted attributes besides bitterness.

Therefore, in order to validate our *in silico* results that strongly suggest that thee heterodimeric complex, composed by the hT1R2 and hT1R3 subunits, is required for activation of the sweetness receptor by sweet proteins as well as the calculated binding affinities of evaluated sweeteners with the taste receptor, we are currently working on evaluating the response of the HEK293 cells - transiently expressing hT1R2, hT1R3 or hT1R2/hT1R3 - to natural sweeteners, including sucrose, steviol glycosides, thaumatin.

6. PERSPECTIVES

The *in silico* results obtained in this thesis will be validated experimentally by activation *in vitro* essays of sweet taste receptor to sweeteners of different families, including glucose, sucrose, stevioside, rebaudioside A and thaumatin. The experimental essays will be carried out at the School of Medicine at the Pontificia Universidad Católica de Chile. *In vitro* affinity assays of interactions sweetener-receptor will be carried out as follows:

6.1 Molecular cloning of hT1R2 and hT1R3 subunits

The coding sequences of the hT1R2 and hT1R3 subunits retrieved from the NCBI (accession number NM_152232 and NM_152228, respectively) will be synthesized by Genscript (Piscataway, NJ, USA) and then linked to the pcDNA3.1 N-HA and pcDNA3.1 N-6histag commercial expression vectors by Gibson Assembly. These vectors allow the detection and quantification of the receptors through the Western Blot technique. In addition, the $G_{\alpha 16Gus44}$ chimeric G protein, described as a promiscuous G protein, will be synthesized allowing the activation cascade of various GPCRs (Ueda, Ugawa, Yamamura, Imaizumi, & Shimada, 2003)(Ohta, Masuda, Tani, & Kitabatake, 2011b).

6.2 Cell cultures and transfection of HEK 293 cells

Human embryonic cells 293, also known as HEK 293, will be cultured at 37°C, with 5% CO2 and 100% moisture, in DMEM medium with 4.5 g/L glucose, 10% FBS, 2 mmol/L l-glutamine, 100 U/ml penicillin and 100 U/ml streptomycin. Cell transfection will be performed by the lipofection method (Lipofectamine 2000, # 11668-027, Life technologies) using different concentrations of hT1R2 and hT1R3; and 50 ng of $G_{\alpha 16Gus44}$ protein. Transfections of the pcDNA3.1 N-HA and pcDNA3.1 N-6 histag empty vectors along with the $G_{\alpha 16Gus44}$ protein will be used as negative control (mock). The amount of transfected DNA will be the same in both cell types. Subsequently, the localization of taste receptor in the cell membrane will be checked through the indirect immunofluorescence technique at 24 or 48 hour post-transfection.

6.3 Activation *in vitro* assays of sweet taste receptors

The activation of taste receptors to different type of tastants will be evaluated by cell-based functional assay. This type of assay is very popular for evaluating the activity of GPCRs due to the availability of fluorescent markers sensitive to Ca^{2+} capable of permeating the cell membrane and the existence of automatic fluorescence readers (Hodder, 2004). Furthermore, this technique has been widely used to study taste receptors in general. For example, the contact site of the sweet protein thaumatin to the sweetness receptor was elucidated by expressing receptor chimeras in HEK 293 cells, and measuring their activity through Ca^{2+} measurements using Fluo-8AM (Ohta et al., 2011b).

In this study, the response of the HEK 293 cells - transiently expressing hT1R2, hT1R3 or hT1R2/hT1R3 – to sweet tastants will be analyzed by monitoring the level of intracellular Ca^{2+}. To do this, the taste receptor-expressing cells will be loaded with Ca^{2+}-sensitive fluorescent dyes, for example fluo-3, fluo-4 and fura-2, so that the cellular responses can be easily detected by measuring the changes in the fluorescent intensity produced by those indicators using quantitative fluorescence microscopy. It is worth noting that the response of taste receptor to glucose and caffeine will be used as positive and negative control, respectively.

The results obtained in cell-based functional assay will be used to validate the mode of interaction both of small sweeteners and sweet protein previously proposed by a molecular modeling-based docking simulation for sweet taste receptor, for example both subunits of receptor are required to be activated by sweet protein.

8. REFERENCES

Acevedo, W., Gonzalez-Nilo, F. D., & Agosin, E. (2016). Docking and Molecular Dynamics of Steviol Glycosides-Human Bitter Receptors Interactions. *Journal of Agricultural and Food Chemistry*, *64*(40), 7585–7596.

Adcock, S. A., & McCammon, J. A. (2006). Molecular dynamics: Survey of methods for simulating the activity of proteins. *Chemical Reviews*, *106*(5), 1589–1615.

Adler, E., Hoon, M. A., Mueller, K. L., Chandrashekar, J., Ryba, N. J., & Zuker, C. S. (2000). A Novel Family of Mammalian Taste Receptors. *Cell*, *100*(6), 693–702.

Amino, Y., Kawahara, S., Mori, K., Hirasawa, K., & Sakata, H. (2016). Preparation and Characterization of Four Stereoisomers of Monatin. *Chemical and Pharmaceutical Bulletin*, *64*(8), 1161–1171.

Andersen, H., & Vigh, M. (2002). Synergistic Combination of Sweeteners Including D-Tagatose. US.

Angelo, S., & O. Lord, J. (2010). Talin and Stevia - the natural choice. Retrieved from http://www.thaumatinnaturally.com/stevia.html

Assadi-Porter, F. M., Maillet, E. L., Radek, J. T., Quijada, J., Markley, J. L., & Max, M. (2010). Key amino acid residues involved in multi-point binding interactions between brazzein, a sweet protein, and the T1R2-T1R3 human sweet receptor. *Journal of Molecular Biology*, *398*(4), 584–99.

Avila-Salas, F., Sandoval, C., Caballero, J., Guiñez-Molinos, S., Santos, L. S., Cachau, R. E., & González-Nilo, F. D. (2012). Study of interaction energies between the PAMAM dendrimer and nonsteroidal anti-inflammatory drug using a distributed computational strategy and experimental analysis by ESI-MS/MS. *The Journal of Physical Chemistry*, *116*(7), 2031–2039.

Bassoli, A., Drew, M. G. B., Merlini, L., & Morini, G. (2002). General Pseudoreceptor Model for Sweet Compounds: A Semiquantitative Prediction of Binding Affinity for Sweet-Tasting Molecules. *Journal of Medicinal Chemistry*, *45*(20), 4402–4409.

Basu, S., McKee, M., Galea, G., & Stuckler, D. (2013). Relationship of soft drink consumption to global overweight, obesity, and diabetes: A cross-national analysis of 75 countries. *American Journal of Public Health*, *103*(11), 2071–2077.

Behrens, M., Brockhoff, A., Kuhn, C., Bufe, B., Winnig, M., & Meyerhof, W. (2004). The

human taste receptor hTAS2R14 responds to a variety of different bitter compounds. *Biochemical and Biophysical Research Communications*, *319*(2), 479–85.

Behrens, M., & Meyerhof, W. (2006). Bitter taste receptors and human bitter taste perception. *Cellular and Molecular Life Sciences*, *63*(13), 1501–1509.

Bertelsen, H., Jensen, B. B., & Buemann, B. (1999). D-tagatose - A Novel Low-Calorie Bulk Sweetener with Prebiotic Properties. *World Review of Nutrition and Dietetics*, *85*, 98–109.

Biasini, M., Bienert, S., Waterhouse, A., Arnold, K., Studer, G., Schmidt, T., … Schwede, T. (2014). SWISS-MODEL: modelling protein tertiary and quaternary structure using evolutionary information. *Nucleic Acids Research*, *42*(W1), W252–W258.

Birch, G. G., & Mylvaganam, A. R. (1976). Evidence for the proximity of sweet and bitter receptor sites. *Nature*, *260*(5552), 632–634.

Bradstock, M. K., Serdula, M. K., Marks, J. S., Barnard, R. J., Crane, N. T., Remington, P. L., & Trowbridge, L. (1986). Evaluation aspartame of reactions to food additives : the aspartame experience. *American Journal of Clinical Nutrition*, *43*(3), 464–469.

Brockhoff, A., Behrens, M., Niv, M. Y., & Meyerhof, W. (2010). Structural requirements of bitter taste receptor activation. *Proceedings of the National Academy of Sciences of the United States of America*, *107*(24), 11110–5.

Brooks, C. L. (2001). Ligand Protein Database. Retrieved May 30, 2015, from http://lpdb.chem.lsa.umich.edu/

Buemann, B., Toubro, S., Raben, A., & Astrup, A. (1999). Human tolerance to a single, high dose of D-tagatose. *Regulatory Toxicology and Pharmacology : RTP*, *29*(2), S66–S70.

Bufe, B., Breslin, P. A. S., Reed, D. R., Tharp, C. D., Slack, J. P., Kim, U.-K., … Meyerhof, W. (2005). The Molecular Basis of Individual Differences in Phenylthiocarbamide and Propylthiouracil Bitterness Perception. *Current Biology*, *15*(4), 322–327.

Bufe, B., Hofmann, T., Krautwurst, D., Raguse, J. D., & Meyerhof, W. (2002). The human TAS2R16 receptor mediates bitter taste in response to beta-glucopyranosides. *Nat Genet*, *32*(3), 397–401.

Canadian Sugar Institute. (2015). Sweetness of Sugar. Retrieved April 7, 2015, from http://www.sugar.ca/Nutrition-Information-Service/Consumers/Cooking-with-Sugar/Sweetness-of-Sugar.aspx

Carakostas, M., Prakash, I., Kinghorn, A. D., Wu, C. D., & Soejarto, D. D. (2012). Steviol glycosides. In L. B. Nabors (Ed.), *Alternative Sweeteners, 4th ed.* (Marcel Dek, pp. 159–180). New York, NY, USA.

Chandrashekar, J., Hoon, M. a, Ryba, N. J. P., & Zuker, C. S. (2006). The receptors and cells for mammalian taste. *Nature*, *444*(7117), 288–94.

Chéron, J.-B., Casciuc, I., Golebiowski, J., Antonczak, S., & Fiorucci, S. (2016). Sweetness prediction of natural compounds. *Food Chemistry*.

Choi, J. hye, & Chung, S. jin. (2014). Optimal sensory evaluation protocol to model concentration-response curve of sweeteners. *Food Research International*, *62*, 886–893.

Chun, L., Zhang, W., & Liu, J. (2012). Structure and ligand recognition of class C GPCRs. *Acta Pharmacologica Sinica*, *33*(3), 312–23.

Comeau, S. R., Gatchell, D. W., Vajda, S., & Camacho, C. J. (2004). ClusPro: a fully automated algorithm for protein-protein docking. *Nucleic Acids Research*, *32*(Web Server issue), W96-9.

Cowart, B. J. (1998). The Addition of CO2 to Traditional Taste Solutions Alters Taste Quality. *Chemical Senses*, *23*(1984), 397–402.

Cui, M., Jiang, P., Maillet, E., Max, M., Margolskee, R. F., & Osman, R. (2006). The heterodimeric sweet taste receptor has multiple potential ligand binding sites. *Current Pharmaceutical Design*, *12*(35), 4591–4600.

Deshmukh, M. M., Bartolotti, L. J., & Gadre, S. R. (2008). Intramolecular hydrogen bonding and cooperative interactions in carbohydrates via the molecular tailoring approach. *Journal of Physical Chemistry A*, *112*(2), 312–321. http://doi.org/10.1021/jp076316b

Di Salle, F., Cantone, E., Savarese, M. F., Aragri, A., Prinster, A., Nicolai, E., … Cuomo, R. (2013). Effect of carbonation on brain processing of sweet stimuli in humans. *Gastroenterology*, *145*(3), 537–539.

DiPizio, A., & Niv, M. Y. (2014). Computational studies of smell and taste receptors. *Israel Journal of Chemistry*, *54*, 1205–1218.

Donner, T. W., Wilber, J. F., & Ostrowski, D. (1999). D-tagatose, a novel hexose: acute effects on carbohydrate tolerance in subjects with and without type 2 diabetes. *Diabetes, Obesity & Metabolism*, *1*(5), 285–291.

DuBois, G. E., & Prakash, I. (2012). Non-caloric sweeteners, sweetness modulators, and

sweetener enhancers. *Annual Review of Food Science and Technology*, *3*, 353–80.

Espinoza, M. I., Vincken, J. P., Sanders, M., Castro, C., Stieger, M., & Agosin, E. (2014). Identification, quantification, and sensory characterization of steviol glycosides from differently processed stevia rebaudiana commercial extracts. *Journal of Agricultural and Food Chemistry*, *62*(49), 11797–11804.

Esposito, V., Gallucci, R., Picone, D., Saviano, G., Tancredi, T., Temussi, P. A., … Cnr, B. (2006). The Importance of Electrostatic Potential in The Interaction of Sweet Proteins with the Sweet Taste Receptor. *Journal of Molecular Biology*, *360*, 448–456.

Fan, C. F., Olafson, B. D., Blanco, M., & Hsu, S. L. (1992). Application of Molecular Simulation To Derive Phase Diagrams of Binary Mixtures, 3667–3676.

Findlay, C. J., Castura, J. C., & Lesschaeve, I. (2007). Feedback calibration: A training method for descriptive panels. *Food Quality and Preference*, *18*, 321–328.

Floriano, W. B., Hall, S., Vaidehi, N., Kim, U., Drayna, D., & Goddard, W. a. (2006). Modeling the human PTC bitter-taste receptor interactions with bitter tastants. *Journal of Molecular Modeling*, *12*(6), 931–41.

Fogh, R. H., Boucher, W., Vranken, W. F., Pajon, A., Stevens, T. J., Bhat, T. N., … Laue, E. D. (2005). A framework for scientific data modeling and automated software development. *Bioinformatics*, *21*(8), 1678–1684.

Fujimaru, T., Park, J. H., & Lim, J. (2012). Sensory Characteristics and Relative Sweetness of Tagatose and Other Sweeteners. *Journal of Food Science*, *77*(9), S323–S328.

Gorman, J. W., & Hinman, J. E. (1962). Simplex lattice designs for multicomponent systems. *Technometrics*, *4*(October 2013), 463–487.

Granato, D., & de Araújo Calado, V. M. (2013). The use and importance of design of experiments (DOE) in process modelling in food science and technology. In D. Granato (Ed.), *Mathematical and Statistical Methods in Food Science and Technology* (pp. 1–18).

Grant E. DuBois, Walters, D. E., Schiffman, S. S., Warwick, Z. S., Booth, B. J., Pecore, S. D., … 1, L. M. B. (1991). Concentration—Response Relationships of Sweeteners. *ACS Symposium Series*, *450*, 261–276.

Grosdidier, A., Zoete, V., & Michielin, O. (2011). SwissDock, a protein-small molecule docking web service based on EADock DSS. *Nucleic Acids Research*, *39*(SUPPL. 2), 270–277.

Heikel, B., Krebs, E., Köhn, E., & Busch-Stockfisch, M. (2012). Optimizing Synergism of

Binary Mixtures of Selected Alternative Sweeteners. *Journal of Sensory Studies*, *27*(5), 295–303.

Hellfritsch, C., Brockhoff, A., Stähler, F., Meyerhof, W., & Hofmann, T. (2012). Human Psychometric and Taste Receptor Responses to Steviol Glycosides. *Journal of Agricultural and Food Chemistry*, *60*(27), 6782–93.

Hewson, L., Hollowood, T., Chandra, S., & Hort, J. (2009). Gustatory, olfactory and trigeminal interactions in a model carbonated beverage. *Chemosensory Perception*, *2*(2), 94–107.

Hodder, P. (2004). Miniaturization of Intracellular Calcium Functional Assays to 1536-Well Plate Format Using a Fluorometric Imaging Plate Reader. *Journal of Biomolecular Screening*, *9*(5), 417–426.

Hu, F. B., & Malik, V. S. (2010). Sugar-sweetened beverages and risk of obesity and type 2 diabetes: epidemiologic evidence. *Physiology & Behavior*, *100*(1), 47–54.

Humphrey, W., Dalke, A., & Schulten, K. (1996). VMD: Visual Molecular Dynamics. *Journal of Molecular Graphics*, *14*, 33–38.

James J. P. Stewart. (2016). Stewart Computational Chemistry - MOPAC Home Page. Retrieved March 22, 2017, from http://openmopac.net/

Ji, M., Su, X., Su, X., Chen, Y., Huang, W., Zhang, J., … Lu, X. (2014). Identification of Novel Compounds for Human Bitter Taste Receptors. *Chemical Biology & Drug Design*, *84*(1), 63–74.

Jiang, P., Ji, Q., Liu, Z., Snyder, L. a, Benard, L. M. J., Margolskee, R. F., & Max, M. (2004). The cysteine-rich region of T1R3 determines responses to intensely sweet proteins. *The Journal of Biological Chemistry*, *279*(43), 45068–75.

Kaneko, R., & Kitabatake, N. (2001). Structure-sweetness relationship in thaumatin: importance of lysine residues. *Chemical Senses*, *26*, 167–177.

Kant, R. (2005). Sweet proteins - potential replacement for artificial low calorie sweeteners. *Nutrition Journal*, *4*(5), 1–6.

Kappes, S. M., Schmidt, S. J., & Lee, S. Y. (2006). Descriptive analysis of cola and lemon/lime carbonated beverages. *Journal of Food Science*, *71*(8), S583–S589.

Kinghora, A. D., Soejarto, D. D., & Inglett, G. E. (1986). Sweetening agents of plant origin. *Critical Reviews in Plant Sciences*, *4*(2), 79–120.

Kinghorn, A. D., Chin, Y., Pan, L., & Ohio, T. (2010). *Natural Products as Sweeteners and Sweetness Modifiers*. *Comprehensive Natural Products II: Chemistry and*

Biology.

Kroyer, G. (2010). Stevioside and Stevia-sweetener in food: Application, stability and interaction with food ingredients. *Journal of Consumer Protection and Food Safety*, *5*(2), 225–229.

Kubota, A., & Kubo, I. (1969). Bitterness and Chemical Structure. *Nature*, *223*, 97–99.

Kuhn, C., Bufe, B., Winnig, M., Hofmann, T., Frank, O., Behrens, M., … Meyerhof, W. (2004). Bitter Taste Receptors for Saccharin and Acesulfame K. *The Journal of Neuroscience*, *24*(45), 10260–5.

Lawless, H. T., Science, F., & Hall, S. (1998). Theoretical note: Tests of synergy in sweetener mixtures. *Chemical Senses*, *23*, 447–451.

Lee, T., Radko, G., Chen, H., & Chang, P. K. (2010). Use of Erythritol and D-tagatose in Diet or Reduced-calorie Beverages and Food Products. United States.

Li, X., Staszewski, L., Xu, H., Durick, K., Zoller, M., & Adler, E. (2002). Human receptors for sweet and umami taste. *Proceedings of the National Academy of Sciences of the United States of America*, *99*(7), 4692–96.

Liao, F., Xu, H., Torrey, N., Road, P., & Jolla, L. (2015). Physical Approaches to Masking Bitter Taste: Lessons from Food and Pharmaceuticals. *Pharmaceutical Research*, *2*(74), 2921–2939.

Liu, B., Ha, M., Meng, X.-Y., Khaleduzzaman, M., Zhang, Z., Li, X., & Cui, M. (2012). Functional characterization of the heterodimeric sweet taste receptor T1R2 and T1R3 from a New World monkey species (squirrel monkey) and its response to sweet-tasting proteins. *Biochemical and Biophysical Research Communications*, *427*(2), 431–7.

Lobley, A., Sadowski, M. I., & Jones, D. T. (2009). pGenTHREADER and pDomTHREADER: new methods for improved protein fold recognition and superfamily discrimination. *Bioinformatics (Oxford, England)*, *25*(14), 1761–7.

Loncharich, R. J., & Brooks, B. R. (1989). The effects of truncating long-range forces on protein dynamics. *Proteins: Structure, Function, and Genetics*, *6*(1), 32–45.

Lovell, S. C., Davis, I. W., Arendall, W. B., de Bakker, P. I. W., Word, J. M., Prisant, M. G., … Richardson, D. C. (2003). Structure validation by Calpha geometry: phi,psi and Cbeta deviation. *Proteins*, *50*(3), 437–450.

Maillet, E. L., Cui, M., Jiang, P., Mezei, M., Hecht, E., Quijada, J., … Max, M. (2015). Characterization of the binding site of aspartame in the human sweet taste receptor.

Chemical Senses, *40*(8), 577–586.

Malik, V., Popkin, B., Bray, G., Després, J.-P., & Hu, F. (2010). Sugar Sweetened Beverages, Obesity, Type 2 Diabetes and Cardiovascular Disease risk. *Circulation*, *121*(11), 1356–1364.

Malik, V. S., Popkin, B. M., & Bray, G. A. (2010). Sugar-Sweetened Beverages and Risk of Metabolic Syndrome and Type 2 Diabetes. *Reviews/Commentaries/ADA Statements*, *33*(11), 2477–81.

Marchiori, A., Capece, L., Giorgetti, A., Gasparini, P., Behrens, M., Carloni, P., & Meyerhof, W. (2013). Coarse-grained/molecular mechanics of the TAS2R38 bitter taste receptor: experimentally-validated detailed structural prediction of agonist binding. *PloS One*, *8*(5), 1–12.

Masuda, K., Koizumi, A., Nakajima, K., Tanaka, T., Abe, K., Misaka, T., & Ishiguro, M. (2012). Characterization of the modes of binding between human sweet taste receptor and low-molecular-weight sweet compounds. *PloS One*, *7*(4), 1–10.

Masuda, T., Ohta, K., Ojiro, N., Murata, K., Mika, B., Tani, F., … Kitabatake, N. (2016). A Hypersweet Protein: Removal of The Specific Negative Charge at Asp21 Enhances Thaumatin Sweetness. *Scientific Reports*, *6*, 1–9.

Masuda, T., Taguchi, W., Sano, A., Ohta, K., Kitabatake, N., & Tani, F. (2013). Five amino acid residues in cysteine-rich domain of human T1R3 were involved in the response for sweet-tasting protein, thaumatin. *Biochimie*, *95*(7), 1502–5.

Mayank, & Vikas, J. (2015). Interaction model of steviol glycosides from Stevia rebaudiana (Bertoni) with sweet taste receptors: A computational approach. *Phytochemistry*, *116*, 12–20.

Meyerhof, W. (2005). Elucidation of mammalian bitter taste. *Reviews of Physiology, Biochemistry and Pharmacology*, *154*(July), 37–72.

Meyerhof, W., Batram, C., Kuhn, C., Brockhoff, A., Chudoba, E., Bufe, B., … Behrens, M. (2010). The molecular receptive ranges of human TAS2R bitter taste receptors. *Chemical Senses*, *35*(2), 157–70.

Meyerhof, W., Born, S., Brockhoff, A., & Behrens, M. (2011). Molecular biology of mammalian bitter taste receptors. A review. *Flavour and Fragrance Journal*, *26*(4), 260–268.

Mirzadeh, M., Theillard, M., Helgadóttir, A., Boy, D., & Gibou, F. (2013). An adaptive, finite difference solver for the nonlinear poisson-boltzmann equation with applications to biomolecular computations. *Communications in Computational*

Physics, *13*(1), 150–173.

Morini, G., Bassoli, A., & Temussi, P. a. (2005). From small sweeteners to sweet proteins: anatomy of the binding sites of the human T1R2_T1R3 receptor. *Journal of Medicinal Chemistry*, *48*(17), 5520–29. http://doi.org/10.1021/jm0503345

Morris, G. M., Huey, R., Lindstrom, W., Sanner, M. F., Belew, R. K., Goodsell, D. S., & Olson, A. J. (2009). AutoDock4 and AutoDockTools4: Automated Docking with Selective Receptor Flexibility. *Journal of Computational Chemistry*, *30*(16), 2785–2791.

Muto, T., Tsuchiya, D., Morikawa, K., & Jingami, H. (2007). Structures of the extracellular regions of the group II/III metabotropic glutamate receptors. *Proceedings of the National Academy of Sciences*, *104*(10), 3759–3764. http://doi.org/10.1073/pnas.0611577104

National Cancer Institute. (2009). Artificial Sweeteners and Cancer - National Cancer Institute. Retrieved June 19, 2014, from http://www.cancer.gov/cancertopics/factsheet/Risk/artificial-sweeteners

National Center for Biotechnology Information. (2004). The PubChem Project. Retrieved November 26, 2015, from http://pubchem.ncbi.nlm.nih.gov/

Nelson, G., Hoon, M. A., Chandrashekar, J., Zhang, Y., Ryba, N. J. P., & Zuker, C. S. (2001). Mammalian Sweet Taste Receptors. *Cell*, *106*(3), 381–390.

Ngatchou, P., Zarei, A., & El-Sharkawi, A. (2005). Pareto Multi Objective Optimization. *Proceedings of the 13th International Conference On, Intelligent Systems Application to Power Systems*, 84–91.

Niccolai, N., Spadaccini, R., Scarselli, M., Bernini, A., Crescenzi, O., Spiga, O., … Temussi, P. A. (2001). Probing the surface of a sweet protein : NMR study of MNEI with a paramagnetic probe. *Protein Science*, *10*, 1498–1507.

Nilges, M., Bernard, A., Bardiaux, B., Malliavin, T., Habeck, M., & Rieping, W. (2008). Accurate NMR Structures Through Minimization of an Extended Hybrid Energy. *Structure*, *16*(9), 1305–1312.

Nofre, C., & Tinti, J. M. (1996). Sweetness reception in man: The multipoint attachment theory. *Food Chemistry*, *56*(3), 263–274.

Nordström, K. J. V, Sällman Almén, M., Edstam, M. M., Fredriksson, R., & Schiöth, H. B. (2011). Independent HHsearch, Needleman-Wunsch-based, and motif analyses reveal the overall hierarchy for most of the g protein-coupled receptor families. *Molecular Biology and Evolution*, *28*(9), 2471–2480.

Normén, L., Lærke, H. N., Jensen, B. B., Langkilde, A. M., & Andersson, H. (2001). Small-bowel absorption of D-tagatose and related effects on carbohydrate digestibility : an ileostomy study. *American Journal of Clinical Nutrition*, *73*, 105–10.

O'Boyle, N. M., Banck, M., James, C. A., Morley, C., Vandermeersch, T., & Hutchison, G. R. (2011). Open Babel: An Open chemical toolbox. *Journal of Cheminformatics*, *3*(10), 1–14.

Ohta, K., Masuda, T., Ide, N., & Kitabatake, N. (2008). Critical molecular regions for elicitation of the sweetness of the sweet-tasting protein, thaumatin I. *The FEBS Journal*, *275*(14), 3644–52.

Ohta, K., Masuda, T., Tani, F., & Kitabatake, N. (2011a). Introduction of a negative charge at Arg82 in thaumatin abolished responses to human T1R2-T1R3 sweet receptors. *Biochemical and Biophysical Research Communications*, *413*(1), 41–5.

Ohta, K., Masuda, T., Tani, F., & Kitabatake, N. (2011b). The cysteine-rich domain of human T1R3 is necessary for the interaction between human T1R2-T1R3 sweet receptors and a sweet-tasting protein, thaumatin. *Biochemical and Biophysical Research Communications*, *406*(3), 435–8.

Parmentier, M., Prézeau, L., Bockaert, J., & Pin, J. (2002). A model for the functioning of family 3 GPCRs, *23*(6), 268–274.

Phillips, J. C., Braun, R., Wang, W., Gumbart, J., Tajkhorshid, E., Villa, E., … Schulten, K. (2005). Scalable molecular dynamics with NAMD. *Journal of Computational Chemistry*, *26*(16), 1781–802.

Picone, D., & Temussi, P. A. (2012). Dissimilar sweet proteins from plants: oddities or normal components? *Plant Science : An International Journal of Experimental Plant Biology*, *195*, 135–42.

Pin, J.-P., Galvez, T., & Prézeau, L. (2003). Evolution, structure, and activation mechanism of family 3/C G-protein-coupled receptors. *Pharmacology & Therapeutics*, *98*(3), 325–354.

Pin, J., Kniazeff, J., Goudet, C., Bessis, A., Liu, J., & Galvez, T. (2004). The activation mechanism of class-C G-protein coupled receptors, *96*, 335–342.

Pineau, N., Chabanet, C., & Schlich, P. (2007). Modeling the evolution of the performance of a sensory panel: A mixed-model and control chart approach. *Journal of Sensory Studies*, *22*(2), 212–241.

Portmann, M. O., & Kilcast, D. (1996). Psychophysical characterization of new sweeteners of commercial importance for the EC food industry. *Food Chemistry*, *56*(3), 291–302.

Prakash, I., Dubois, G. E., Clos, J. F., Wilkens, K. L., & Fosdick, L. E. (2008). Development of rebiana, a natural, non-caloric sweetener. *Food and Chemical Toxicology : An International Journal Published for the British Industrial Biological Research Association*, *46*, S75-82.

Prakash, I., Markosyan, A., & Bunders, C. (2014). Development of Next Generation Stevia Sweetener: Rebaudioside M. *Foods*, *3*(1), 162–175.

Pronin, A. N., Tang, H., Connor, J., & Keung, W. (2004). Identification of ligands for two human bitter T2R receptors. *Chemical Senses*, *29*(7), 583–593.

Pronin, A. N., Xu, H., Tang, H., Zhang, L., Li, Q., & Li, X. (2007). Specific Alleles of Bitter Receptor Genes Influence Human Sensitivity to the Bitterness of Aloin and Saccharin. *Current Biology*, *17*(16), 1403–1408.

Pydi, S. P., Bhullar, R. P., & Chelikani, P. (2012). Constitutively active mutant gives novel insights into the mechanism of bitter taste receptor activation. *Journal of Neurochemistry*, *122*(3), 537–44.

Pydi, S. P., Singh, N., Upadhyaya, J., Bhullar, R. P., & Chelikani, P. (2014). The third intracellular loop plays a critical role in bitter taste receptor activation. *Biochimica et Biophysica Acta*, *1838*(1), 231–36.

Rezácová, P., Borek, D., Moy, S. F., Joachimiak, A., & Otwinowski, Z. (2008). Crystal structure and putative function of small Toprim domain-containing protein from Bacillus stearothermophilus. *Proteins*, *70*(2), 311–319.

Rocha, I. F. de O., & Bolini, H. M. A. (2015). Passion fruit juice with different sweeteners: sensory profile by descriptive analysis and acceptance. *Food Science & Nutrition*, *3*(2), 129–39.

Roth, T. (2012). qualityTools: Statistical Methods for Quality Science.

Roudnitzky, N., Bufe, B., Thalmann, S., Kuhn, C., Gunn, H. C., Xing, C., … Wooding, S. P. (2011). Genomic, genetic and functional dissection of bitter taste responses to artificial sweeteners. *Human Molecular Genetics*, *20*(17), 3437–3449.

Schifferstein, H. N. J. (1996). Cognitive factors affecting taste intensity judgments. *Food Quality and Preference*, *7*(3), 167–175.

Schiffman, S. S., Booth, B. J., Losee, M. L., Pecore, S. D., & Warwick, Z. S. (1995). Bitterness of sweeteners as a function of concentration. *Brain Research Bulletin*, *36*(5), 505–513.

Schiffman, S. S., Sattely-miller, E. A., Graham, B. G., Zervakis, J., Butchko, H. H., &

Stargel, W. W. (2003). Effect of Repeated Presentation on Sweetness Intensity of Binary and Ternary Mixtures of Sweeteners. *Chemical Senses*, *28*, 219–229.

Schweden, T., Kopp, J., Guex, N., & Peitsch, M. C. (2003). SWISS-MODEL: an automated protein homology-modeling server. *Nucleic Acids Research*, *31*(13), 3381–3385.

Serio, C. Di, Lio, P., Nonis, A., & Tagliaferri, R. (2014). *Computational Intelligence Methods for Bioinformatics and Biostatistics*. Springer Verlag.

Shallenberger, R. S., & Acre, T. E. (1967). Molecular Theory of Sweet Taste. *Nature*, *216*, 480–482.

Shankar, P., Ahuja, S., & Sriram, K. (2013). Non-nutritive sweeteners: review and update. *Nutrition*, *29*(11–12), 1293–9.

SIB Swiss Institute of Bioinformatics and the Biozentrum, & der Universität Basel, S. (2003). SWISS-MODEL. Retrieved November 26, 2015, from http://swissmodel.expasy.org/

Singh, N., Pydi, S. P., Upadhyaya, J., & Chelikani, P. (2011). Structural basis of activation of bitter taste receptor T2R1 and comparison with Class A G-protein-coupled receptors (GPCRs). *The Journal of Biological Chemistry*, *286*(41), 36032–41.

Singla, R., & Jaitak, V. (2016). Synthesis of rebaudioside A from stevioside and their interaction model with hTAS2R4 bitter taste receptor. *Phytochemistry*, *125*, 106–111.

Sippl, M. J., & Wiederstein, M. (2008). Structural bioinformatics A note on difficult structure alignment problems. *Structural Bioinformatics*, *24*(3), 426–427.

Sippl, M. J., & Wiederstein, M. (2012). Detection of spatial correlations in protein structures and molecular complexes. *Structure*, *20*(4), 718–728.

Slack, J. P., Brockhoff, A., Batram, C., Menzel, S., Sonnabend, C., Born, S., … Meyerhof, W. (2010). Modulation of bitter taste perception by a small molecule hTAS2R antagonist. *Current Biology : CB*, *20*(12), 1104–9.

Smith, S. O. (2010). Structure and activation of the visual pigment rhodopsin. *Annual Review of Biophysics*, *39*, 309–28.

Soffritti, M., Belpoggi, F., Degli Esposti, D., Lambertini, L., Tibaldi, E., & Rigano, A. (2006). First experimental demonstration of the multipotential carcinogenic effects of aspartame administered in the feed to Sprague-Dawley rats. *Environmental Health Perspectives*, *114*(3), 379–385.

Sommer, B. (2013). Membrane Packing Problems: A short Review on computational

Membrane Modeling Methods and Tools. *Computational and Structural Biotechnology Journal*, *5*(6), e201302014.

Stewart, J. J. P. (2013). Optimization of parameters for semiempirical methods VI: More modifications to the NDDO approximations and re-optimization of parameters. *Journal of Molecular Modeling*, *19*(1), 1–32.

Suez, J., Korem, T., Zeevi, D., Zilberman-Schapira, G., Thaiss, C. A., Maza, O., … Elinav, E. (2014). Artificial sweeteners induce glucose intolerance by altering the gut microbiota. *Nature*, *514*(7521), 181–197.

Tan, J., Abrol, R., Trzaskowski, B., & Goddard, W. A. (2012). 3D structure prediction of TAS2R38 bitter receptors bound to agonists phenylthiocarbamide (PTC) and 6-n-propylthiouracil (PROP). *Journal of Chemical Information and Modeling*, *52*(7), 1875–1885.

Tancredi, T., Pastore, A., Salvadori, S., Esposito, V., & Temussi, P. a. (2004). Interaction of sweet proteins with their receptor. A conformational study of peptides corresponding to loops of brazzein, monellin and thaumatin. *European Journal of Biochemistry / FEBS*, *271*(11), 2231–40.

Temussi, P. a. (2006). Natural sweet macromolecules: how sweet proteins work. *Cellular and Molecular Life Sciences : CMLS*, *63*(16), 1876–88.

Temussi, P. A. (2002). Why are sweet proteins sweet? Interaction of brazzein, monellin and thaumatin with the T1R2-T1R3 receptor. *FEBS Letters*, *526*(1–3), 1–4.

Temussi, P. A. (2011). *New insights into the characteristics of sweet and bitter taste receptors. International review of cell and molecular biology* (1st ed., Vol. 291). Elsevier Inc.

Toniolo, C., & Temussi, P. (2016). Conformational flexibility of aspartame. *Biopolymers*, *106*(3), 376–384.

Trott, O., & Olson, A. J. (2009). AutoDock Vina: Improving the Speed and Accuracy of Docking with a New Scoring Function , Efficient Optimization , and Multithreading. *Journal of Computational Chemistry*, *31*(2), 455–61.

Ueda, T., Ugawa, S., Yamamura, H., Imaizumi, Y., & Shimada, S. (2003). Functional interaction between T2R taste receptors and G-protein alpha subunits expressed in taste receptor cells. *The Journal of Neuroscience : The Official Journal of the Society for Neuroscience*, *23*(19), 7376–80.

Upadhyaya, J., Pydi, S. P., Singh, N., Aluko, R. E., & Chelikani, P. (2010). Bitter taste receptor T2R1 is activated by dipeptides and tripeptides. *Biochemical and Biophysical*

Research Communications, *398*(2), 331–5.

Vangone, A., & Bonvin, A. M. (2015). Contacts-based prediction of binding affinity in protein-protein complexes. *eLife*, *4*(e07454), 1–20.

Vanommeslaeghe, K., Hatcher, E., Acharya, C., Kundu, S., Zhong, S., Shim, J., … Jr, A. D. M. (2010). CHARMM General Force Field: A Force Field for Drug-Like Molecules Compatible with the CHARMM All-Atom Additive Biological Force Fields. *Journal of Computational Chemistry*, *31*(4), 671–690.

Vartanian, L. R., Schwartz, M. B., & Brownell, K. D. (2007). Effects of soft drink consumption on nutrition and health: a systematic review and meta-analysis. *American Journal of Public Health*, *97*(4), 667–75.

Verdi, R. J., & Hood, L. L. (1993). Advantages of alternative sweetener blends. *Food Technology*, *47*(6), 94–101.

Vigues, S., Dotson, C. D., & Munger, S. D. (2009). The receptor basis of sweet taste in mammals. *Chemosensory Systems in Mammals, Fishes, and Insects*, *47*, 187–202.

Waldrop, M. E., & Ross, C. F. (2014). Sweetener blend optimization by using mixture design methodology and the electronic tongue. *Journal of Food Science*, *79*(9), 1782–94.

Wallace, A. C., Laskowski, R. A., & Thornton, J. M. (1995). LIGPLOT: a program to generate schematic diagrams of protein-ligand interactions. *Protein Engineering*, *8*(2), 127–134.

Wang, Z., & Rangaiah, G. P. (2017). Application and Analysis of Methods for Selecting an Optimal Solution from the Pareto-Optimal Front obtained by Multiobjective Optimization. *Industrial & Engineering Chemistry Research*, *56*(2), 560–574.

Wintjens, R., Viet, T. M. V. N., Mbosso, E., & Huet, J. (2011). Hypothesis/review: the structural basis of sweetness perception of sweet-tasting plant proteins can be deduced from sequence analysis. *Plant Science : An International Journal of Experimental Plant Biology*, *181*(4), 347–54.

World Health Organization. (2013). About Noncommunicable Diseases and Mental Health. Retrieved November 7, 2013, from http://www.who.int/mediacentre/factsheets/fs355/en/

Worth, C. L., Kreuchwig, A., Kleinau, G., & Krause, G. (2011). GPCR-SSFE: a comprehensive database of G-protein-coupled receptor template predictions and homology models. *BMC Bioinformatics*, *12*(1), 185–195.

Xu, H., Staszewski, L., Tang, H., Adler, E., Zoller, M., & Li, X. (2004). Different functional roles of T1R subunits in the heteromeric taste receptors. *Proceedings of the National Academy of Sciences of the United States of America*, *101*(39), 14258–63.

Xue, L. C., Rodrigues, J. P., Kastritis, P. L., Bonvin, A. M., & Vangone, A. (2016). PRODIGY: a web server for predicting the binding affinity of protein–protein complexes. *Bioinformatics*, *32*(23), 3676–3678.

Zhang, F., Klebansky, B., Fine, R. M., Liu, H., Xu, H., Servant, G., … Li, X. (2010). Molecular mechanism of the sweet taste enhancers. *Proceedings of the National Academy of Sciences of the United States of America*, *107*(10), 4752–7.

ANNEXES

Supplementary figure 2-1: Ramachandran plots for hT2R4 (a), hT2R14 (b) and hT2R1 (c) receptors. The dark blue region indicates the favoured regions; the clear blue region represents the permitted regions; yellow indicates the generously allowed regions; and white, the outlier regions. hT2R1 is used as a negative control.

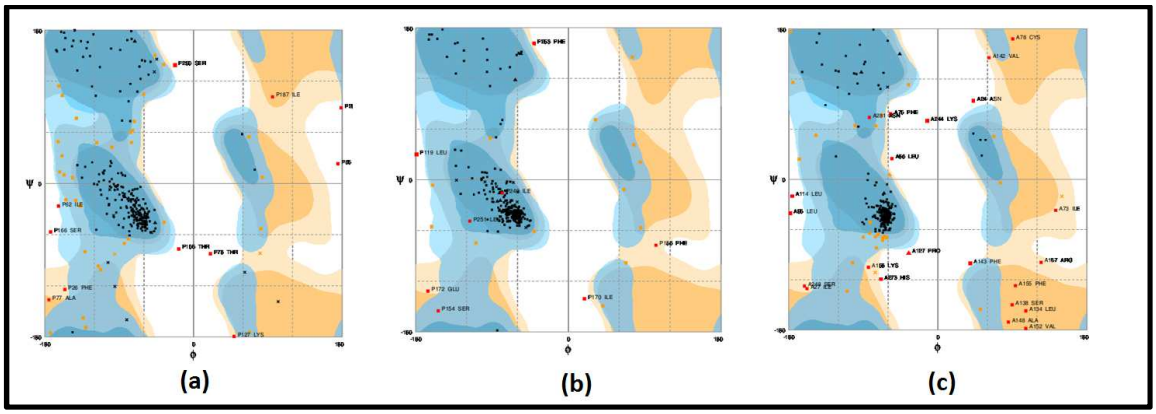

Supplementary figure 2-2: Energy minimization of different complexes for 1000 steps.

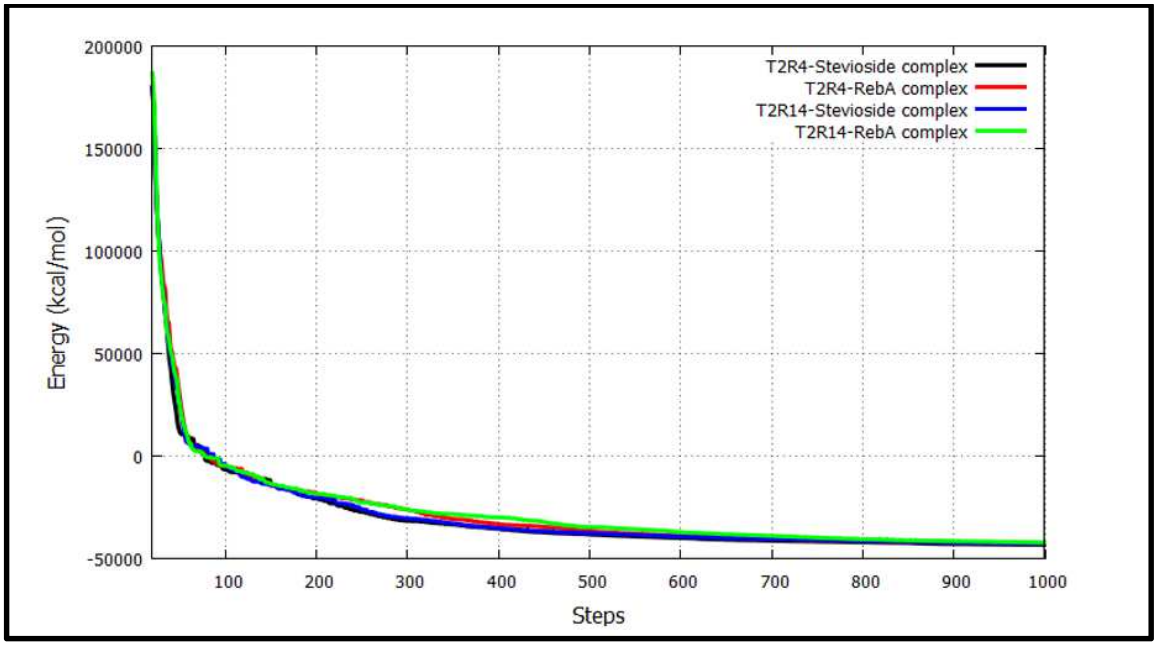

Supplementary figure 2-3: RMSD values show the conformational stability of both hT2R4 and hT2R14.

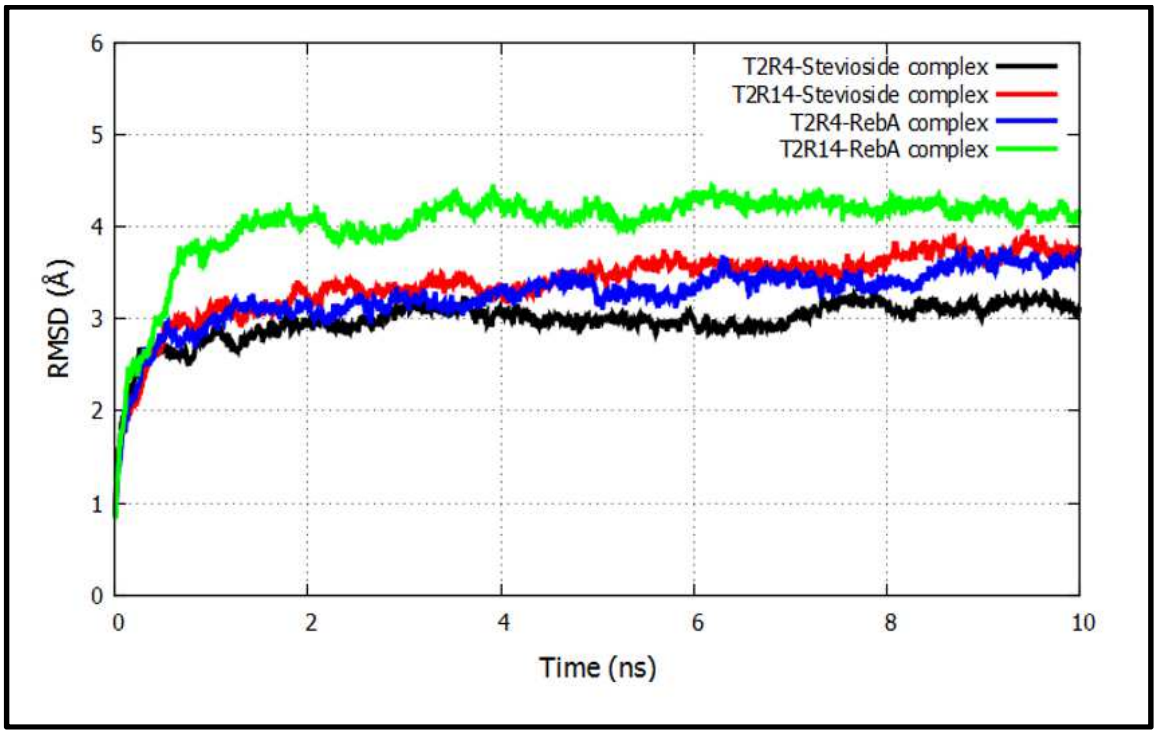

Supplementary figure 2-4: RMSD values show the conformational stability of both stevioside and rebaudioside A.

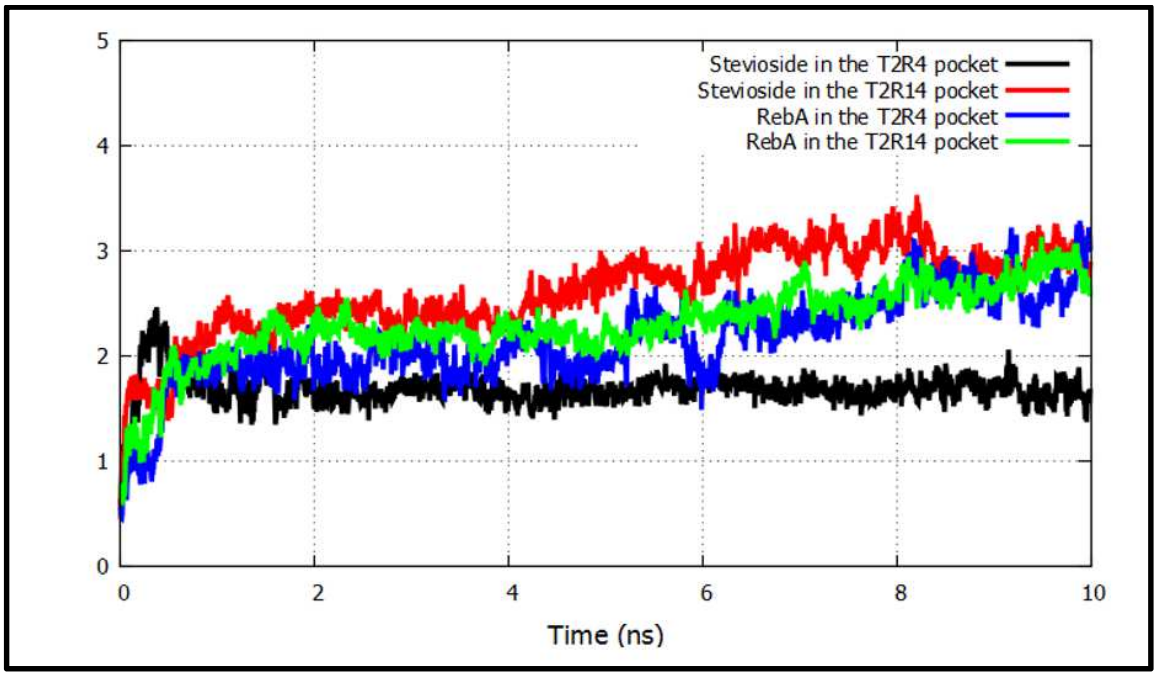

Supplementary figure 2-5: Frequency of hydrogen bonds between the receptor and ligand during 10 ns simulations.

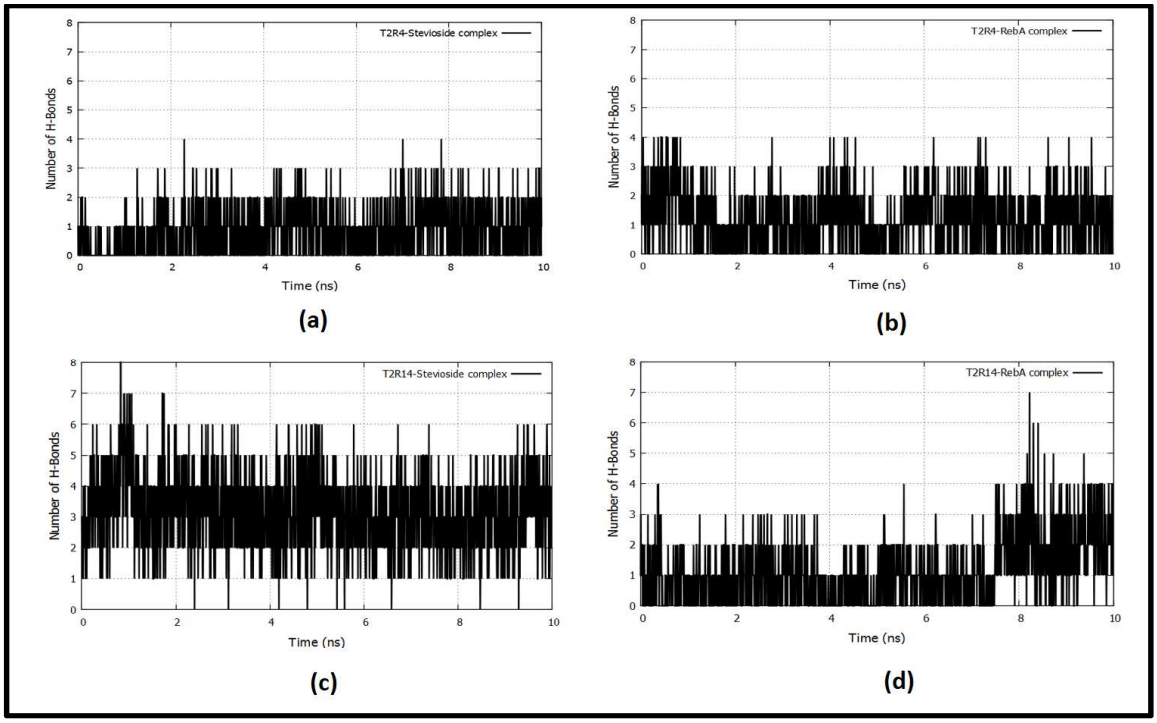

Supplementary figure 2-6: Conformational changes of hT2R4 (a) and hT2R14 (b) with the corresponding RMSF value during the stevioside and rebaudioside A unbinding process.

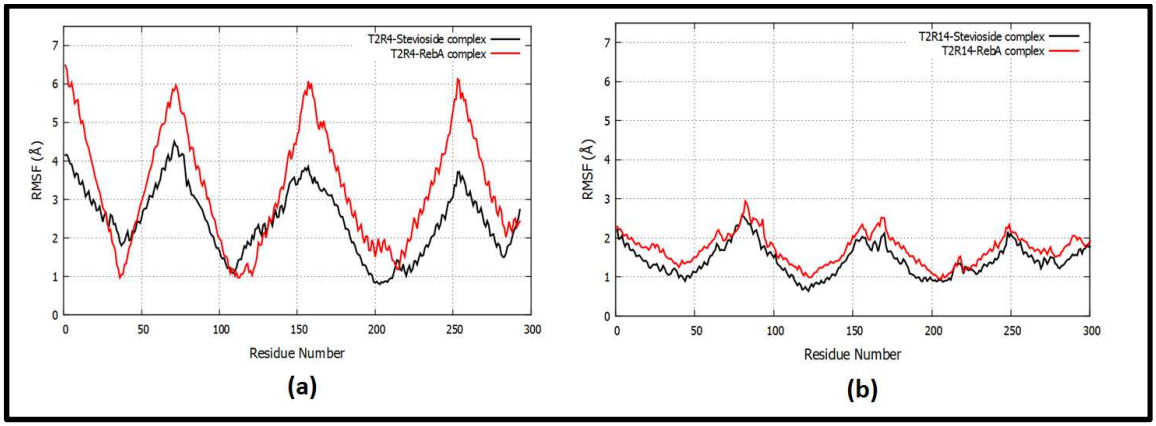

Supplementary figure 2-7: Structural comparison of the hT2R4 (a) and hT2R14 (b) models generated by single template (blue color) and by fragment approach (green color), both generated by TopMatch. The regions of similar structure are colored in red and orange.

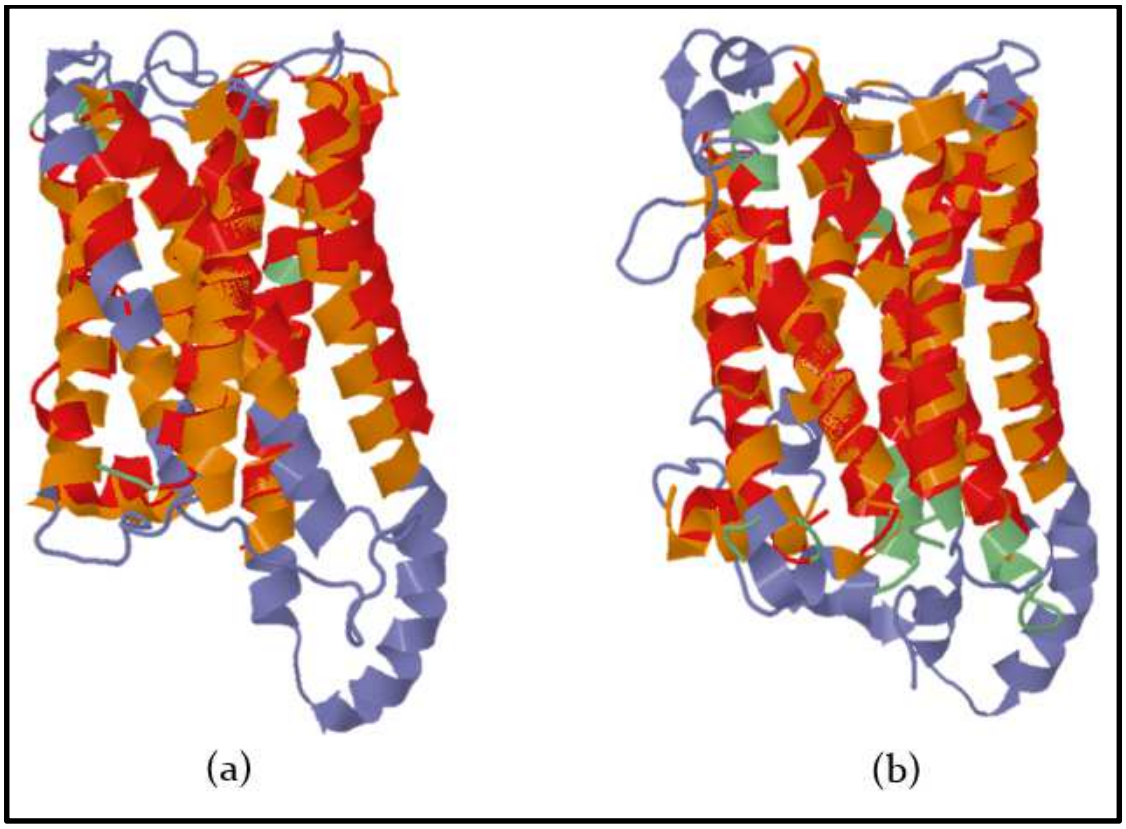

Supplementary figure 3-1: Ramachandran Plots for the hT1R2 (a) and hT1R3 (b) subunits. The dark blue region indicates the favoured regions; the clear blue region represents the permitted regions; yellow indicates the generously allowed regions; and white, the outlier regions.

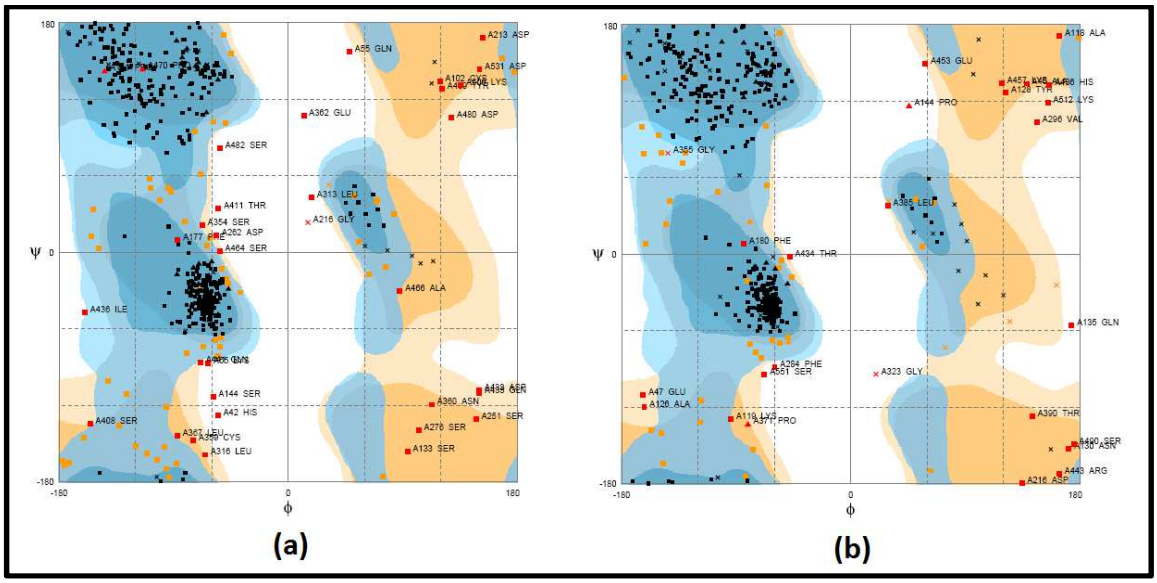

Supplementary figure 3-2: Comparative models of (a) hT1R2 and (b) hT1R3 generated using SWISS-MODEL. Alpha helical structures, beta sheets and loops are represented with red, yellow and cyan, respectively, whereas side chains are shown in green.

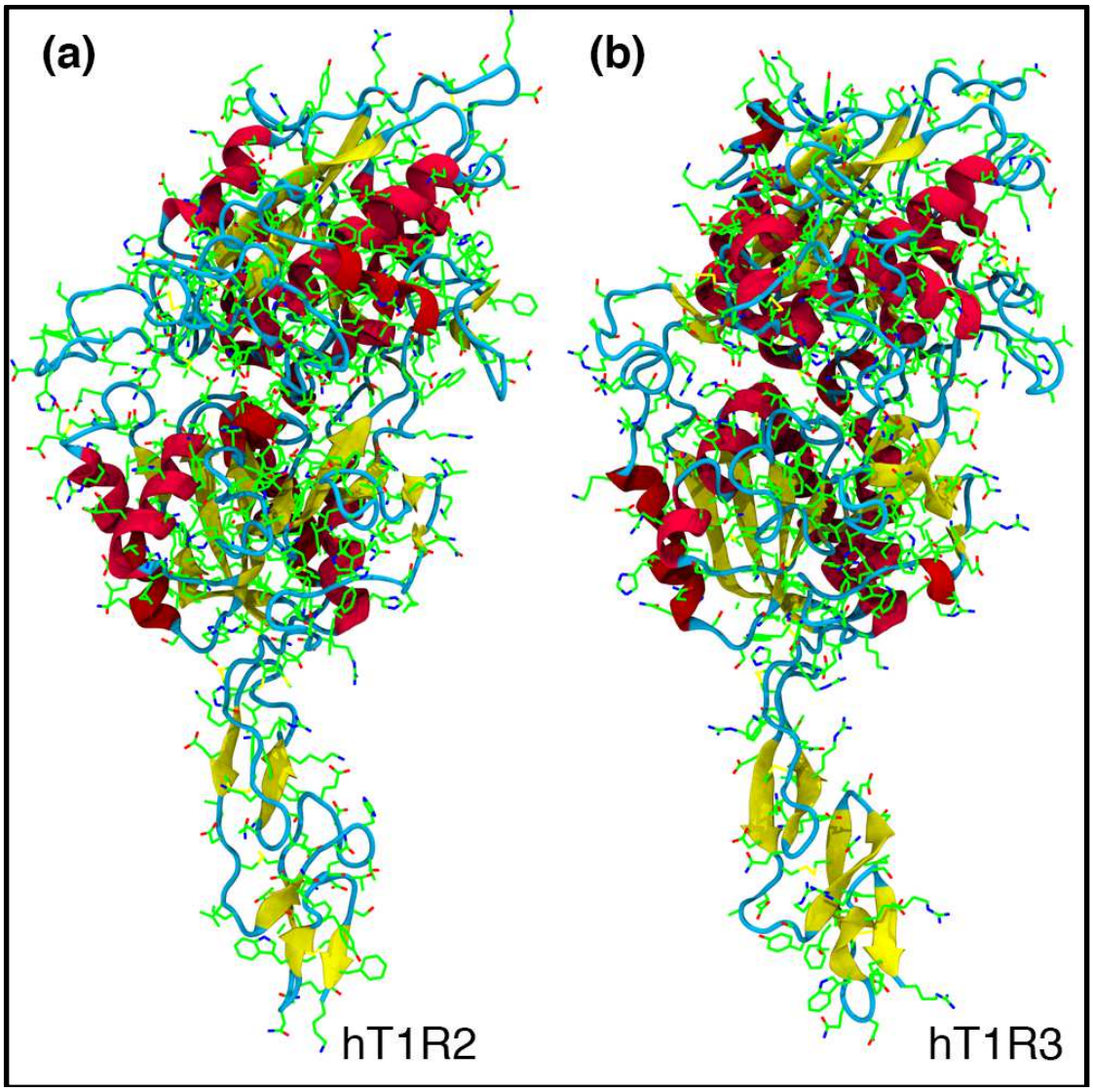

Supplementary figure 3-3: Surface representation of the comparative model of heterodimeric complex composed of hT1R2 (blue) and hT1R3 (red) subunits obtained through protein-protein docking.

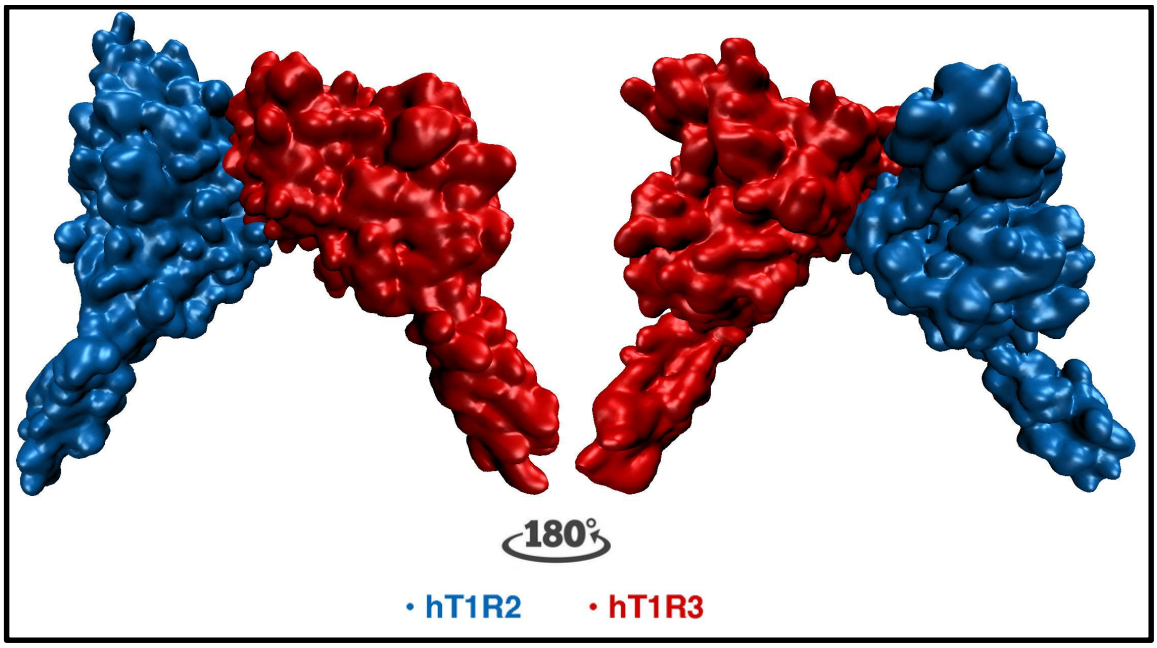

Supplementary figure 3-4: Structural comparison of the comparative model of hT1R2-hT1R3 heterodimeric complex (blue color) with its structure refined by molecular dynamics for 30 nanoseconds (green color), both generated by TopMatch. The regions of similar structure are colored in red and orange.

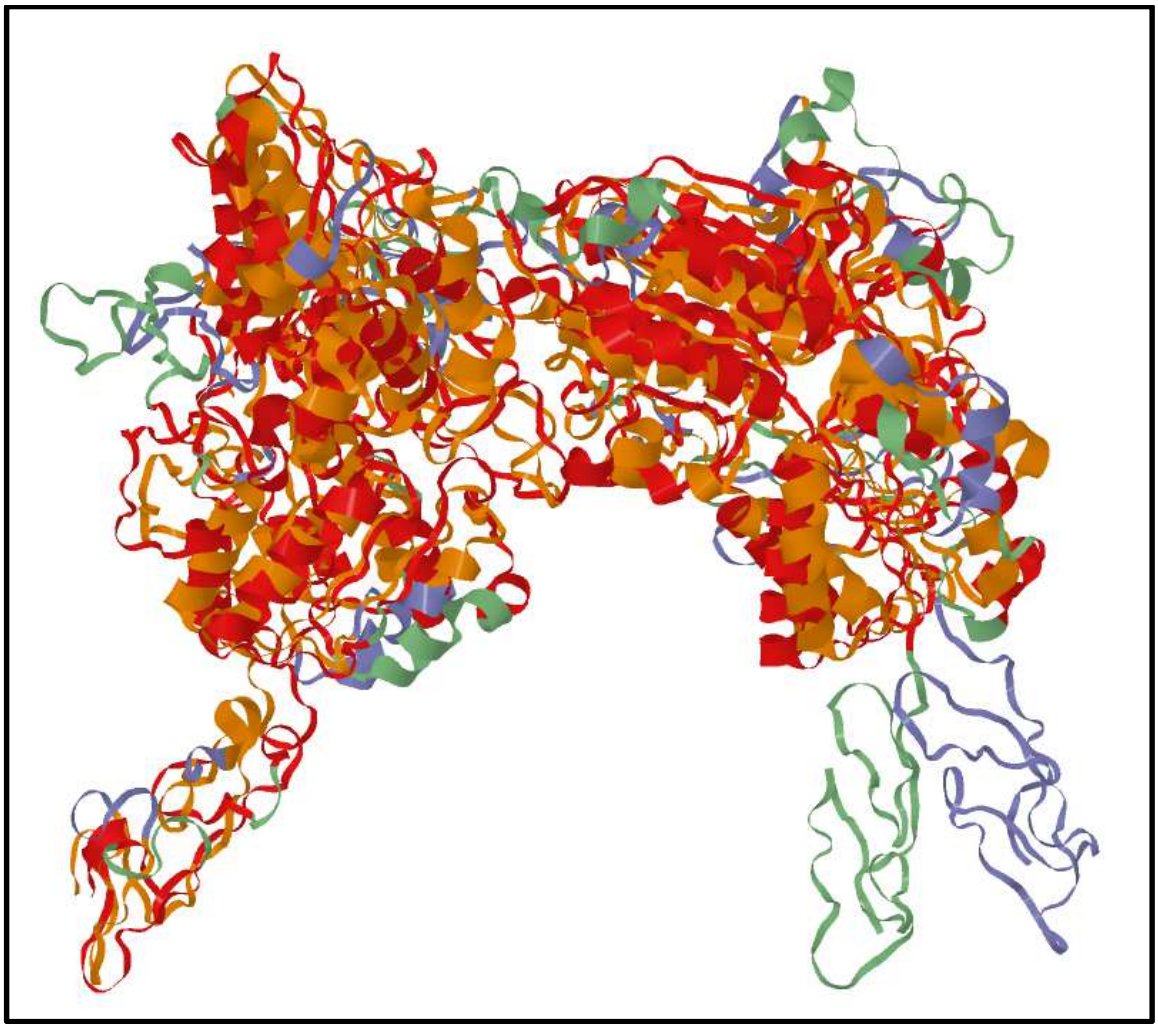

Supplementary figure 3-5: Binding patterns of GTs with the hT1R2-hT1R3 receptor. The amino acids responsible for hydrogen bonds and hydrophobic interactions are represented by three letter codes in green and black, respectively. Carbon, oxygen and nitrogen atoms are shown as filled black, red and blue circles, respectively.

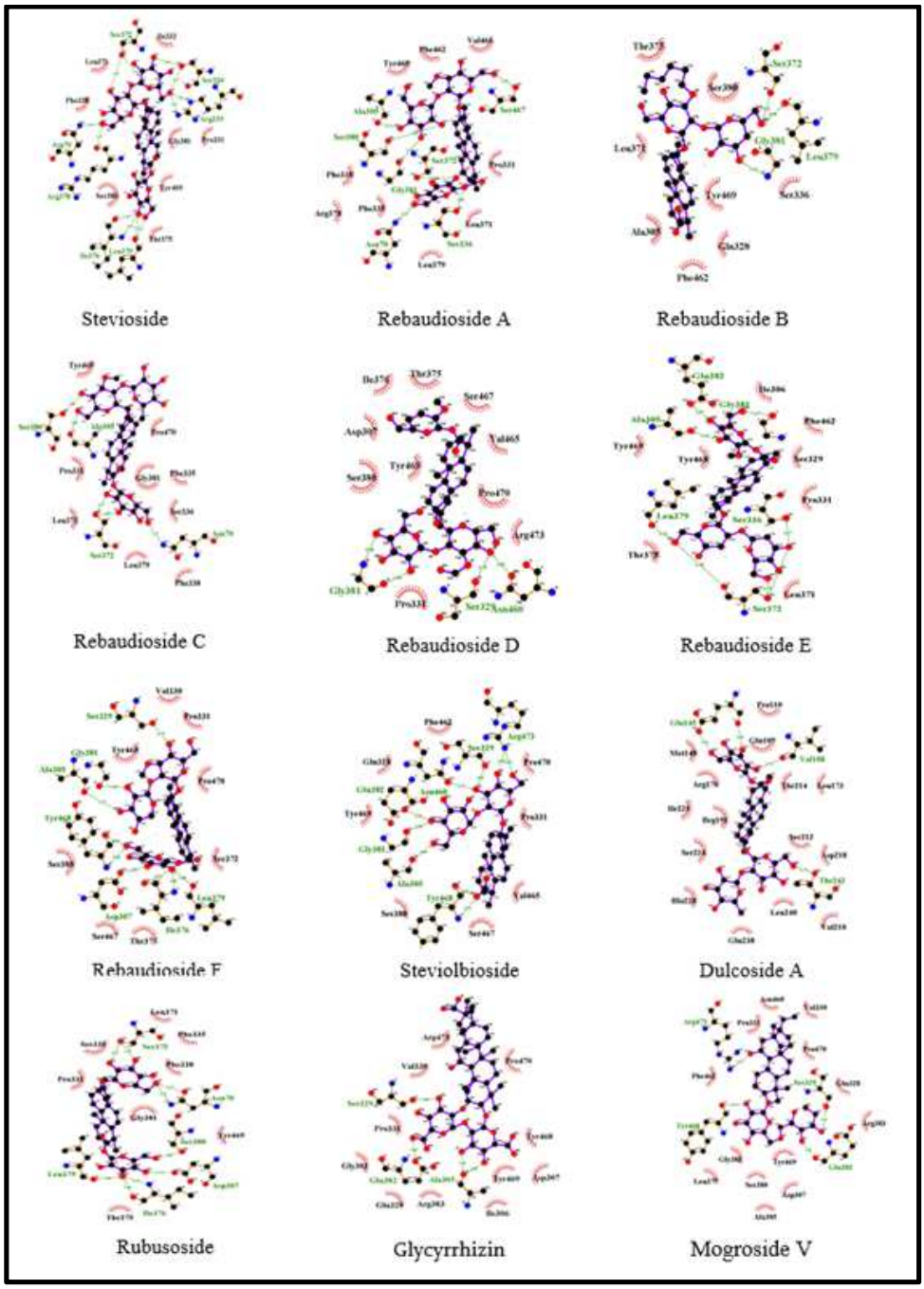

Supplementary figure 3-5: Comparison of the electrostatic surface potentials of (a) hT1R2-hT1R3 (b) brazzein, (c) monellin, (d) thaumatin and (e) neoculin. A green line encircles the interaction surfaces on the sweet taste receptor and the sweet proteins.

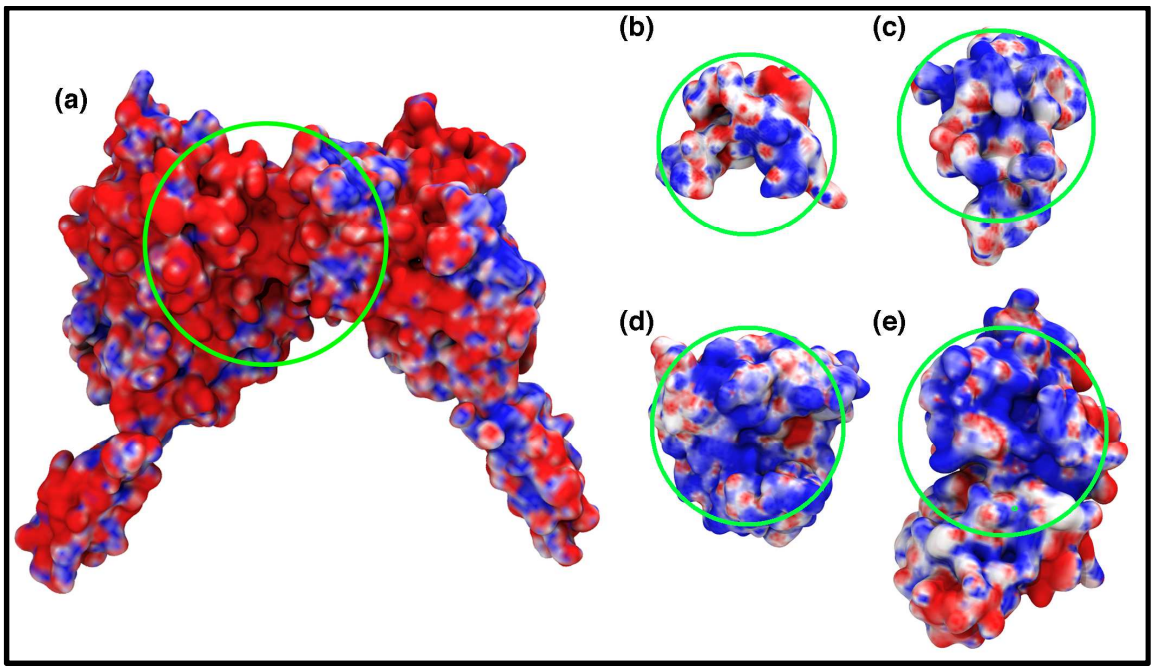

Supplementary figure 4-1: Histogram of frequency of interaction energies of 100.000 pairs configurations sampled. SUC: sucrose. TAG: tagatose. STE: stevioside. REB: rebaudioside A.

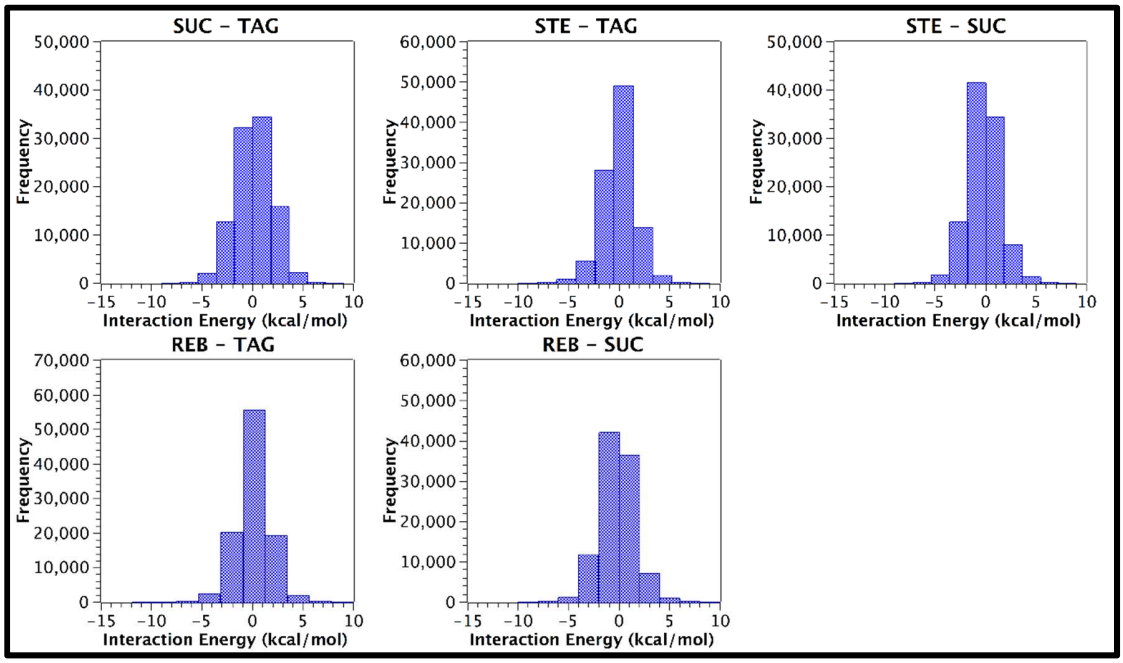

Supplementary figure 4-2: Four checkpoint samples indicated in the ternary diagram. The proportion of sweeteners is represented as sucrose/stevia/tagatose.

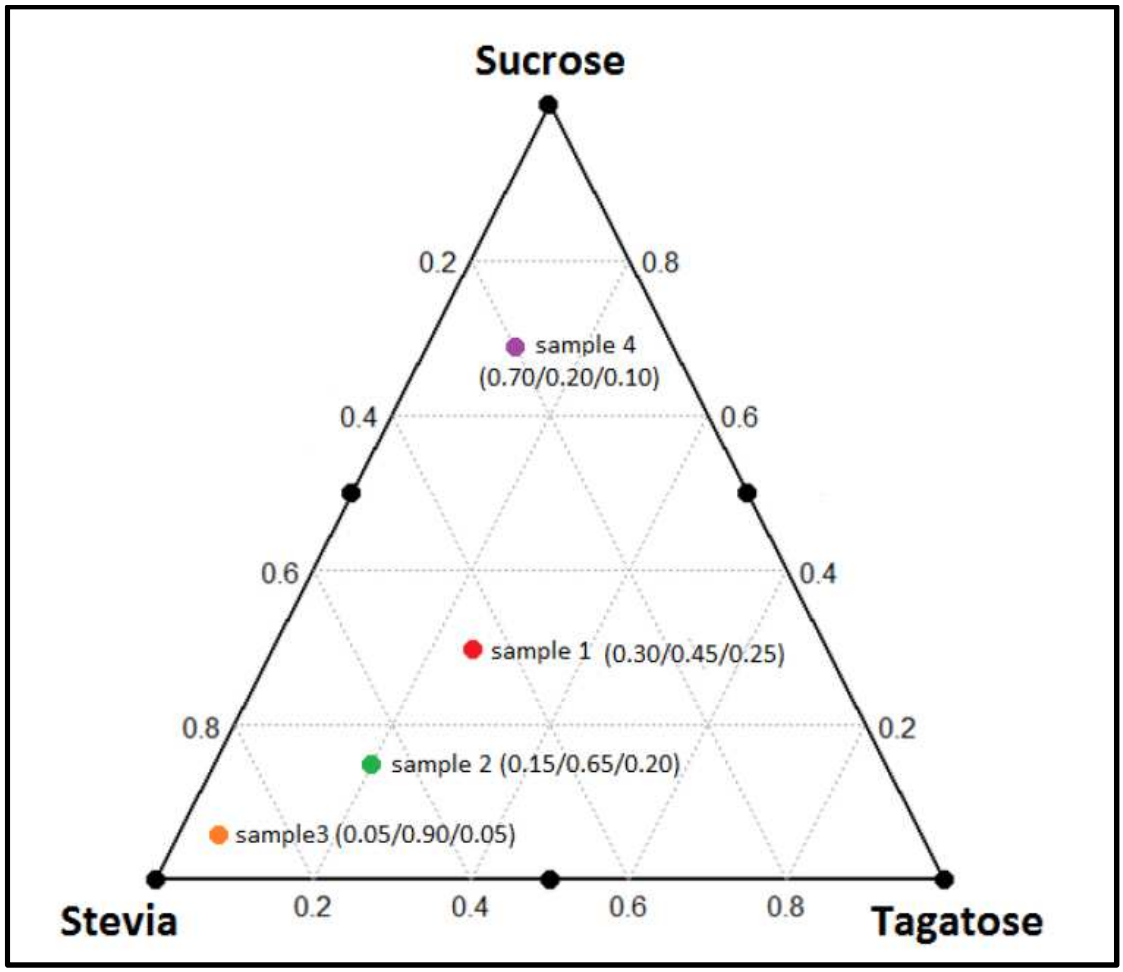

Supplementary figure 4-3: Structural comparison of the molecular model of (a) sucrose, (b) tagatose, (c) stevioside and (d) rebaudioside A extracted from PubMed database (blue color) with its geometry optimized by PM3 semi-empirical quantum mechanics (red color), both generated by the VMD software.

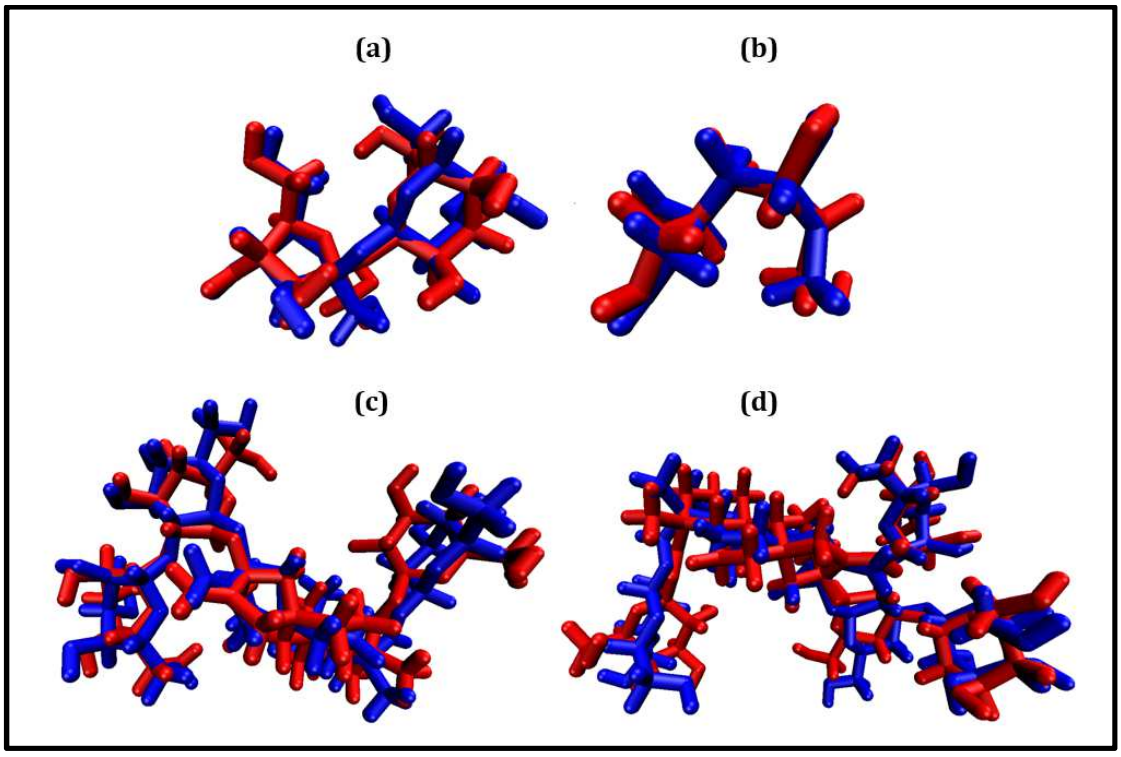

Supplementary figure 4-4: Molecular representation of the best configuration between the (a - d) binary and (e and f) ternary interactions. SUC: sucrose, TAG: tagatose, STE: stevioside, REB: rebaudioside A.

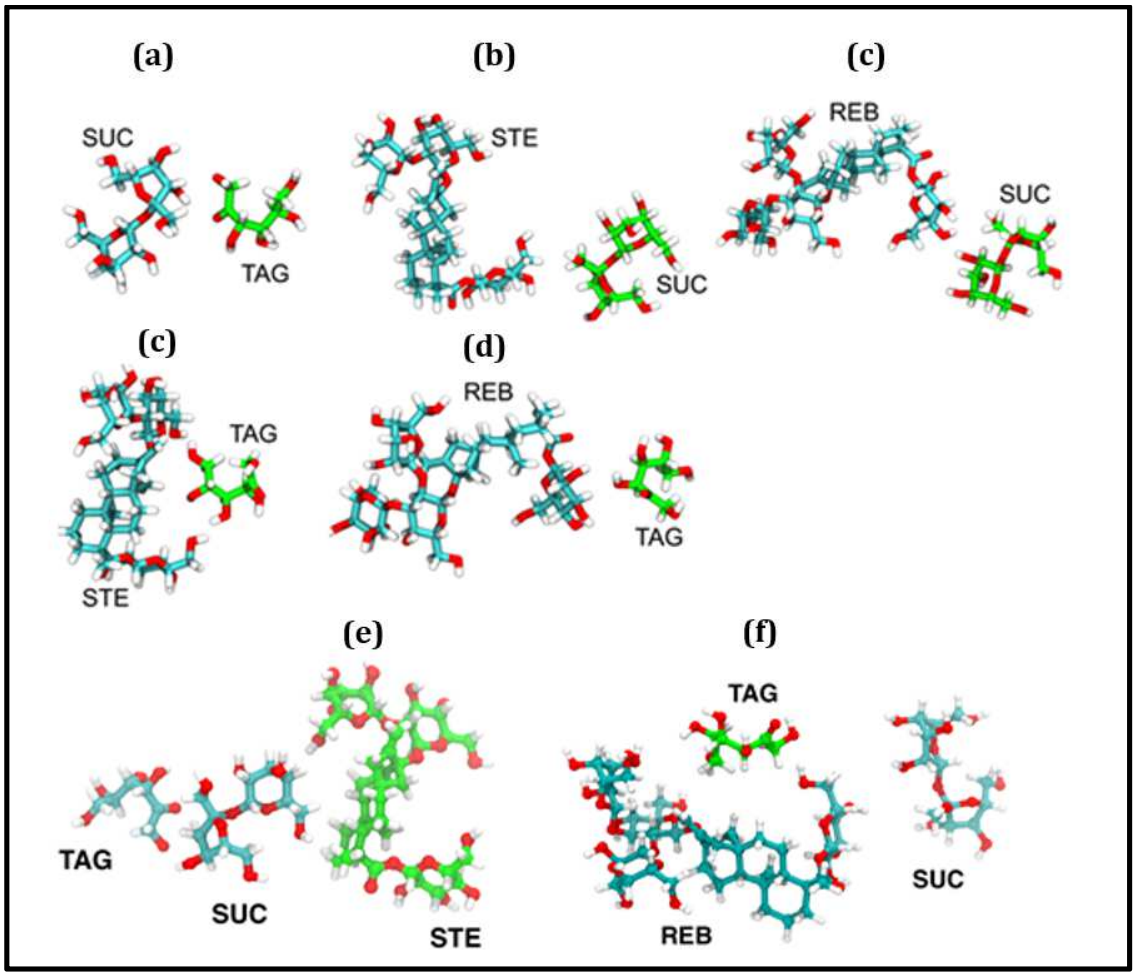

Supplementary figure 4-5: Evolution of curve by weighted aggregation for combinations of (a and c) sucrose-stevioside-tagatose and (b and d) sucrose-rebaudioside A-tagatose. f1-norm and f2-norm correspond to normalized functions for sweetness and bitterness, respectively.

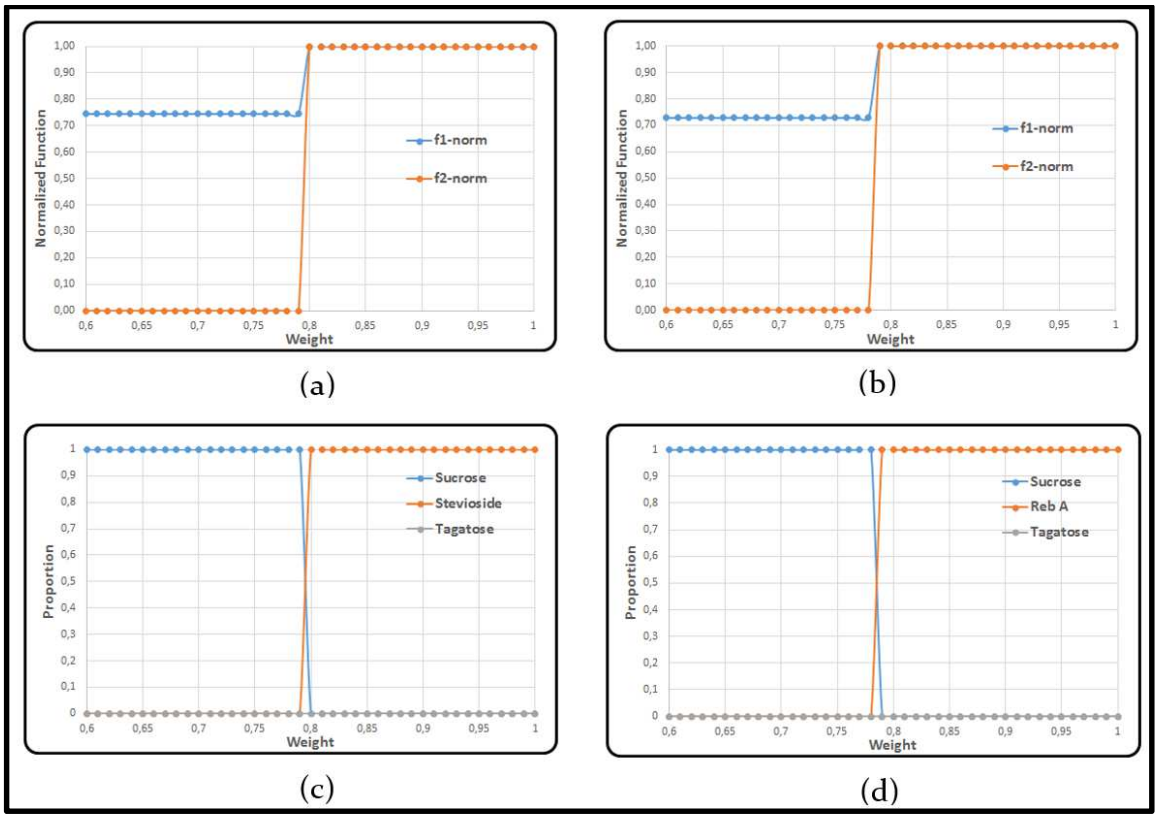

Supplementary figure 4-6: Evolution of curve by weighted aggregation for combinations of (a and c) sucrose-stevioside-tagatose and (b and d) sucrose-rebaudioside A-tagatose. f1-norm and f2-norm correspond to normalized functions for sweetness and bitterness, respectively.

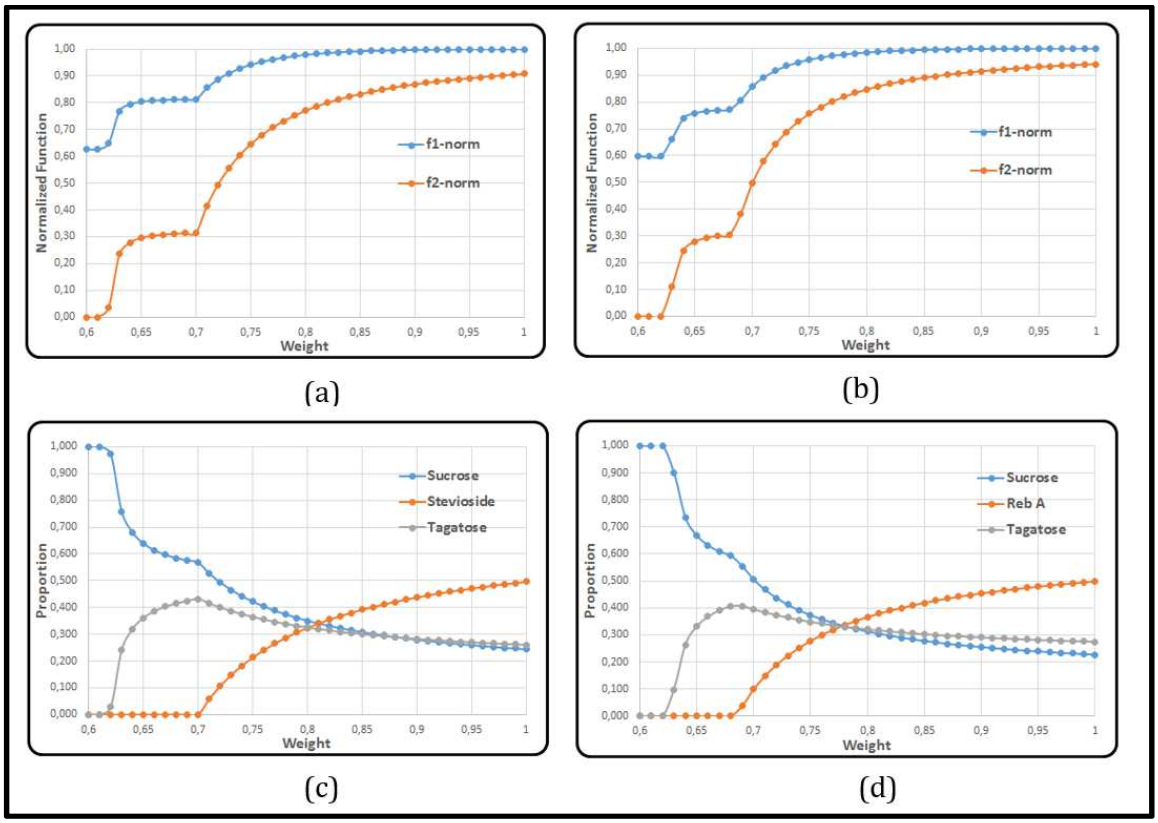

Supplementary figure 4-7: Calories and price contour plots. A. The amount of calories per portion (360 mL); 4*[Sucrose] + 1.5*[Tagatose]; where [] represents the concentration in g/360mL of the corresponding sweetener. This formula was calculated considering the follow energetic values: sucrose 4 cal/g; tagatose 1.5 cal/g and stevia 0 cal/g. B. The cost per 100 liter of product; 0.045*[Sucrose] + 15*[Stevia] + [Tagatose], where [] represents the concentration in g/L of the corresponding sweetener. This formula was calculated considering an average price of each pure sweeteners: sucrose US$ 0.45/Kg; tagatose US$ 10/Kg and stevia US$ 150/Kg. Due to the relatively small amount of stevia used in each sample, the limiting ingredient in terms of cost is tagatose. Both equations are below the corresponding contour plot.

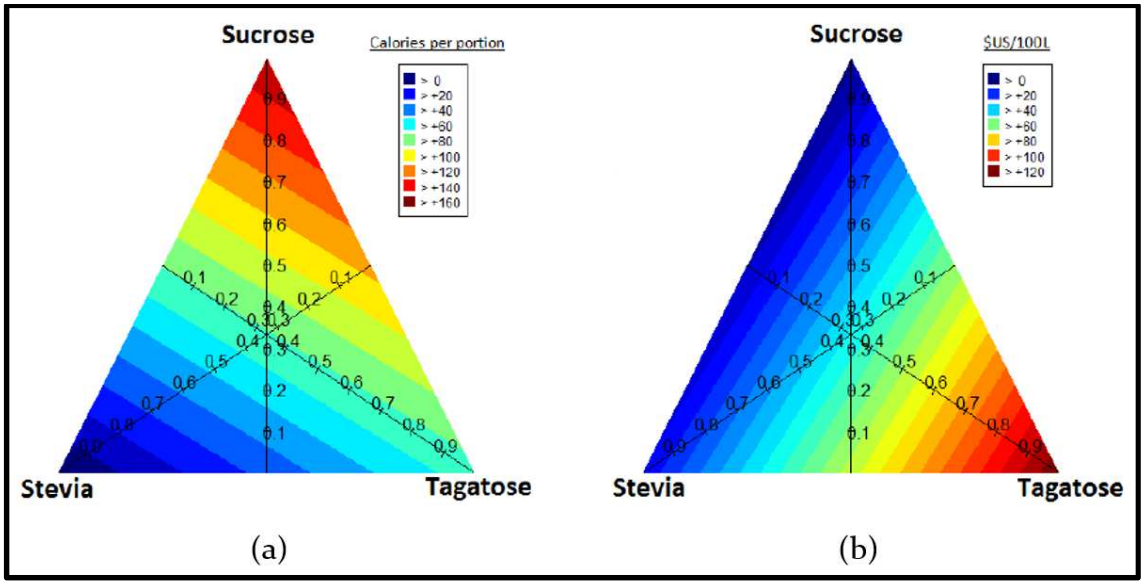

Supplementary table 3-1: Interaction Energies and Potential Binding Sites of Sweeteners for hT1R2-hT1R3 Sweet Taste Receptor.

Number[a]	Compound	$\Delta G_{binding}$ for hT1R2-hT1R3 (Kcal/mol)	Binding site in hT1R2	Binding site in hT1R3	Surface Area of the binding site (Å)	Relative sweetness to sucrose on a weight basis[b]
1	Glucose	-6.6	Leu 54, Gln 55, Val 56, Pro 57, Met 58, Asn 106	-	458	0.65
2	Galactose	-6.4	Lys 46, Leu 54, Gln 55, Val 56, Pro 57, Met 58	-	469	0.7
3	Fructose	-5.8	Leu 54, Gln 55, Val 56, Pro 57, Asn 106	-	437	1.2
4	Xylose	-6.3	Tyr 103, Asp 142, Asn 143, Ser 303	-	114	1.0
5	Sucrose	-6.7	Leu 54, Gln 55, Asn 246	.	343	1.0
6	Tagatose	-6.3	Lys 46, Gly 47, Val 49, His 50, Gln 55, Asn 248, Thr 250, Glu 252	-	784	0.9
7	Sucralose	-8.2	Leu 54, Gln 55	Glu 172, Se 189	388	600
8	Sacharin	-7.3	Thr 183, Gln 454	-	540	300
9	Aspartame	-8.2	Asn 106, Asn 246	Asp 445, Ser 447	309	200
10	Monatin 2S,4S	-8.0	-	Glu 172, Se 189, Asp 445, Asn 449	360	50
11	Monatin 2S,4R	-8.7	-	Ser 189, Asp 445, Asn 449	295	300
12	Monatin 2R,4S	-9.0	Asn 106, Gln 109	Glu 172, Se 189, Asp 445, Asn 449	408	1300
13	Monatin 2R,4R	-9.1	Leu 54, Gln 55, Met 58, Asn 106	Ser 189, Asp 445, Asn 449	418	2700
14	Stevioside	-9.0	Asn 70, Ser 372, Ile 376, Arg 378, Leu 379	-	862	210
15	Rebaudioside A	-9.2	Asn 70, Ala 305, Ser 336, Ser 380, Gly 381, Ser 467	-	1155	242
16	Rebaudioside B	-8.5	Ser 372, Leu 379, Gly 381	-	1018	150
17	Rebaudioside C	-7.4	Asn 70, Ala 305, Ser 380	-	1175	30
18	Rebaudioside D	-8.5	Ser 329, Gy 381, Asn 460	-	990	221

19	Rebaudioside E	-8.9	Ala 305, Ser 336, Ser 372, Leu 379, Gly 381, Glu382	-	1133	174
20	Rebaudioside F	-8.9	Ala 305, Asp 307, Ser 329, Ile 376, Leu 379, Gly 381, Tyr 468	-	1034	200
21	Steviolbioside	-7.9	Ala 305, Ser 329, Gly 381, Glu 382, Asn 460, Tyr 468, Arg 473	-	1023	90
22	Dulcoside A	-8.0	Val 108, Glu145, Thr 242	-	1046	30
23	Rubusoside	-8.8	Asn 70, Asp307, Ser 372, Ile 376, Leu 379, Ser 380	-	934	114
24	Glycyrrhizic acid	-8.4	Ala 305, Ser 329, Glu 382	-	752	50
25	Mogroside V	-9.3	Ser 329, Glu 382, Tyr 468, Arg 473	-	1065	300
26	Brazzein	-11.8	Val111, Ser 129, Asn130, Tyr131, Asn152, Ser155	Lys155, Phe159, Arg177, Asp419	1267	2000
27	Monellin	-14.4	Tyr 131, Glu145, Glu170, Gln244	Gln133, Arg177	1606	3000
28	Thaumatin	-15.6	Gln109, Leu156, Lys174	Phe159, Ser158, Arg177, Glu178	1824	3000
29	Neoculin	-19.2	Val108, Ser129, Tyr131, Glu145, Asn152,Leu156, Phe157, Val175, Asp218, Arg413, Val414	Asp124, Gln133, Lys155, Arg177, Glu178	2685	4000

[a]Compound number refers to structures given in Figure 1 and Table 1. [b]Relative sweetness values extracted from the Canadian Sugar Institute (2015), Shankar et al. (2013), Amino at al. (2016), and Kinghorn et al. (2010),. [c] Values extracted from the PubChem database (National Center for Biotechnology Information, 2004)

Supplementary table 4-1: Sweetness, bitterness, licorice, metallic average of each sample in three-component mixture design in soft drink matrix.

	Sweetness proportion			Sweetness	Bitterness	Licorice	Metallic
Sample	Sucrose (X1)	Stevia (X2)	Tagatose (X3)				
1	1	0	0	7.00	0.77	0.20	0.40
2	0.75	0.25	0	7.14	0.57	0.28	0.32
3	0.50	0.50	0	6.75	0.58	0.50	0.33
4	0.25	0.75	0	7.81	1.88	4.26	0.60
5	0	1	0	5.64	7.31	8.14	2.56
6	0.75	0	0.25	7.19	0.63	1.52	0.38
7	0.50	0.25	0.25	7.07	0.49	1.50	0.33
8	0.25	0.25	0.25	7.13	0.77	2.26	0.74
9	0	0.75	0.25	6.38	2.25	2.82	0.69
10	0.50	0	0.50	7.76	0.64	1.75	0.54
11	0.25	0.25	0.50	6.71	0.44	1.13	0.19
12	0	0.50	0.50	5.94	1.26	1.14	0.52
13	0.25	0	0.75	6.56	0.89	1.89	0.66
14	0	0.25	0.75	6.19	0.71	0.95	0.64
15	0	0	1	6.13	0.83	1.94	0.58
16	0.33	0.33	0.33	7.20	0.88	1.76	0.46

Supplementary table 4-2: Coefficients values and statistical analysis of the canonical Scheffé's equation for bitterness.

Coefficients	Estimate	Standard Error	Pr(>|t|)
β_2	6.33	0.50	8.55e-08
β_3	1.23	0.44	0.01
β_{12}	-9.53	1.93	0.0003
β_{23}	-10.57	2.29	0.0006
$*\beta_1$	1.07	0.50	0.06
$*\beta_{13}$	1.75	2.35	0.47
$*\beta_{123}$	17.83	13.23	0.21
Statistics:	Multiple R-squared: 0.93	F-statistic: 38.91	p-value: 8.84e-07
* The t-test indicates that these parameters are not significant therefore were removed from the equation			

Supplementary table 4-3: Difference between observed and predicted values for bitterness of four additional samples (checkpoints).

	Bitterness		
Checkpoint	Observed	Predicted	Difference
1	1.33	0.68	0.65
2	1.88	2.05	0.17
3	4.13	4.85	0.72
4	1.57	0.15	1.42

Supplementary table 4-4: Set of Pareto optimal solutions for different combination of sweeteners.

	Sweetness proportion			f1-norm[a]	-f2-norm[a]	Price[b]	Calories[b]
Product	Sucrose	Stevioside	Tagatose				
1	0.275	0.445	0.280	1.00	-0.87	46	57
2	0.271	0.452	0.277	1.00	-0.88	46	56
3	0.267	0.459	0.275	1.00	-0.88	46	56
4	0.263	0.465	0.272	1.00	-0.89	46	55
5	0.259	0.471	0.270	1.00	-0.89	46	54
6	0.256	0.476	0.268	1.00	-0.90	46	54
7	0.253	0.482	0.266	1.00	-0.90	45	53
8	0.250	0.487	0.264	1.00	-0.90	45	53
9	0.247	0.491	0.262	1.00	-0.91	45	52
10	0.244	0.496	0.260	1.00	-0.91	45	51
Product	Sucrose	Rebaudioside A	Tagatose				
11	0.259	0.448	0.293	1.00	-0.91	48	56
12	0.255	0.454	0.291	1.00	-0.92	48	55
13	0.252	0.460	0.289	1.00	-0.92	48	54
24	0.248	0.465	0.287	1.00	-0.92	48	54
25	0.245	0.470	0.285	1.00	-0.93	47	53
26	0.242	0.475	0.283	1.00	-0.93	47	53
27	0.239	0.479	0.282	1.00	-0.93	47	52
28	0.236	0.483	0.280	1.00	-0.93	47	52
29	0.234	0.487	0.279	1.00	-0.94	47	51
30	0.232	0.491	0.277	1.00	-0.94	47	51
31	0.229	0.495	0.276	1.00	-0.94	47	50
32	0.227	0.498	0.275	1.00	-0.94	47	50

[a]f1 and f2 correspond to normalized functions for sweetness and bitterness, respectively

[b]Price and calories were calculated as US$/100L and cal per portion (360 mL), respectively, using the formulas described in Figure S3